Attempts to Quantify Mitochondrial DNA Deletions in Single *Drosophila melanogaster* Flies

Masters by Research Thesis

Lewis Huzzard BSc (Hons)

Lancaster University

July 2020

I, Lewis Huzzard, confirm that the work presented in this thesis is my own and has not been submitted in substantially the same form for the award of a higher degree elsewhere. Where information has been derived from other sources, I confirm this has been indicated in the thesis.

Submitted in fulfilment of the requirements for the degree of Research Masters

Abstract

Research to date has not clearly described the role mitochondrial DNA (mtDNA) deletions may have in normal ageing. Therefore, a high throughput method of mtDNA deletion detection and quantification is required. The goal of this project was to develop such an assay using individual *Drosophila melanogaster*, which allowed for rapid generation of aged animals and manipulation of conditions which could affect deletion generation. An assay composed of DNA extraction and Quantitative Polymerase Chain Reaction (QPCR) was designed for deletion amplification. Primers were designed to amplify deletions within the *cytochrome oxidase* (COX) region with primers in *nadh ubiquinone oxidoreductase 1* (*ND1*) used as a control to quantify total mtDNA.

Optimising QPCR methods for specific primer pairs improved target amplification and replicability. Redesign of an existing DNA extraction kit improved overall mtDNA yield for assay development but still lacked consistency. QPCR inhibitors present in commercial extraction kits were present in minor concentrations in extracts and likely impacted amplification efficiency. The lack of sufficient mtDNA extraction from single *Drosophila* for consistent deletion amplification lead to mispriming and nonspecific amplification of nuclear DNA (nDNA). Repeated amplification of one deletion across multiple extracts suggests QPCR preferentially amplifies the shortest available target sequence, corresponding to the largest deletion.

Redesign of the DNA extraction method to yield higher mtDNA concentration whilst reducing inhibitors would assist in reducing nonspecific amplification. mtDNA enrichment may be required to remove nDNA if nonspecific amplification still occurs. Differential amplification of deletions depending on size renders comparison and quantification difficult. Targeted amplification of a specific common deletion may eliminate this issue at the cost of quantifying just one deletion. The likelihood of single *Drosophila* harbouring sufficient numbers of a specific deletion should be determined to assess if quantification of mtDNA deletion levels in single *Drosophila* is viable.

Table of Contents

Acknowledgements

I would like to thank my supervisor Dr David Clancy for his support throughout this project. I would also like to thank my family and friends for their love and support, without which I would never have made it through the year.

Literature Review

Introduction

In broad terms ageing can be defined as the increase in the chance of mortality with chronological age (Charlesworth and Partridge, 1997). Ageing is characterised by the time-dependent changes within an organism, focused on the deterioration of cellular function with age that progressively increases mortality risk through disease and dysfunction. This multifactorial process affects a range of cellular elements as seen in figure 1.1 (Lopez-Otin et al., 2013). These processes are impacted by genetic and environmental factors which control the extent to which each process influences ageing (Chandrasekaran et al., 2017).

Figure 1.1. The nine hallmarks of ageing (Lopez-Otin et al., 2013)

Although the literature covers in-depth the wide range of genetic and environmental factors which influence ageing, this literature review will focus on the role mtDNA damage and more specifically mtDNA deletions may have on the ageing process. Within the last 20 years the understanding of how mtDNA damage and deletions impact ageing has improved significantly with the help of model organisms such as mitochondrial mutator mice (Ahlqvist et al., 2012; Trifunovic et al., 2004; Vermulst et al., 2008). Further research into the mechanisms which generate and accumulate mtDNA damage and deletions is essential to establish the extent to which mtDNA deletions are a cause or a consequence of ageing, or both.

This review will begin by establishing the concepts of ageing followed by reviewing the oxidative and mitochondrial theories of ageing and their validity in light of the current literature. The review will then assess how mtDNA damage is caused and accumulated, progressing into the role mtDNA damage accumulation and more specifically mtDNA deletion accumulation has in ageing.

Concepts of Ageing

Evolutionary Theory of Ageing

The evolution of ageing is a major question within evolutionary biology. Within multicellular organisms a gradual functional decline overtime characterises the ageing process, yet there are a few exceptions to this rule across the plant and animal kingdoms such as Hydra (Schaible et al., 2014). Regardless of exceptions, ageing has appeared to have evolved in tandem with higher organisms from unicellular bacteria. However, the way that ageing has evolved may not mimic a programmed process but rather a maladaptive one. Initial evolutionary theories suggested that ageing had evolved to filter a population in order to remove older individuals for the populations benefit. However, progressing knowledge of molecular biology defined evolution as a gene-centred process and ageing as a maladaptive process, discrediting these theories (Gardner and Welch, 2011). As a result, ageing is the effect of declining adaptation for survival which fails to maintain

life in higher organisms. As regulatory genes of ageing have evolved overtime, ageing can be described as a genetically controlled process (Harman, 2006).

The evolutionary theories of ageing are centred on the fact that forces of selection decline with age as mortality, disease, and damage reduces the number of individuals reaching older ages. These forces also decline with age once reproduction is achieved and genes are passed on. These theories lack any actual mechanisms of ageing since they only describe the risk of death increasing with the duration an individual is alive (Kirkwood and Holliday, 1979). These evolutionary theories can be divided into, the mutation accumulation theory, the antagonistic pleiotropy theory, and the disposable soma theory. The theory of mutation accumulation suggests that the accumulation of deleterious mutations which negatively impact the organism in later life accumulate because of a lack of selection against their presence (Medawar, 1952). This theory was further developed into the antagonistic pleiotropy theory, which suggests that the mutations which accumulate are those that confer beneficial effects in early life but deleterious effects in later life. These mutations accumulate because they are strongly selected for in early life and lack selection against in later life (Williams, 1957). The disposable soma theory suggests that ageing is the concession between reproduction of the germline and maintenance of the soma (or organism). This theory implies that all multicellular organisms are just biological machines whose purpose is simply to continue passing on genes (Kirkwood and Holliday, 1979).

Mechanistic Theory of Ageing

The mechanistic approach to understanding ageing aims to define the molecular and cellular mechanisms responsible. The rate of living theory first described by Pearl based on *Drosophila* observations, suggested that lifespan is determined by the average rate of metabolism within an organism in an inverse manner (Alpatov and Pearl, 1929). The concept of replicative senescence or the 'Hayflick Limit' was established by Leonard Hayflick in the 1960s through *in vitro* observations of human diploid cells displaying a limited replication capacity of ~50 cycles (+/- 10) (Hayflick,

1965). As cells approach their replicative capacity they start to display features including increasing generation time, before cellular division ceases altogether. Hayflick noted that chromosomal aberrations increased *in vivo* within a cell alongside division count. These observations were also seen with chronological age of human peripheral blood leukocyte samples (Hayflick, 1965).

Hayflicks observations led to a hypothesis suggesting that cellular deterioration is the result of telomere shortening (Olovnikov, 1973). Telomeres are repetitive, protective sequences (TTAGG) which cap the ends of chromosomes to prevent them from adhering to one another. They also serve to prevent the loss of genetic information from cell division, since a short portion of sequence from the ends of each chromosome is lost during replication. Telomeres are maintained by a ribonucleoprotein called Telomerase which extends these sequences by adding further TTAGG repeats to the 3' end of chromosomes. However, Telomerase activity is absent in the majority of somatic tissues and thus telomeres shorten with each cell cycle, leading to the loss of genetic information (Lopez-Otin et al., 2013). This exhaustion of telomeres provides part of the explanation to the replication limit first described by Hayflick.

Cellular senescence describes the cessation of cell division caused by a wide variety of stress inducing factors (Campisi, 2013). These stress factors include internal and external sources of damage, telomere shortening, autophagy, and oxidative stress. Under cellular senescence cells develop specific phenotypic changes which include tumour suppressor activation, chromatin changes, and secretome changes (Kuilman et al., 2010). Cell senescence is important in preventing carcinogenesis but more recently has been identified to possess a role in ageing and tissue repair (Baker et al., 2011; Krizhanovsky et al., 2008; van Deursen, 2014).

Evidence both supporting and contradicting mechanistic theories has made the identification of a 'common' mechanism for all ageing processes difficult. However, this information suggests that each of these theories have identified mechanisms that mediate the ageing process through genetic and non-genetic means. Collectively

the identification of these mechanisms provides insight into the complex ageing process and further supports the concept that ageing is a collection of mechanisms rather than an underlying common process (Lopez-Otin et al., 2013).

Oxidative Theory of Ageing

Free Radical Theory of Ageing

The Free Radical Theory of Ageing (FRTA, or oxidative theory of ageing) is the most widely studied basic molecular mechanistic theory of ageing to date. The use of a wide range of model organisms underpins the evidence used to build these theories, including *Drosophila melanogaster*. The FRTA initially described by Denham Harman in 1956 proposed that the generation of oxygen radicals (specifically hydroxyl and hydroperoxyl) through respiration results in cellular damage which accumulates with age (Harman, 1956). This accumulation of damage offered an explanation to the mechanistic 'rate of living' theory proposed by Pearl in 1929 (Alpatov and Pearl, 1929). Further studies provided evidence of *in vivo* oxygen radical production through the discovery of the anti-oxidant enzyme superoxide dismutase (SOD) (McCord and Fridovic.I, 1969) and hydrogen peroxide (H_2O_2) (Boveris and Chance, 1973). These studies provided a base to Harman's concept and further research into the theory.

Over time Harman's concepts have been refined from the FRTA into the oxidative stress theory of ageing to encompass additional forms of reactive oxygen species (ROS), including peroxides and aldehydes. While not technically free radicals, these reactive species contribute to oxidative damage in the cell (Muller et al., 2007). Intracellular ROS are generated by various pathways with multiple contributors including cyclooxygenases, NAPDH oxidases, and lipid metabolism enzymes (Massudi et al., 2012). Close to 90% of intracellular ROS generation occurs from the mitochondria, more specifically the Electron Transport Chain (ETC) (Gomez and Hagen, 2012). The modification of the FRTA highlighted a constant state of oxidative stress within aerobic organisms, even under normal physiological state. This state

suggests an imbalance between oxidant and antioxidant systems (or redox systems) leads to the gradual accumulation of oxidative damage to macromolecules with age. Oxidative damage and modification to macromolecules include DNA damage, lipid peroxidation, and the formation of sulphur bridges in proteins (Valko et al., 2007). According to the FRTA this accumulation of oxidative damage leads to the progressive decline of cellular function and efficiency.

Redox Homeostasis

Excessive ROS generation past physiological levels result in oxidative modification of cellular components and the accumulation of oxidative damage with age. At physiologically low levels however, ROS act as intracellular messengers in signalling and regulation (Circu and Aw, 2010). Majority of cell types have demonstrated a small oxidative increase generating minor concentrations of ROS when stimulated by growth factors, cytokines, and hormones including tumour necrosis factor α, interleukin 3 and 6, and angiotensin 2 (Thannickal and Fanburg, 2000). The dysregulation of ROS signalling may also influence various pathological conditions, including the rate of ageing (Balaban et al., 2005). This implies a role for ROS in the initiation and/or continuation of multiple signal transduction pathways, suggesting ROS act as important physiological secondary messengers.

Redox homeostasis describes the systems of oxidants and antioxidants which maintain balanced physiological ROS levels. Cellular antioxidants function as competitive substrates against oxidisable substrates to delay or inhibit their oxidation in order to preserve cellular function (Bratic and Larsson, 2013). Enzymatic antioxidants include SOD, glutathione peroxidase, and catalase. Non-enzymatic antioxidants include vitamins E and C, and carotenoids. Central to ROS control are cellular redox systems which include: the glutathione redox system, the thioredoxin redox system, the pyridine nucleotide redox system, NADPH and antioxidant defence, and NAD^+ and sirtuins proteins (Circu and Aw, 2010).

Redox homeostasis is primarily maintained by the glutathione and thioredoxin redox systems which represent the major cellular 'buffer' against excessive ROS generation (Valko et al., 2007). Alongside these major systems are minor antioxidants present in high concentrations which can contribute significantly to the overall ROS scavenging effort. These include proteins, peptides, and amino acids which when oxidised become substrates for proteolytic digestion, contributing to the maintenance of redox homeostasis (Droge, 2002). Redox signalling describes the regulation of redox systems through either an increase in ROS or a decrease in antioxidant systems. A shift in ROS generation towards more oxidisable conditions induces signalling mechanisms to enhance antioxidant systems which reduce ROS concentration to physiological levels (Figure 1.2). These signalling mechanisms include bacterial OxyR, MAPK and JNK signalling pathways, and insulin receptor kinase activity (Valko et al., 2007). Large shifts in ROS under pathological conditions potentially leads to permanent changes in signalling and gene expression (Chandrasekaran et al., 2017).
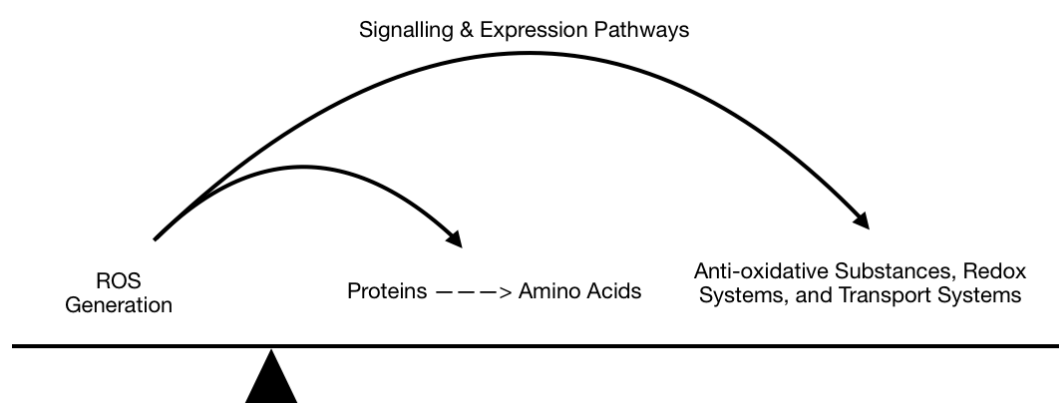
Figure 1.2. The balance between ROS generation and clearance. Major scavenging mechanisms occur through enzymes, substrates, and transport systems at low cellular concentrations. Minor scavenging mechanisms occur through proteolysis at high cellular concentrations.

Redox state shifts in an opposing manner within the cytosol and endoplasmic reticulum (ER) in response to ageing and proteotoxic stresses, with the ER becoming further reduced in disease-associated protein expression, in proteosomal inhibition, and when the cytosol redox state shifts to become more oxidising (Feleciano and Kirstein, 2016). The shift of redox state in part may be a natural product of the 'back and forward' feedback regulation of redox homeostasis through metabolic systems

(Murray et al., 2007). Although assumptions can be made on the roles age-related ROS increase has on the age-related changes in gene expression and redox state, a clear cause-effect relationship is currently lacking.

The Role of Reactive Oxygen Species in Ageing

In 1998 Beckman and Ames suggested that the theories on the role of ROS in ageing should be divided into both a 'strong' and 'weak' theory. The strong theory hypothesised that oxidative modification and damage determines lifespan whereas the weak theory hypothesised that oxidative damage is associated with the ageing process (Beckman and Ames, 1998). The question is which theory, if at all, best describes the role of ROS in ageing?

The FRTA states that lifespan is dictated by the rate of ROS damage and that antioxidant defences protect against this, meaning redox homeostasis is essential to maintaining cellular function and longevity. From this information, increasing antioxidant defences should reduce ageing progression and prolong lifespan. In contrast to this statement, manipulating antioxidant defence genes within model organisms demonstrates no clear association of oxidative damage and longevity (Doonan et al., 2008; Mockett et al., 2010; Zhang et al., 2009). The overexpression of antioxidant enzymes does not extend lifespan in model organisms and shortens lifespan in certain cases (Mockett et al., 2010). Within human studies, dietary supplementation using antioxidants such as vitamins A and E provide no beneficial effects in protecting against age-related diseases (Bjelakovic et al., 2007; Bjelakovic et al., 2012). This suggests that dietary supplementation of antioxidants lack beneficial effects for extending lifespan and protecting against age-related disease. It should be noted that differences between human and model organism studies may be the result of different conditions for antioxidant treatment. Some human studies relied on subjects already displaying clinical symptoms prior to treatment.

Comparison between species of insect, avian, and mammalian origin with variable lifespans demonstrate a positive correlation between mitochondrial H_2O_2 production

and age, suggesting that ROS generation is a potential factor in lifespan determination. (Cocheme et al., 2011). There are however, exceptions to this concept such as the naked-mole rat which has the longest lifespan of all rodent species (25-30 years) but maintains similar levels of ROS generation as mice (3-4 years). Naked-mole rats demonstrate no age-related variation in antioxidant enzyme expression whilst showing increasing levels of oxidative damage with age (Lewis et al., 2013). This information is consistent with suggestions that increased ROS generation may extend lifespan in model organisms (Yang and Hekimi, 2010). Collectively these studies support the concept that ROS act as essential regulators of cell signalling, senescence, and apoptosis alongside other cellular processes (Chandrasekaran et al., 2017). Note that this does not suggest that ROS levels are the sole determinant of age and age-related functional decline, rather that they're important in controlling overall cellular function and longevity.

Reviewing Beckman and Ames' theories on ROS and ageing, current information suggests that the weak approach is most appropriate. Age-related differences in ROS generation and oxidative damage are minor and do not explain the significant physiological changes which happen throughout the ageing process (Jackson and McArdle, 2016). The lack of a direct correlation between oxidative stress and lifespan suggests that ROS-mediated damage does not play a central role in the ageing process nor in age-related disease. Rather the accumulation of oxidative damage with age appears to be the product of multiple aspects of declining cellular function (Valko et al., 2007).

Mitochondrial Theory of Ageing

The origin of the mitochondria has been a source of much debate since it's identification as an organelle in 1890 (Ernster and Schatz, 1981) In 1970 Margulis proposed that the mitochondria had evolved from bacteria through symbiosis within a eukaryotic cell (Margulis and Sagan, 2000). The actual mechanism of this evolution is still widely debated with two theories, the Archezoan Scenario and the Symbiogenesis Scenario, considered the two potential mechanisms of symbiosis

(Gray, 2012; Koonin, 2010). The identification of at least 840 orthologous groups within eukaryotes that possess a clear α-Proteobacterial signature provide the candidate which likely underwent symbiosis (Gabaldon and Huynen, 2007). Comparisons amongst α-Proteobacterial genomes suggest that this mitochondrial ancestor initially contained between 3000-5000 genes and lost between 1000-3000 genes in its transition from symbiont to organelle (Szklarczyk and Huynen, 2010). Of the more than 800 human genes that possess α-Proteobacterial signatures only around 200 are actually found within the mitochondrial proteome. This suggests that the contribution of α-Proteobacteria to eukaryotic cell evolution progresses past the mitochondria itself to include the shuffling of genes to additional cellular elements (Gray, 2012). In summary the evolution of the mitochondria is characterised by its loss of multiple original functions, a retargeting of other functions to different locations within the cell, and the inclusion of host-derived proteins (Gabaldon and Huynen, 2007).

The Mitochondrial Theory of Ageing

The mitochondrial theory of ageing was initially proposed in 1972 by Harman as a modification of the FRTA. This Mitochondrial FRTA (MFRTA) is focused on the mitochondria because of the disproportionately high quantities of ROS generated by these organelles (Harman, 1972). The MFRTA is centred on the fact that mitochondrial ROS generation increases with age due to both declining mitochondrial function and declining ROS-scavenging enzyme activity (Bratic and Larsson, 2013). Within the MFRTA, the accumulation of mtDNA mutations throughout ageing and the resulting impairment of respiratory chain function is through ROS-associated damage. This impairment then further enhances both ROS generation and oxidative damage as the respiratory chain becomes less efficient (Bratic and Larsson, 2013). The MFRTA and increasing ROS-associated damage with age is supported to an extent, by studies on various age-associated diseases (Schapira, 2012). The various mitochondrial molecules and processes impacted by ROS generation are summarised in figure 1.3:
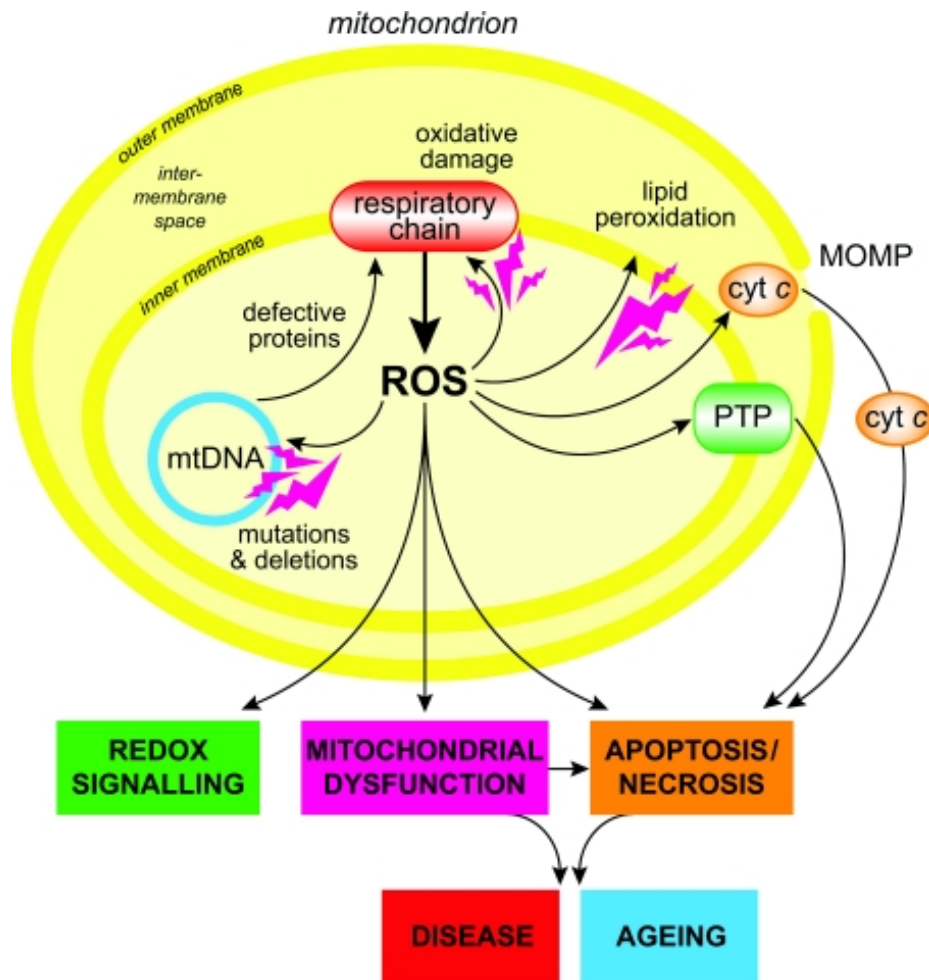
Figure 1.3. An overview of the molecules and processes impacted by mitochondrial ROS. Mitochondrial outer membrane permeabilization (MOMP), PTP = mitochondrial permeability transition pore (Murphy, 2009).

The primary role of the mitochondria is to generate ATP through oxidative phosphorylation, performed by four respiratory complexes embedded in the inner mitochondrial membrane (complexes I-IV) and ATP synthase (complex V). The sequential transfer of electrons through the ETC exposes oxygen to electrons. Leakage of electrons at complexes I and III causes the partial reduction of free oxygen molecules into free radicals (O_2-) as summarised in figure 1.4 (Li et al., 2013). Referring back to the previous sections on ROS and the conclusions on ROS role in ageing, the MFRTA appears to have progressed in the correct direction. Although the theories focus on ROS is still dated, the inclusion of the mitochondria as a major factor in ageing fits current ageing models (Bratic and Larsson, 2013).
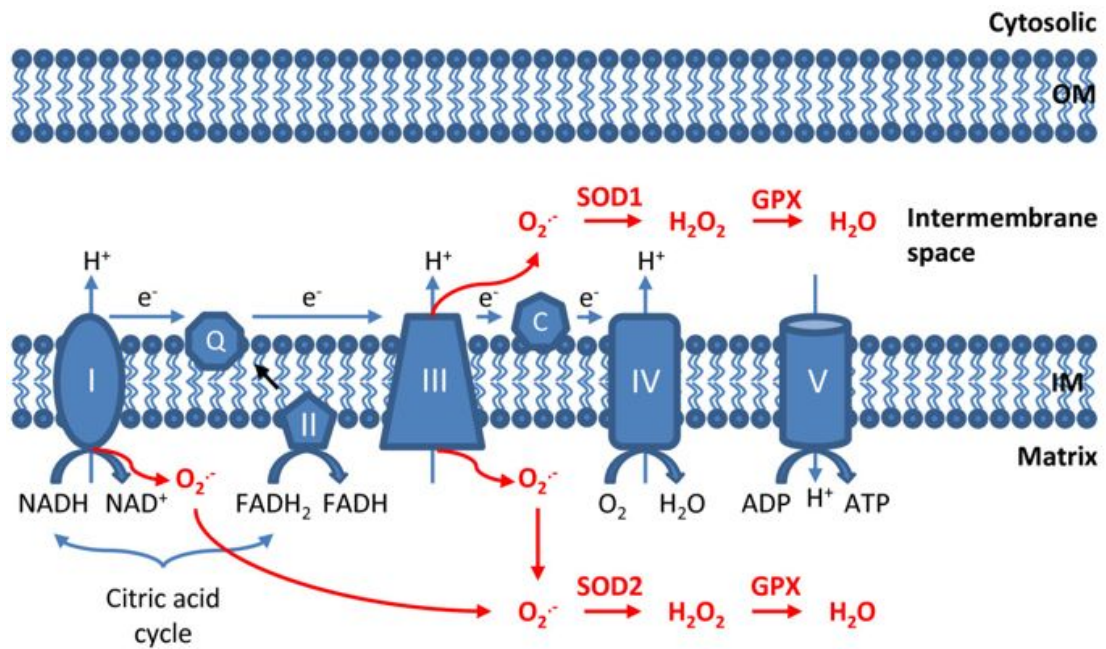
Figure 1.4. Generation and disposal of mitochondrial ROS. Leakage of electrons by complexes I and III generate O_2-. O_2- is produced in the matrix by complex I and in the matrix and intermembrane space by complex III. O_2- is then dismutated to H_2O_2 by superoxide dismutase 1 and 2 (SOD1 and SOD2). H_2O_2 is then reduced to water by catalase and glutathione peroxidase (GPX). Both H_2O_2 and O_2- are considered to be mitochondrially generated ROS. IM = inner membrane, OM = outer membrane (Li et al., 2013).

The functional decline of mitochondria with age is the defining characteristic of the mitochondrial theory of ageing and is already widely established through studies on model organisms and humans (Sun et al., 2016). The mitochondrial activity and count in liver cells declines with age in mice (Herbener, 1976) and humans (Yen et al., 1989). Liver cell respiratory chain capacity declines up to 40% in 24 month old rats compared to 3-4 month old rats (Stocco et al., 1977). Respiratory chain capacity has also been found to decline in human skeletal muscle (Short et al., 2005) and heart (Ojaimi et al., 1999). It should be noted that these changes in respiratory capacity may be in response to a shift in hormone and physical activity rather than a decline in mitochondrial mass and function (Brierley et al., 1997). More specifically, complex I and IV activity declines with age in heart, brain, liver, and kidney of mice and rats but activity remains unchanged in complexes II, III, and V (Navarro and Boveris, 2007). The cause of respiratory chain component decline has been associated with increasing levels of mtDNA mutations and declining mtDNA expression with age

(Manczak et al., 2005). The differences with age between studied species, cellular type, and cellular composition should be reiterated. As tissue composition differs with age so will mitochondrial function and respiratory capacity, complicating the interpretation of these conclusions (Picard et al., 2011).

Although the functional decline of the mitochondria is associated with ageing, it does not suggest causality since mitochondrial functional decline may be secondary to other mechanisms (Koopman and van Loon, 2009). Given that mitochondrial dysfunction is important in ageing, it should be noted that multiple elements control mitochondrial biogenesis. This includes hormonal regulation via thyroid-hormones (Knuever et al., 2012) and oestrogens (Chen et al., 2009). Changes in mitochondrial biology are also documented in physical activity studies through reduced oxidative damage and increased mitochondrial function (Radak et al., 2013). Multiple studies have demonstrated the importance of mitochondrial metabolism in controlling lifespan through dietary restriction (Choi et al., 2011) and nutrient sensing (Holzenberger et al., 2003). The two major mitochondrial nutrient sensing pathways, insulin (IIS) and rapamycin (TOR), are linked to lifespan manipulation. Impaired TOR and ISS activity extends lifespan in mammals, flies, and worms (Holzenberger et al., 2003; Kapahi et al., 2004; Vellai et al., 2003). Caloric restriction has already been established in improving health and lifespan in mammals and model organisms (Colman et al., 2009). The age-related effects of caloric restriction have been associated with reduced oxidative damage and metabolic rate which subsequently inhibit various signalling pathways in redox homeostasis (Dai et al., 2012).

In conclusion the age-related decline of mitochondrial function can be attributed to additional age-related changes including declining hormonal levels and nutrient sensing. Recent mitochondrial ageing models have suggested that mtDNA damage and more specifically mtDNA mutations propel the ageing process and are responsible for respiratory chain dysfunction (Stewart and Chinnery, 2015).

Mitochondrial DNA

Mitochondrial genetic composition can differ between species. Most animal mtDNA is supercoiled and compact in nature approximately 16kb in length. *Drosophila* mtDNA is approximately 19517bp in length, much longer than human mtDNA at approximately 16569bp. The size difference is predominantly because of the expanded 'AT rich' region in *Drosophila* species (Sen and Cox, 2017). Aside from differences in size, the positions of genes within the *Drosophila* genome are drastically different from their human counterpart (figure 1.5). The natural absence of introns, high genetic density, frequency of direct repeats, and a non-coding 'D-loop' characterise mtDNA. mtDNA is divided into a Heavy (H) and Light (L) strand which are composed of mainly purines and pyrimidines respectively, with the H-strand having greater molecular weight (Pitceathly et al., 2012). The human mitochondrial proteome is estimated to consist of 1000-1500 different proteins which all contribute to mitochondrial biochemical processes (Madreiter-Sokolowski et al., 2018). In humans there are 13 protein subunits which are required for the respiratory chain to function, with 2 rRNA and 22 tRNA species for gene expression. All genes found in mtDNA are essential for an effective functioning mitochondria (Szczepanowska and Trifunovic, 2015). All complex II subunits are encoded by nDNA alongside other subunits and factors required for biogenesis of the respiratory chain (Lott et al., 2013). Due to the high density of genetic information within mtDNA and lack of intron sequences, several genes overlap one another and lack full termination codons (Nissanka et al., 2019). The mitochondrial genome is packaged into protein complexes called mitochondrial nucleoids, holding similarities to bacterial chromosomes (Chen and Butow, 2005). The genetic density of mtDNA means any mtDNA damage can theoretically cause varying levels of dysfunction, hence the importance of accumulating mtDNA damage in ageing (Stewart and Chinnery, 2015).
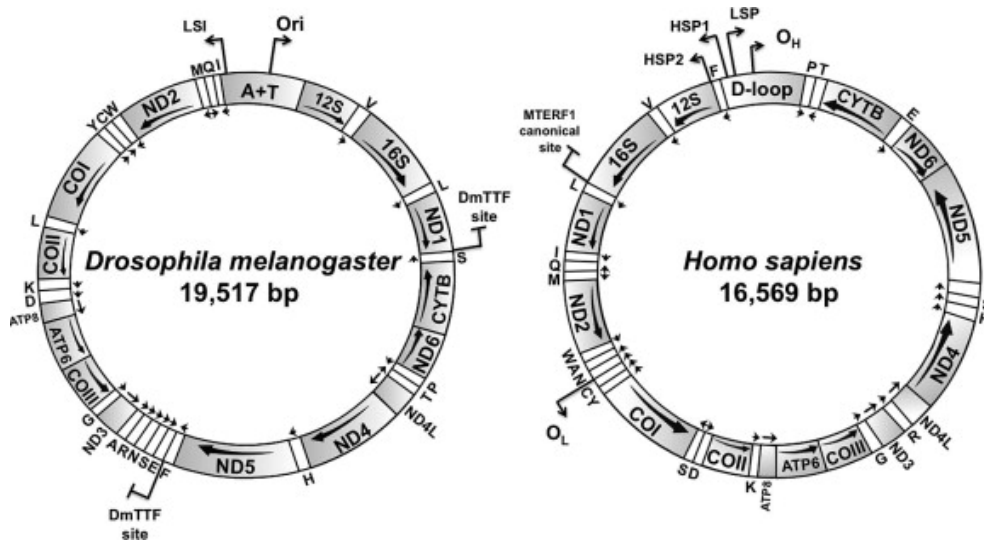
Figure 1.5. *Drosophila melanogaster* **mtDNA genome (left) and human mtDNA genome (right). The major noncoding regions of** *Drosophila* **(A+T) and human (D-loop) mtDNA are the regions where sequence variation is highest within animal species. The arrows underneath each gene show the direction of transcription. In the** *Drosophila* **genome: Ori = Origin of Replication (origin of leading strand synthesis), LSI = Initiation of Lagging Strand Synthesis. In the human genome: O_H = origin of leading (heavy) strand synthesis, O_L = origin of lagging (light) strand synthesis, LSP = light strand promotor, HSP1 and HSP2 = heavy strand promotors 1 and 2 (Oliveira et al., 2010).**

Mitochondrial DNA Repair

Despite extensive study of mitochondrial repair mechanisms the exact components and steps of an advanced mechanism are not fully documented (Kazak et al., 2012). Currently there are two established mechanisms of mtDNA repair, Base Excision Repair (BER) and Microhomology-mediated end joining (MMEJ). BER is a pathway which removes and repairs oxidised, deaminated, and alkylated bases. Mitochondrial and nucleic BER use the same enzymes and process damage in the same way. BER relies on DNA glycosylases to identify and cleave the damaged base, catalysing the first step of the repair pathway. Each end is then 'cleaned', the required DNA base synthesised, and the adjacent nicks sealed (Prakash and Doublié, 2015).

MMEJ is a mutagenic form of repair that uses 5-25bp microhomologous sequences to align double stranded DNA breaks. MMEJ is essential in maintaining the mammalian mitochondrial genome (Tadi et al., 2016). This double stranded repair begins with the nuclear encoded MRE11 nuclease cleaving part of each end leaving single stranded overhangs. These overhangs then anneal to microhomologous sequences, roughly complementary to the overhangs. Any further overhanging bases

are removed, both ends are joined, and the remaining gaps are filled by a DNA polymerase (Sfeir and Symington, 2015). MMEJ was observed by Tadi and colleagues by using DNA substrates with 5-, 8-, 10-, 13-, 16-, 19-, and 22-nt Microhomology, with the length of homology enhancing MMEJ efficiency. Alongside additional observations they concluded the central role for MMEJ in the overall maintenance of the mammalian mitochondrial genome. Furthermore, they concluded on the relevance of MMEJ in causing minor deletions (Tadi et al., 2016).

Initial beliefs and a lack of information regarding mtDNA repair suggested that mitochondrial repair systems were poor and less diverse than their nuclear counterparts. This conclusion coupled with the proximity of mtDNA to the ETC and thus ROS provided an explanation for high mtDNA mutation frequency (Zinovkina, 2018). However, ETC function is reliant on proteins coded within mtDNA and cellular function is reliant on the ETC. If the mitochondrial repair system is poor, then the respiratory chain would eventually be disrupted. Therefore, there must be mitochondrial DNA repair systems capable of maintaining the mitochondrial genome and thus protecting mitochondrial function.

Recent advances in the study of mtDNA repair have begun to identify the presence of various DNA repair components similar to that of nuclear repair systems (Zinovkina, 2018). For example, two key components of nucleotide excision repair (NER), ERCC6 and ERCC8, were detected in mammalian mitochondria and found to sharply increase in concentration when cells were treated with H_2O_2. These NER components were found to only be imported into the mitochondria during oxidative stress (Kamenisch et al., 2010). It should be noted that NER requires additional enzymes not found in the mitochondria, suggesting that these two components either perform different functions or that NER is different in mitochondria. Regardless, further identification and understanding of repair components within the mitochondria will progress understanding of mtDNA repair systems.

Mitochondrial DNA Replication

As with mtDNA repair the exact steps of mtDNA replication are not fully established, with three major theorised mechanisms of mtDNA replication currently debated (Figure 1.6) (Falkenberg, 2018). The first model (strand-displacement model) established in 1972, involves synthesis of the leading mtDNA strand first (from the template H-strand) without synchronous lagging strand synthesis (Robberson et al., 1972). The second model was established in 2000 when mtDNA replication intermediates were identified which displayed properties of coupled leading-lagging strand synthesis within mouse tissues and human tissues and cells (Holt et al., 2000). The third model or RITOL model is essentially an updated strand-displacement model which uses an 'RNA incorporation' mechanism, where the lagging strand is hybridised with complementary RNA molecules rather than proteins (Holt and Reyes, 2012). For the purpose of this review these methods will not be analysed in detail. Regardless of conflicting theories, progressing research into mtDNA replication demonstrates the complexity of the process and how further research is required to establish the exact mechanism of mtDNA replication. It is speculated that the variability of mitochondrial quantity and metabolic state across tissues and cells contributes to the modulation of mtDNA replication, which is essential for mitochondrial function (Yasukawa and Kang, 2018).
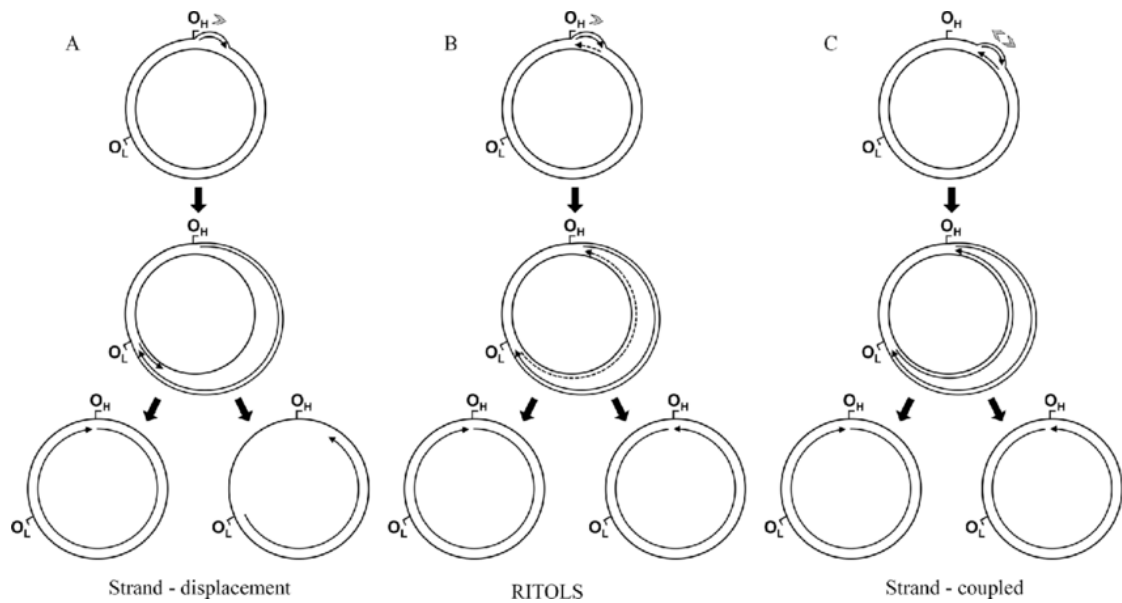
Figure 1.6. Current proposed models of mtDNA replication. The O_H and O_L sites are represented as reference points to the mammalian origins of both heavy (leading) and light (lagging) strand synthesis respectively. Arrows within the replicating mtDNA indicate the 5' to 3' direction of synthesis with dashed and continuous lines representing RNA and DNA respectively (McKinney and Oliveira, 2013).

mtDNA replication occurs independently of cellular replication and thus could be replicated multiple times or not at all during cell division (Clayton, 1982). Mammalian mtDNA replication uses proteins distinct from nuclear DNA replication, with multiple mtDNA replication proteins found to be related to bacteriophage replication factors (Shutt and Gray, 2006). mtDNA replication and maintenance relies on some nuclear encoded proteins including core replicative machinery components and proteins which maintain mitochondrial dNTP levels (Ahmed et al., 2015).

Within humans, mtDNA is replicated by polymerase γ (PolG), a heterotrimeric polymerase comprised of a catalytic subunit encoded by *Polg1* (p140) and a homodimeric subunit encoded by *Polg2* (p55). The catalytic subunit possesses a 3'-5' exonuclease domain that proofreads synthesised DNA strands (Graziewicz et al., 2006). Human mtDNA replication fidelity averages 1 error in 440000 nucleotides, with the average rate of misincorporation of all four individual nucleotides varying widely (Lee and Johnson, 2006). The accessory homodimeric subunit of PolG acts in two ways; the proximal accessory subunit assists the complex in DNA binding

whereas the distal accessory subunit enhances nucleotide incorporation (Graziewicz et al., 2006). PolG can only replicate single stranded mtDNA and so is accompanied by a DNA helicase, Twinkle, which unwinds the mtDNA template ahead of replication machinery. Twinkle forms a hexamer structure with a 5' mtDNA loading site and 3' tail to load mtDNA and initiate unwinding (Korhonen et al., 2003). Single stranded DNA binding proteins bind single stranded mtDNA to protect against nucleases and secondary structure formation. These single stranded proteins also enhance mtDNA synthesis through Twinkle stimulation and increasing PolG processivity (Farr et al., 1999; Korhonen et al., 2003).

Causes of Mitochondrial DNA Damage

There are three major chemical sources of mitochondrial DNA damage; reactive species, alkylation, and hydrolysis (Gates, 2009). Oxidative damage through ROS is by far the most discussed and prevalent form of mtDNA damage due to the role the mitochondrial ETC has in generating ROS, with at least nine separate sites responsible for superoxide anion generation (Balaban et al., 2005). ROS include oxygen, superoxide anions, hydroxyl radicals, and hydrogen peroxide. All of these molecules can oxidise DNA molecules to form damage including oxidised bases and both single and double-stranded DNA breaks (Kazak et al., 2012). Additional reactive species such as reactive nitrogen species (RNS) also oxidise, deaminate, and generate strand breakage in mtDNA (Mangialasche et al., 2009). 8-hydroxydeoxyguanosine (8-oxodG) is the most measureable marker of oxidative damage with its generation enhanced by chemical carcinogens (Helbock et al., 1999; Pisoschi and Pop, 2015).

mtDNA damage through alkylation can occur through exposition to both exogenous elements such as smoke and drugs, and endogenous elements such as S-adenosylmethionine (SAM) and choline (De Bont and van Larebeke, 2004; Rydberg and Lindahl, 1982). This type of DNA damage can result in modifications, such as 7-methylguanine, which can cause mtDNA replication blockage and stalling (Gates, 2009; Tudek et al., 1992). Hydrolytic damage describes the damage, deamination, or total loss of DNA bases. The deamination of DNA bases mainly occurs through the

deamination of cytosine to yield uracil, resulting from either hydroxide attack against a nucleotide or water attack against a protonated base (Gates, 2009). Total loss of a DNA base, known as an apurinic site (AP), is the result of targeting the glycosidic bond between a nucleotide and sugar (Gates, 2009).

Alongside major chemical sources of DNA damage, other damage sources including ultraviolet light, activated compounds, and error from mitochondrial replication and repair contribute to mtDNA damage levels. The formation of DNA adducts called photodimers can arise from exposure to ultraviolet light, with additional adducts arising through activated metabolites from organic contaminants and stimulated endogenous factors (Van Houten et al., 2016). Ultraviolet light exposure can also generate double strand DNA breakage and pyrimidine-dimerization (Sinha and Hader, 2002). The minor infidelity of mtDNA replication machinery can introduce base to base mismatches, insertions, and deletions (Kazak et al., 2012). mtDNA single strand breaks can arise from ineffective BER (Sykora et al., 2012). Minor mtDNA deletion can arise from MMEJ repair (Tadi et al., 2016).

Accumulation of Mitochondrial DNA Damage

There is already clear evidence for increasing mtDNA mutation levels with age in humans, notably mtDNA deletions within human skeletal muscle (Fayet et al., 2002) and human liver cells (Yen et al., 1991). Overall mtDNA mutations appear to arise from unrepaired DNA damage, which can be the result of oxidative modification, modification through additional reactive elements, and mtDNA replication and repair errors (Larsson, 2010). It would be reasonable to assume that increasing mtDNA damage and mutation with age is the result of overall accumulating unrepaired damage, yet current evidence suggests that mtDNA replication errors could hold a much more significant role (Ameur et al., 2011).

The first time that mtDNA mutation accumulation was associated with premature ageing was through the creation of mtDNA mutator mice (Trifunovic et al., 2004). The mutator mice demonstrate multiple ageing phenotypes including hair loss,

hearing loss, weight loss, shortened lifespan, and reduced fertility. These mice are homozygous for a mutation that causes the expression of a proofreading deficient form of PolG. The expression of this mutated polymerase results in mtDNA mutagenesis, producing sporadic point mutations, large deletions, and repeated copies of the mitochondrial control region (Trifunovic et al., 2004; Vermulst et al., 2008). Vermulst and colleagues suggested that a fourth mtDNA mutation circular in nature with large deletions was present and responsible for driving ageing (Vermulst et al., 2008), but further study has refuted this suggestion (Park and Larsson, 2011). Mutations within PolG are associated with diseases including Progressive External Ophthalmoplegia (PEO), myopathy sensory ataxia, myoclonic epilepsy, and ataxia neuropathy disorders (Young and Copeland, 2016). Increased mtDNA point mutations in mutator mice is suggested to cause respiratory complex instability through amino acid substitution across respiratory chain subunits (Edgar et al., 2009). The development of another mouse model expressing a mutant version of Twinkle, demonstrated accumulating large mtDNA deletions within post mitotic tissues (Tyynismaa et al., 2005). Mutations in Twinkle are associated with PEO and mtDNA depletion syndromes (Goffart et al., 2009). Deletion generation and mtDNA depletion within deleter mice has been attributed to replication stalling (Goffart et al., 2009). Despite these mtDNA deleter mice demonstrating progressing mitochondrial myopathy and respiratory dysfunction they maintain a normal lifespan and ageing phenotype suggesting that mtDNA deletion accumulation may not progress ageing on their own (Tyynismaa et al., 2005). Development of a *Drosophila* mtDNA mutator strain similar to mutator mice which express a proofreading deficient form of PolG, demonstrated significantly increased mtDNA mutation frequency. These mutator flies also demonstrated a shortened lifespan, mitochondrial dysfunction, reduced dopaminergic neurons, and declining locomotor activity (Samstag et al., 2018).

The accelerated ageing phenotype seen in mutator mice has been partially associated with the embryonic dysfunction of somatic stem cells (Ahlqvist et al., 2012). This association established that neural progenitor cells demonstrate both reduced numbers in vivo and reduced self-renewal in vitro. This study by Ahlqvist

and colleagues suggests that mtDNA mutation influences stem cell number and quality and impacts the quiescent state, damaging somatic stem cell maintenance. Collectively, the driving force of premature ageing within mutator mice may be attributed to the early dysfunction of somatic stem cells (Ahlqvist et al., 2012). It should be noted that the treatment of mutator mice with an antioxidant (N-acetyl cysteine) restores neural progenitor cell self-renewal suggesting that redox state holds a role in stem cell function (Ahlqvist et al., 2012). However, mutator mice demonstrate no shift in ROS generation or oxidative modification despite respiratory chain capacity being significantly reduced (Trifunovic et al., 2005). This information contradicts the 'vicious cycle' theory of declining respiratory function causing increasing ROS generation, theoretically increasing mtDNA mutation frequency and further respiratory chain decline. Humble and colleagues generated both $Polg2^{+/-}$ and $Polg2^{-/-}$ knockout mice, finding $Polg2^{+/-}$ to develop normally with no variations in mitochondrial function across two years and $Polg2^{-/-}$ to demonstrate embryonic lethality at approximately day 8 (Humble et al., 2013). This lethality was from the loss of mtDNA and gene products, structural defects including disorganised cristae, and lipid accumulation. This suggests that a single copy of $Polg2$ is required for development and that $Polg2$ is essential for mtDNA replication and mammalian embryogenesis (Humble et al., 2013). Overall the majority of age-associated mutations, polymorphisms, and base substitutions within human mtDNA are transition mutations and are prone to arise from the minor infidelity of the mitochondrial DNA polymerase (Szczepanowska and Trifunovic, 2015). Collectively these studies provide valuable insight into the role of inefficient/ineffective mtDNA replication in accumulating mtDNA damage.

Mitochondrial Heteroplasmy

Mitochondrial heteroplasmy describes the existence of multiple mtDNA variants coexisting within a single cell. ~90% of individuals maintain at least one heteroplasmy with ~20% of individuals maintaining heteroplasmies implicated in disease (Ye et al., 2014). High levels of heteroplasmy tends to demonstrate higher pathogenicity and overrepresentation within disease associated loci. That said, heteroplasmies with

derived allele frequencies over 60% demonstrate reduced pathogenicity suggesting selection against excessive presence of heteroplasmies (Ye et al., 2014). If heteroplasmy for a specific mtDNA mutation is high within younger individuals, then said mutation likely occurred early in development and was clonally expanded to high levels of heteroplasmy (Copeland, 2012). Heteroplasmic mtDNA mutations can potentially be maternally inherited, with the quantity of mutated alleles differing considerable between generations (Zhang et al., 2018).

Due to the separate replication of mtDNA, the distribution of mutations across tissues and cells becomes uneven with age (Durham et al., 2006). The divergence of mtDNA composition explains how minor mtDNA deletion and point mutation levels accumulate within individual cells with age in specific tissues such as skeletal muscle (Fayet et al., 2002), brain (Bender et al., 2006), heart, and colon (Larsson, 2010). The percentage of mtDNA heteroplasmy within a cell and/or tissue will determine if mitochondrial dysfunction occurs. The threshold at which this dysfunction occurs depends entirely on the type, location, and frequency of the mutation with most ranging between 60-90% (Larsson, 2010). As previously described, mtDNA heteroplasmy is known to accumulate in stem cells which contributes to age-related cellular decline in regenerative potential and homeostasis (Ahlqvist et al., 2012). This accumulation is partly attributed to replication error and not solely from oxidative damage as first assumed (Kauppila et al., 2017). Clonal expansion of both de novo and inherited mutations from early life can accumulate without negative selection outside of the germline, which explains the mosaic pattern of respiratory chain dysfunction in ageing tissues (Stewart and Chinnery, 2015).

In the majority of multicellular organisms mtDNA is maternally inherited, with paternal sperm mitochondria being marked with ubiquitin to identify them for later destruction within the embryo (Sutovsky et al., 1999). As animals are subject to maternal inheritance of mtDNA with minimal recombination, it may be assumed that the accumulation of deleterious mutations will progress across generations until mitochondrial functionality is lost. This is loss of functionality is avoided by a concept known as the 'genetic bottleneck' theory, with the exact mechanisms of this theory

widely debated (Johnston et al., 2015; Pitceathly et al., 2012). This concept exploits the random processes within a cell to generate cell to cell variability in heteroplasmy as an organism develops. So an egg cell with some level of heteroplasmy will produce an embryo in which each cell may have different levels of heteroplasmy (Cree et al., 2008). Cell-level selection can then remove cells which possess excessive or more damaging heteroplasmy to stabilise or reduce mutation load across generations. It should be reiterated that mtDNA damage which is transmitted will characterise the offspring if maintained during development (Zhang et al., 2018).

Throughout evolution animal mitochondria has maintained its specialised role in aerobic metabolism despite drastic changes in organism physiology and nuclear genome composition (Boore, 1999). This preservation of mitochondrial function occurs despite the high mutation rate caused by the presence of reactive species, damaging elements, and the inefficiency of mtDNA replication and repair (Neiman and Taylor, 2009). Mutation accumulation experiments using *Drosophila melanogaster* found that over 95% of mutations within protein-coding genes are non-synonymous (Haag-Liautard et al., 2008). The nonsynonymous to synonymous ratio of these mutations however, was found to be 1:5 across the *Drosophila* subgroup, suggesting a strong selection against excessive mutation accumulation (Ballard, 2000). The conservation of mitochondrial function despite these pressures is due to the genetic density of mtDNA, where the mitochondrial proteome must function in its entirety for the mitochondria to work effectively (Madreiter-Sokolowski et al., 2018). Because of this requirement, heteroplasmy which impacts mitochondrial function will be selected against between generations (Zhang et al., 2018). To an extent this nullifies the effects of mutation accumulation on following offspring and ensures that the primary functions of the mitochondria are preserved across generations.

The Role of Mitochondrial DNA Damage in Ageing

Generally, the accumulation of mtDNA damage is associated with cancer, neurological disorders, and hereditary diseases (Schapira, 2012). Increased mtDNA mutation, oxidative phosphorylation, and mitochondrial ROS generation have been identified in tumorigenesis (Lisanti et al., 2011). Leber's Hereditary Optic Neuropathy (LHON) is the most common mtDNA-related disorder, resulting in partial loss of central vision. LHON is often caused by homoplasmic mutations within one of three genes, *ND1*, *ND4*, and *ND6* (Giordano et al., 2011). Damaged mtDNA is known to impair bioenergetics, reduce cellular proliferation and apoptosis, atherosclerosis, and hypercholesterolemia (Schapira, 2012). Increased mtDNA damage can cause defective ATP production and reduced protein expression levels that result in impaired organ function and associated disease (Boczonadi and Horvath, 2014). Within neurodegenerative disorders such as Parkinson's, Alzheimer's, and Amyotrophic Lateral Sclerosis (ALS), mtDNA damage is associated with either causing or amplifying these diseases (Martin, 2012). Within the brain tissue of Alzheimer patients mtDNA was found to possess 10 times the oxidised bases when compared to nuclear DNA, with the level of oxidised bases higher overall (Martin, 2012). Huntington's disease (HD) demonstrates elevated levels of oxidative stress within brain tissues of mice and humans (Mena et al., 2015). Within HD mouse models increased superoxide generation and increased Ca^{2+} loading has been identified in embryonic fibroblasts. This confirmed that the regulation of superoxide generation and mitochondrial Ca^{2+} signalling is altered in HD and that manipulating Ca^{2+} uptake can act as a therapeutic strategy for treating HD (Mena et al., 2015).

Excessive accumulation of mtDNA mutation is often associated with respiratory chain deficiency displayed in a mosaic pattern across tissues, following the known uneven distribution of mtDNA mutation load (Boczonadi and Horvath, 2014). Due to the proximity of mtDNA to the ETC, mtDNA is vulnerable to ROS. As mtDNA is damaged its ability to effectively translate information is reduced, producing dysfunctional respiratory chain components and further contributing to ROS production and mitochondrial functional decline (Kennedy et al., 2013). This functional decline

potentially increases the residence time of electrons at areas where oxygen reduction can take place, increasing ROS production (Correa et al., 2012). However, conflicting studies within model organisms on if mtDNA damage actually increases ROS generation makes a complete conclusion difficult (Nissanka and Moraes, 2018; Trifunovic et al., 2005).

The accumulation of somatic mtDNA mutations with age is well documented and supported by various model organisms. Current evidence however, cannot definitively explain if mtDNA damage is a cause or consequence of ageing (Kauppila et al., 2017). Generally, the accumulation of mtDNA mutations throughout lifespan arises from constant exposure to mtDNA damage and replication error. Since this accumulation characterises the natural progression of ageing, it appears appropriate to define mtDNA mutation accumulation as initially a consequence of ageing and overtime increasingly a potential cause (Sun et al., 2016). Despite evidence supporting the damaging effects of age-related mtDNA mutations, understanding if reducing mtDNA damage load increases lifespan will display a clear association between mtDNA damage and age (Bratic et al., 2015).

Mitochondrial DNA Deletion

Accumulation of Mitochondrial DNA Deletions

The accumulation of mtDNA deletions with age is well documented across various organisms including mice (Tanhauser and Laipis, 1995), rat (VanTuyle et al., 1996), nematode (Melov et al., 1995), human (Melov et al., 1999) and flies (Yui et al., 2003). ~85% of mtDNA deletions occur within the major DNA arc (Pitceathly et al., 2012). Large mtDNA deletions are observed in diseases such as PEO (Lee et al., 2007), Pearson's syndrome, and Kearns-Sayre syndrome (Copeland, 2012). It has been shown that mtDNA deletions account for ~25% of all individuals with mtDNA-related disease (Chinnery et al., 2000). mtDNA deletions are rarely inherited and often occur spontaneously through mtDNA replication error. Excessive mtDNA deletion accumulation is associated with primary nuclear defects in genes required for mtDNA

maintenance and can be inherited in a Mendelian pattern (Suomalainen and Kaukonen, 2001). Data from recent studies suggests that double-stranded DNA breaks (DSB) are central to one mechanism of mtDNA deletion with mtDNA replication error is responsible for another (Lee and Wei, 2007; Nissanka et al., 2019).

mtDNA DSBs can occur through exposure to both exogenous and endogenous agents. It has been established that mtDNA is rapidly degraded following DSB with linear mtDNA present for only 2 hours after the DSB event (Bayona-Bafaluy et al., 2005). A mouse model expressing an inducible mitochondrially targeted restriction endonuclease (PstI), demonstrates DSBs when triggered and deletion of mtDNA in subsequent generations (Fukui and Moraes, 2009). However, recombination was identified between free ends produced by PstI and between one free end and a region close to the D-loop (Fukui and Moraes, 2009). The concept of repair between these free ends has been suggested to occur because of the relaxed three-strand conformation of the D-loop which allows single-strand annealing and recombination (Lee and Clayton, 1998). PolG, MGME1, and Twinkle mouse models demonstrate degradation of linear mtDNA after DSBs. These studies demonstrated that persisting linear mtDNA after DSB cause increased generation of mtDNA rearrangements resulting in mtDNA deletion and depletion (Nissanka et al., 2018). There is an increased presence of recombined mtDNA in PolG, Twinkle, and MGME1 knockdown samples compared to controls exposed to mitochondrial PstI (Peeva et al., 2018). These recombination events following mtDNA DSBs demonstrate a process of mtDNA rearrangement and partial deletion when linear mtDNA is left undegraded by replication machinery. The exact mechanisms of this repair however are not established, given the lack of specific DSB repair machinery including nuclear Rad51 (Zinovkina, 2018).

Most mtDNA deletion occurs through strand displacement during DNA replication, often resulting from mtDNA damage from endogenous and exogenous sources (Nissanka et al., 2019; Yui and Matsuura, 2006). Almost 60% of deletions are flanked by short, directly repeated sequences between 4bp and 13bp in length, named class

1 deletions. 30% of deletions are flanked by imperfect repeats called class 2 deletions, and remaining deletions are flanked by non-repetitive sequences called class 3 deletions (Krishnan et al., 2008). There are two theorised mechanisms of replication slippage which generate mtDNA deletions. The first, slipped-strand replication, occurs through the mispairing of a newly synthesising H-strand and the template strand between repeated single nucleotide sequences or short, directly repeated sequences (Shoffner et al., 1989). Slipped-strand replication requires mtDNA replication machinery to pause and dissociate, displacing the currently replicating H-strand (Viguera et al., 2001). Once displaced a repeating sequence on the newly synthesised strand aligns to a homologous sequence on the template strand at a different position. This misalignment loops out the sequence between these two repeating elements on the template strand (Phillips et al., 2017). The end result is one wild-type and one deleted mtDNA molecule. The second, more recent model called copy-choice recombination, suggests that mtDNA deletion occurs during synthesis of the L-strand (Persson et al., 2019). Here the 3' end of the synthesising L-strand is displaced after passing a sequence of a tandem repeat on the template strand. The L-strand then reanneals to the following repeating sequence on the template strand leading to mtDNA deletion after another round of replication (Persson et al., 2019).

Collectively, mtDNA replication machinery plays an essential role in both synthesising and degrading mtDNA. mtDNA deletions can occur if linear mtDNA is not degraded shortly after DSB and if mtDNA replication machinery is sufficiently stalled during replication. mtDNA damage directly contributes to DSB frequency and replication stalling, influencing mtDNA deletion frequency (Lakshmanan et al., 2018). It should be noted however, that functionally impactful levels of mtDNA deletions are suggested to only accumulate when mutations within the replication machinery are present (Nissanka et al., 2019). Although this suggestion follows a known bias for mtDNA mutation frequency in PolG deficient mice, it is however a broad statement which lacks sufficient direct study to be conclusive.

Impacts of Mitochondrial DNA Deletion

There is a plethora of studies which highlight the role mtDNA deletions have in causing disease, dysfunction, and accelerated ageing within humans and model organisms. The point at which a deletion is first established has been suggested to determine the location and frequency of the deletion as well as the clinical phenotype and affected tissues (Lopez-Gallardo et al., 2009). Individuals harbouring mtDNA deletions tend to exhibit a wide variation in clinical phenotypes dependent on the age of onset and disease severity (Pitceathly et al., 2012). Human males suffering from infertility and subfertility with low sperm motility tend to have a 4977bp mtDNA deletion within sperm cells (Kao et al., 1995). Disruption of the Guided Entry of Tail-anchored protein (GET) system and deletion of Msp1 gene in humans causes the accumulation of Pex15 and Gos1 tail-anchored proteins to the mitochondrial outer membrane (Chen et al., 2014). This accumulation causes severe mitochondrial damage and growth defects including protein loss, mtDNA loss, and damaging mitochondrial morphology (Chen et al., 2014). Large scale deletion of mitochondrial tRNAs increases the likelihood of developing Kearns-Sayre syndrome (KSS) (Yamashita et al., 2008). Human ageing is associated with declining skeletal muscle mass and function known as sarcopenia. Clonal expansion of mtDNA deletions within humans occurs at sites of muscle fibre breakage and are associated with causing sarcopenia (Lakshmanan et al., 2018).

The deletion of *DNM1* required for mitochondrial fission alters cellular redox state, increases H_2O_2 resistance, and extends lifespan in fungal ageing models (Scheckhuber et al., 2007). Homozygous deletion of *CEP89* in humans is associated with complex IV oxidative phosphorylation deficiency, intellectual disability, and multi-systemic issues (van Bon et al., 2013). Knockdown of *CEP89* in *Drosophila* reduces complex IV activity and results in total lethality. *CEP89* was found to play a wider role in synaptic transmission of photoreceptor neurons and organisation of *Drosophila* larval neuromuscular junction (van Bon et al., 2013). *Drosophila simulans* deletion of DTrp85 and DVal86 reduces *COX* activity by 30% in females and 26% in males (Melvin and Ballard, 2011). This deletion causes greater physical activity in

mutant females compared to wild-type, reducing age (Melvin and Ballard, 2011). The deletion of *Drosophila* 'ATPase's Associated with diverse cellular Activities' (AAA) protease (*dYME1L*) exhibited premature ageing, neurodegeneration and locomotor deficiencies that are similar to mitochondrial AAA diseases (Qi et al., 2016). *dYME1L* deleted, aged *Drosophila* demonstrated reduced complex 1 activity, mitochondrial membrane disorganisation, increased ROS generation, and thus increased apoptosis (Qi et al., 2016). Aged primates demonstrate increased DNA damage and reduced mtDNA transcription compared to younger primates (Mao et al., 2012). The development of a D-Galactose-Induced (DGI) ageing rat model demonstrated increased mtDNA deletions within the hippocampus compared to controls with age (Du et al., 2012). DGI models demonstrate damaged mitochondrial structural elements within the hippocampus alongside increased NADPH oxidase (NOX) and uncoupling protein 2 (UCP2) (Du et al., 2012).

The Common Deletion

The 4977bp 'common deletion' is the best described class 1 deletion within human mtDNA, occurring between 8470nt to 13446nt (Wei, 1992). The common deletion is generated through replication error and strand slippage between two 13bp perfect repeats (Samuels et al., 2004). The common deletion results in the partial or total truncation of *cytochrome c oxidase*, the ATPase subunits of F0-F1, and *nicotinamide adenine dinucleotide-coenzymeQ oxidoreductase*, which subsequently impairs mitochondrial capacity in controlling apoptosis (Shen et al., 2016). The loss of several coding regions within the common deletion disables mitochondrial protein synthesis and biogenesis (Figure 1.7) (Yusoff et al., 2019). The major potential effect of the common deletion is total failure of ATP synthesis and thus mitochondrial function (Wei et al., 2001). The common deletion generally accumulates with age and is suggested to be an indication of oxidative stress on mtDNA (Meissner et al., 2008).
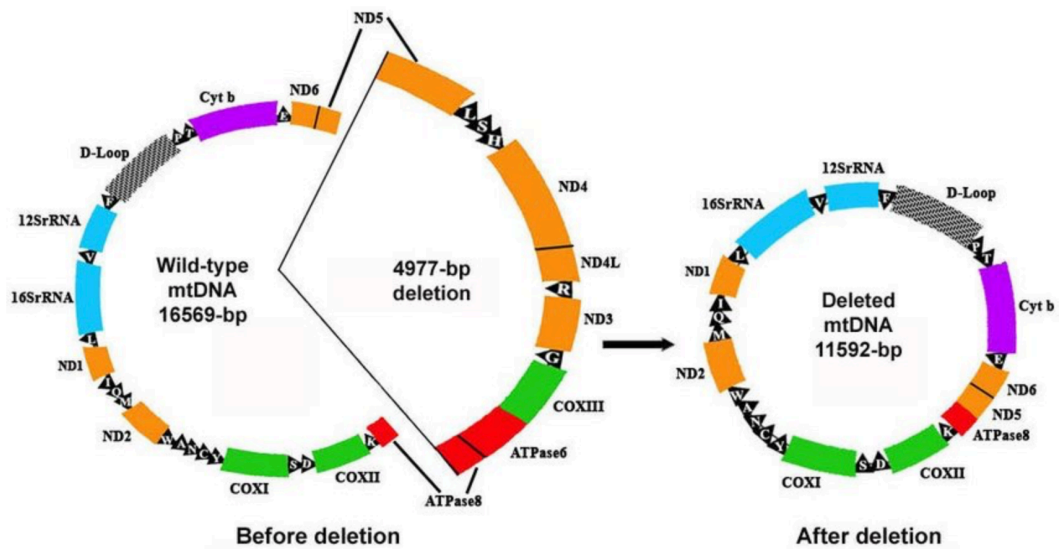
Figure 1.7. The 4977bp common deletion within human mtDNA. This deletion eliminates 5 tRNA genes, 4 complex 1 subunits (ND3, ND4, ND4L, and part of ND5), 1 complex 4 subunit (COX 3), and 2 complex 5 subunits (ATPase6 and part of ATPase8) (Yusoff et al., 2019).

Common deletion frequency is higher in tissues with low mitotic activity and high oxygen demand such as brain, heart, and skeletal muscle (Meissner et al., 2008). Common deletion frequency is described as a biomarker of multiple cancers but various types of carcinoma select against its presence (Nie et al., 2013; Yusoff et al., 2019). Factors including genetic, environmental, lifestyle, and disease have been demonstrated to impact common deletion levels (Iwai et al., 2003; von Wurmb-Schwark et al., 2008; von Wurmb-Schwark et al., 2010). The common deletion has also been identified in Alzheimer's disease (Corraldebrinski et al., 1994), Pearson's syndrome (Wallace et al., 1995), and myopathies (Holt et al., 1989). Decreased levels of common deletion within tumour tissue have been identified when compared to adjacent non-tumour tissues in colorectal cancer (Dani et al., 2004). The common deletion accumulates in all tumour and non-tumour tissues of hepatocellular cancer patients (Yin et al., 2004). Long-term alcohol intake increases common deletion prevalence and reduces mtDNA content (Yin et al., 2004). Increased levels of common deletion within blood leucocytes are associated with higher risk of melanoma through both sun exposure history and pigmentation (Shen et al., 2016).

Since the common deletion is generated through replication stalling and strand slippage, any mtDNA damage which can stall mtDNA replication can influence

common deletion generation (Yusoff et al., 2019). The hypoxic environment of cancerous cells can generate excessive ROS and cause mtDNA damage and genomic instability, providing a partial explanation for common deletion prevalence in some cancerous cells (Jezierska-Drutel et al., 2013). Patients with the common deletion demonstrate varying clinical symptoms and factors which are postulated to contribute to the distribution and load of deleted mitochondrial molecules.

The Role of Mitochondrial DNA Deletions in Ageing

Model organisms are frequently used to study ageing and identify targets for manipulation and intervention. Data on mtDNA deletion within model organisms however, is relatively recent and sparse, with conflicting studies on the natural accumulation of mtDNA deletions within model organisms with age (Ameur et al., 2011; Gruber et al., 2015; Lakshmanan et al., 2018). Mitochondrial Genome Maintenance Exonuclease 1 (MGME1) knockout mice were recently generated which demonstrate deletion, depletion, and duplication of mtDNA similarly to PEO patients (Nicholls et al., 2014). MGME1 mice do not prematurely age like mutator mice which suggests that mtDNA deletion load does not contribute to premature ageing (Nicholls et al., 2014). The accumulation of mtDNA deletions by PstI mice leads to decreased oxidative phosphorylation activity (Fukui and Moraes, 2009). This suggests that mtDNA deletions contribute to an extent, in the age-related dysfunction of oxidative phosphorylation. The age-related accumulation of mtDNA deletions within *COX* genes increases *COX* deficiency, which suggests that this deficiency may contribute to declining oxidative phosphorylation capacity with age (Yu-Wai-Man et al., 2010).

The modelling of mtDNA dynamics in *C. elegans* suggests that animals with shorter lifespans cannot develop significant clonal expansion of mtDNA deletions. Thus clonal expansion of mtDNA deletions requires an organism to have a long enough lifespan for dysfunctional effects to occur and influence the ageing process (Lakshmanan et al., 2018). Within *Drosophila* the age-related accumulation of mtDNA mutations does not heavily influence lifespan or physiology (Kauppila et al.,

2018). Artificially excessive accumulation of mtDNA mutation load will reduce *Drosophila* lifespan but is not representative of natural ageing (Kauppila et al., 2018).

It is well established that mtDNA deletions accumulate in an age-dependent and tissue-specific manner within humans (Kazachkova et al., 2013). Tissue-specific accumulation of mtDNA deletions is often seen in tissues which are exposed to high levels of ROS and thus mtDNA damage (Nissanka and Moraes, 2018). That said, tissue-specific differences are clearly observed between organisms (Guo et al., 2010). The differences in deletion accumulation between these organisms is attributed to extensive cellular and tissue variation (Odom et al., 2007). The type of mtDNA deletion accumulation described is sporadic and accumulates throughout lifespan as a consequence of mtDNA damage and replication error. As a result, the clonal expansion of a deletion within a tissue to a level which causes enough dysfunction to influence ageing is unlikely to occur within normal lifespan (Lakshmanan et al., 2018). For functionally impactful levels of mtDNA deletions to be generated, a deletion must have either been established prior to the genetic bottleneck and clonally expanded during development or rapidly accumulated overtime through mutated replication machinery (Nissanka et al., 2019). Functionally impactful levels of a mtDNA deletion may be established by clonal expansion across a minor subset of cells within a tissue if the deletion is established early enough within a long-lived organism's lifespan (Herbst et al., 2007).

Overall, the natural accumulation of mtDNA deletions with age is a consequence of mtDNA damage and replication error over an extended period of time. Following the mtDNA damage model, accumulating mtDNA deletions throughout a long-lived organism's lifespan will gradually contribute to the overall age-related functional decline of the mitochondria (Bratic and Larsson, 2013). To directly cause early age-related dysfunction and decline mtDNA deletions must be established within early development or within genes required for mtDNA replication and repair (Nissanka et al., 2019).

Detection & Quantification of Mitochondrial DNA Deletions

QPCR is a molecular biology technique which monitors a DNA molecules amplification at regular intervals during a PCR reaction. The key component of a QPCR reaction is a fluorescent dye which allows the detection of a target molecule once excited to a required wavelength. QPCR can detect amplification real time through two methods. The first using non-specific fluorescent dyes which can intercalate with dsDNA and the second using sequence-specific probes where oligonucleotides labelled with a specialised fluorescent reporter allow detection once the probe is bound to its target sequence (Forootan et al., 2017). Sensors within the thermocycler detect the fluorophore in its excited state which subsequently detects the target, allowing the targets rate of generation to be monitored at each cycle. This data can then be used in computational analysis to calculate relative gene expression and target abundance within the sample (Wong and Medrano, 2005). A QPCR reaction can be divided into four phases: linear phase, initial exponential phase, exponential phase, and the plateau phase. The linear phase denotes when the reaction is beginning and the time before target fluorescence surpasses background fluorescence. Reaching early exponential phase is the result of reaction fluorescence increasing to high enough levels to be detectable. This point is often called the cycle threshold (Ct or Cq), more specifically it is the time when the total fluorescence intensity of the reaction surpasses background fluorescence. This Cq value is indicative of the initial copy number of target template and valuable for analysis. Within a reaction the more starting material containing target sequence the faster the fluorescent signal surpasses the threshold for detection, resulting in a lower Cq value (Dang et al., 2016). Once the exponential phase has been reached the PCR reaction has achieved optimal amplification. This results in the quantity of target product doubling with each cycle if reaction conditions are optimal (Rudkjobing et al., 2014). Finally, the plateau phase is reached when one (or all) reaction component(s) begin to impact the PCR reaction, here the reactions value for data analysis is lost (Wong and Medrano, 2005).

Amplification of mtDNA deletions works on the principle that QPCR is optimised for short products of 60-150bp in length (Udvardi et al., 2008). If a primer pair is designed to encompass a region known to harbour deletions, then amplification of sequence in between the two primers will only occur if a deletion is present. Without a deletion the sequence between the two primers will be longer than what standard QPCR reactions can amplify. Thus the amplification data of mtDNA deletions within a sample will theoretically be indicative of the total number of mtDNA molecules harbouring a deletion within the target region. It should be noted that for reliable amplification and accurate quantification of deletions the amplified sequence must be as close to the recommended 60-150bp range. The longer this target sequence is the lower the amplification efficiency will be and in the case of amplifying deletions, the more likely nonspecific amplification will occur (Debode et al., 2017).

Most mtDNA deletions are identified by flanking short direct repeats. Identification of higher levels of mtDNA deletions within one gene or region presents a target for deletion amplification and study (Yui et al., 2003). In order to identify that deletions are not a result of nuclear pseudogenes, flanking repeats of deletions should be identified and matched. With flanking regions identified, primers should be designed to encompass the most amount potential deletion sites within one region. Yui and colleagues identified the age-related accumulation of mtDNA deletions within *Drosophila* was highest between 1866nt to 4737nt (Yui et al., 2003). In 2006 Yui and Matsuura identified that 30 out of 33 identified deletions between 1866nt and 4737nt had flanking or near-flanking repeats, confirming the prevalence of deletion generation within this region of *Drosophila* mtDNA (Yui and Matsuura, 2006).

A control region of mtDNA with known minimal deletion presence should be identified and primers should be designed to encompass this region. A control region with minimal deletion will be the most representative of mtDNA copy number in QPCR (Phillips et al., 2014). Previous mtDNA deletion quantification efforts tend to use the ND1 gene as a control, as it has the lowest deletion frequency in mtDNA (He et al., 2002). The shorter this control region is the lower the number of deletions

spanning this region will likely be and so the more representative of mtDNA copy number it will likely be.

Previous mtDNA deletion quantification studies first established the QPCR reactions efficiency over a range of different template concentrations for both the deletion and control primer pairs (He et al., 2002). In order to perform quantification serial dilutions of a standard template with known concentrations are made, often in 10-fold dilutions. The Cq values from each serial dilution are plotted on a base-10 semi-logarithmic graph (where X = Log concentration and Y = Cq) and fitted to a straight line. If amplification efficiency is 100% for a calibration curve, the slopes value will be 3.32 (Bustin and Huggett, 2017). The Cq of a target sample can then be aligned with this lines equation to determine the starting target quantity. In absolute quantification the amplification efficiency of standard and target samples is assumed to be equal (Svec et al., 2015). Relative quantification does not require the same level of accuracy as absolute quantification, instead relying on an external standard or reference sample (Livak and Schmittgen, 2001). Serial dilutions are still used to construct a calibration curve, the quantity of experimental samples are calculated using the curve, and the samples are expressed relative to the reference sample. The reference sample method establishes a calibrator as 'one fold', so all reactions are compared as an X-fold difference relative to the calibrator (Livak and Schmittgen, 2001). This method is often used when the amplification efficiencies of the target and reference samples are unequal. Relative quantification is easier to perform as the reference sample does not require quantification and exogenous standards are not required (Bustin, 2002). However, normalisation of relative quantification is important in accounting for sample-sample variation in amplification efficiency, identifying target copy number, and to identify any errors including sample loading, reaction composition, and machine error (Bustin et al., 2009). Normalisation against an endogenous control will not work if variation is present in the control, which will obscure target variation and produce artificial variation (Bustin et al., 2009). Comparison of the target Cq values against control Cq values will thus be indicative of the proportion of mtDNA molecules harbouring a deletion in that sample (Bustin et al., 2009).

Experimental Aims

Age-Related Functional Decline

As previously stated, chronological age is not indicative of the functional status of an organism. As a result, ageing research focuses on specific biomarkers which correspond to the biological age of an organism. These biomarkers can differ between organisms but generally can be assayed to monitor the processes underlying ageing (Johnson, 2006). The factors which contribute to the ageing process across different organisms can be divided into nine tentative hallmarks. These hallmarks include; changing intracellular communication, stem cell exhaustion, cellular senescence, mitochondrial dysfunction, deregulated nutrient sensing, loss of proteostasis, epigenetic changes, telomere deterioration, and genomic instability. These hallmarks fit the following criteria to varying degrees; it should occur during normal ageing, its aggravation should accelerate ageing, and its amelioration should alter normal ageing and extend lifespan (Lopez-Otin et al., 2013).

The progressive physiological decline of an organism with age is the key characteristic used to study ageing. This decline is the product of declining tissue and organ function through molecular ageing mechanisms. Within humans, this functional decline is characterised by declining cognitive and physical capacity, reducing quality of life (Santoro et al., 2018). Studying the functional decline of organisms provides insight into the molecular mechanisms of ageing and subsequently improves the treatment of age-related cognitive and physical decline. In model organisms, functional decline is often identified as changes in physical behaviour. Within mice studies the impairment of multiple sensorimotor dependent behaviours including exploration occurs with age (Fahlstrom et al., 2011). *Drosophila* are optimal for studying ageing due to the quantity of behavioural factors influenced by the process. These factors include phototaxis, exploratory walking, negative geotaxis, and fecundity (Grotewiel et al., 2005).

Non-genetic Manipulation of Lifespan

Manipulation of conditions subjected to model organisms has provided insight into how non-genetic factors can influence lifespan. The first demonstration of targeted non-genetic lifespan manipulation was through restricting caloric intake of rats which subsequently extended lifespan (Masoro, 2005). Studies have demonstrated similar effects of caloric restriction in mice, nematodes, and flies. The study of caloric restriction in primates and humans is still ongoing with initial results suggesting similar prolongation of life and forestalling of age-associated disease (Roth and Polotsky, 2012). However, the exact molecular mechanisms of lifespan extension through caloric restriction have not yet been completely established.

The exposure of enough 'stress' to an organism is harmful, yet exposure to minor levels of stress over time extends lifespan in model organisms and cultured human cells (Rattan, 2008). Exposure to low levels of stress enhances an organism's capacity to resist these stresses in larger quantities. This resistance in *Drosophila* is party attributed to heat shock protein induction through minor stresses which reduces mortality rate after minor stresses have ceased (Sarup et al., 2014). Within *Drosophila* studies lifespan and stress response are closely associated, with long-lived populations generally being more stress resistant (Haigis and Yankner, 2010). Common physiological assays used to test *Drosophila* stress response and lifespan include oxidative stress, dietary restriction, temperature shock, and locomotor activity (Sun et al., 2013).

Lifetime reproductive output is used in lifespan studies due to the concept of negative correlation between lifespan and reproductive output (Tatar, 2010). In *Drosophila* studies sterile flies live longer than fertile controls (Barnes et al., 2008) and long-lived mutants have reduced fertility (Flatt, 2011). Arguably the most important lifespan assay in *Drosophila* studies is locomotor activity which can reflect mobility, sleep, cognitive function and circadian rhythm. Generally, locomotor activity declines with age in most species including *Drosophila* (Iliadi and Boulianne,

2010). Key methods of locomotor study in *Drosophila* include negative geotaxis and *Drosophila* Activity Monitoring (DAM) (Sun et al., 2013).

cytochrome c oxidase

COX is a mitochondrially encoded protein complex forming *cytochrome c oxidase*. This complex; also called respiratory complex IV, is the final enzyme of the ETC. As a result, *COX* holds an essential role within oxidative phosphorylation. Within *Drosophila melanogaster* mtDNA, *COX* consists of a 4051bp long sequence coded from 1474nt to 5525nt composed of *COX1*, *COX2*, and *COX3* (including ATP8 and ATP6). Mutations to mtDNA encoding *COX* have been associated with diseases such as colorectal cancers, complex IV deficiencies, Leber's hereditary optic neuropathy (LHON), and acquired idiopathic sideroblastic anaemia (Williams et al., 1999), (Roos et al., 2019), (Suen et al., 2010). Decision to use *COX* as a region for deletion detection within *Drosophila* was made based off Yui and colleagues who detected deletions in approximately 50% of PCR products for the *COX* region (Yui et al., 2003). Their primer pair for this region was also chosen due to previous evidence of success between 1866nt to 4737nt within the mitochondrial genome in both 2003 and 2006 studies (Yui and Matsuura, 2006).

NADH ubiquinone oxidoreductase 1

ND1 is a mitochondrially encoded protein forming one of the subunits of *NADH dehydrogenase*. *NADH dehydrogenase* is located within the inner membrane of the mitochondria and acts as the largest complex of the ETC. Within *Drosophila melanogaster* mtDNA, *ND1* is a 938bp long sequence coded from 11712nt to 12650nt. Mutations to mtDNA encoding *ND1* have been associated with diseases such as LHON, Leigh's syndrome, mitochondrial encephalomyopathy, and lactic acidosis. The *ND1* gene falls into the minor deletion arc; an area known to have few deletions and thus has seen use in quantifying mtDNA copy number (Chen et al., 2017; He et al., 2002). *ND1* has however, been reported to be involved in a deletion encompassing the entire 12S rRNA, 16S rRNA and *ND1* regions and a section of *ND2*

within the mitochondria genome (Harbottle et al., 2004). This human deletion removed any trace of *ND1* rendering the gene useless as a control. Further PCR of the deletion saw 73% of tumour samples carry the deletion (Harbottle et al., 2004). Note that this deletion is present in humans with no direct evidence this same deletion reoccurs within *Drosophila*.

Experimental Aims

In order to further understand the role mtDNA deletions play in the ageing process, an assay which can rapidly amplify and quantify deletions is essential. Rapid generation of mtDNA deletion data across a range of ages and conditions will provide vital insight into what conditions impact deletion generation and if deletion accumulation influences lifespan to any degree.

The current study aimed to develop a QPCR assay to detect and amplify mtDNA deletions using *Drosophila* mtDNA. This assays conditions will be optimised for each primer pair to achieve the best possible amplification efficiency. The region containing *COX1*, *COX2*, and *COX3* genes was selected for assay development due to previous evidence of high deletion frequency (Yui and Matsuura, 2006; Yui et al., 2003). This assay will aim to quantify these deletions using *ND1* as a control. *ND1* was chosen as a control gene for QPCR study due to its presence within the minor deletion arc and previous use in QPCR studies to determine mtDNA copy number (Chen et al., 2017; Grady et al., 2014). The assay will be composed of DNA extraction to generate template and QPCR to detect and amplify mitochondrial deletions. Additional use of agarose gel electrophoresis and purification will be used to identify amplified products and isolate those required for sequencing.

Non-mammalian model organisms compliment mammalian models with key attributes including a relatively cost-effective maintenance, short generation time, and large quantities of offspring per generation (Furda et al., 2012). The use of *Drosophila* allows for rapid processing into usable DNA extracts providing relatively fast deletion detection and amplification across a range of individual organisms. The

study will age the *Drosophila melanogaster* strain White Dahomey (wDah) under varying conditions known to influence lifespan. These conditions include temperature, locomotor activity, reproductive output, and free radical generation (Sun et al., 2013). The effects of these conditions on lifespan will be recorded and their effects on deletion generation may be explored if an assay is successfully developed.

Methods

Drosophila Egg Hatching & Food

In order to produce *Drosophila* for any lifespan experiments, eggs had to be collected from existing stock flies. This was done using old stock bottles which contained large quantities of recently laid eggs. These were kept until hatched and developed, then distributed evenly amongst new bottles and maintained with additional dry yeast at 25°C. At maturity they were then transferred to cages which contained a petri dish of the standard food mix with additional yeast paste (yeast and water). Here they were left in optimal mating conditions; 25°C, covered with a black bin liner with breathing holes, and damp paper towels to maintain humidity. After periodically checking the flies until sufficient eggs had been laid, the flies were gathered and returned to their stock bottles. The petri dishes were gathered and Phosphate Buffered Saline (PBS) was used to wash the eggs into a single falcon tube. The eggs were then mixed thoroughly and ~300 eggs were pipetted into the required bottles. These bottles were then maintained at 25°C until hatched and developed, after which they were then ready for ageing.

Ageing flies were composed solely of white Dahomey, a mass-bred strain derived from flies wild-caught in 1970 from Benin, now made white eyed. *Drosophila* were fed on a ratio of 80g sugar, 80g yeast, and 16g agar, with 30ml Nipagen (10% w/v in ethanol), and 5ml propanoic acid as a preservative, per litre of water. The required volume of water was heated until boiling, then dry ingredients were mixed and added. The temperature was then lowered to a simmer and continuously mixed for

several minutes. The mixture was then cooled in a water bath until it reached ~60°C, preservatives were then added in their required volumes and mixed thoroughly.

Once the food had been cooked and cooled it was distributed into either vials (4ml), sloped vials for cages (12ml), or bottles (40ml) using a peristaltic fluid pump. In order to produce sloped vials, standard vials were stood at a 60-degree angle. The distributed food was then loosely wrapped and left overnight to set, after which each vial/bottle was matched with a bung and stored at 17°C.

Fly Ageing

The goal of subjecting flies to different conditions throughout their lifespan was to assess if any conditions influenced deletion load. Conditions were selected based on controlling body temperature, controlling muscle activity, controlling sexual activity, and influencing intramitochondrial reactive species generation (Paraquat).

Once the new generation of flies were hatched and developed they were sorted based on sex and number into vials or bottles. Unless specified, food vials/bottles were changed every Monday, Wednesday, and Friday, any dead flies were disposed of and recorded if necessary. All flies were frozen at -20°C.

10 vials of 20 male flies were each kept at 25°C and 17°C. Their deaths were recorded each time food vials were changed. 5 flies from each vial were frozen at 60 days old. The final quantity of flies was frozen at 125 days old.

3 cages of 100 male flies were each kept at 25°C and 17°C. Their deaths were recorded each time food vials were changed. 5 flies from each vial were frozen at 60 days old. Remaining flies was frozen at 125 days old.

10 vials of 20 male flies were kept at 25°C for 10 days. After 10 days they were kept at 25°C however each weekday they endured 4.5 hours of gradual shaking (clashing

against the side of the shaker for an average of 30 times per minute). Remaining flies were frozen at 60 days old.

10 vials of 20 virgin males, 10 vials of 20 virgin females, and 20 vials of 20 mixed flies were kept at 25°C. Remaining flies were frozen at 60 days old.

3 bottles of 120 males were kept at 25°C having their food changed every Tuesday and Friday. From 10 days these flies were exposed to food containing 10mM Paraquat (100mg per 40ml). This continued for two weeks until sufficient flies had died to return the flies back to normal food. The remaining flies were unable to be frozen due to rapid death rate.

DNA Extraction

DNA extractions were performed according to the manufacturer's instructions. Homogenisation of flies was performed at 6000g for 10 seconds twice through unless specified. For Invitrogen and Qiagen extraction kits dry homogenisation was used to yield the required tissue, then vortexed briefly with each kit's starting component(s) to retrieve the homogenised tissue. For the Zymo extraction kit homogenisation was an existing part of the protocol. In order to improve total DNA extraction an additional elution step was added as well as incubation periods prior to each elution step of 5 minutes. The eluted DNA was then Nano-dropped to test DNA purity and concentration. All DNA extractions were stored at -20°C. The DNA extraction kits and protocols used are as follows:

Zymo Quick-DNA Tissue/Insect Microprep Kit.
1. Add specimen(s) to a BashingBead^{TM} Lysis Tube (2.0 mm). Add 750μl BashingBead^{TM} Buffer to the tube and cap tightly.
2. Homogenise the required number of specimens at 6000g for ten seconds twice through.
3. Centrifuge the BashingBead^{TM} Lysis Tube (2.0 mm) in a microcentrifuge at ≥10,000g for 1 minute.

4. Transfer up to 400μl supernatant to the Zymo-Spin^{TM} III-F Filter in a Collection Tube and centrifuge at 8,000g for 1 minute. Discard the Zymo-Spin^{TM} III-F Filter.

5. Add 1,200μl of Genomic Lysis Buffer to the filtrate in the Collection Tube from Step 4. Mix well.

6. Transfer 800μl of the mixture from Step 5 to a Zymo-Spin^{TM} IC Column in a collection Tube and centrifuge at 10,000g for 1 minute.

7. Discard the flow through from the Collection Tube and repeat Step 6.

8. Add 200μl DNA Pre-Wash Buffer to the Zymo-Spin^{TM} IC Column in a new Collection Tube and centrifuge at 10,000g for 1 minute.

9. Add 500μl g-DNA Wash Buffer to the Zymo-Spin^{TM} IC Column and centrifuge at 10,000g for 1 minute.

10. Transfer the Zymo-Spin^{TM} IC Column to a clean 1.5ml microcentrifuge tube and add ≥ 20μl (10μl minimum) DNA Elution Buffer directly to the column matrix. Centrifuge at 10,000g for 30 seconds to elute the DNA (In order to improve DNA extraction an additional 5-minute incubation step was added prior to elution).

Invitrogen Purelink Genomic DNA Mini Kit

1. Set a water bath or heat block at 55°C.

2. Homogenise the required number of specimens at 6000g for ten seconds twice through.

3. Add 180μL PureLink® Genomic Digestion Buffer and 20μL Proteinase K (supplied with the kit) to the tube. Ensure the tissue is completely immersed in the buffer mix.

4. Incubate at 55°C with occasional vortexing until lysis is complete (1–4 hours).

5. To remove any particulate materials, centrifuge the lysate at maximum speed for 3 minutes at room temperature. Transfer supernatant to a new, sterile microcentrifuge tube.

6. Add 20μL RNase A (supplied in the kit) to the lysate, mix well by brief vortexing, and incubate at room temperature for 2 minutes.

7. Add 200μL PureLink® Genomic Lysis/Binding Buffer and mix well by vortexing.

8. Add 200μL 96–100% ethanol to the lysate. Mix well by vortexing for 5 seconds.

9. Add the lysate (~640μL) prepared with PureLink® Genomic Lysis/Binding Buffer and ethanol to a PureLink® Spin Column.

10. Centrifuge the column at 10,000g for 1 minute at room temperature.

11. Discard the collection tube and place the spin column into a clean PureLink® Collection Tube supplied with the kit.

12. Add 500μL Wash Buffer 1 prepared with ethanol to the column.

13. Centrifuge column at room temperature at 10,000g for 1 minute.

14. Discard the collection tube and place the spin column into a clean PureLink$^{®}$ collection tube supplied with the kit.

15. Add 500μL Wash Buffer 2 prepared with ethanol to the column.

16. Centrifuge the column at maximum speed for 3 minutes at room temperature. Discard collection tube.

17. Place the spin column in a sterile 1.5-mL microcentrifuge tube.

18. Add 25μL of PureLink$^{®}$ Genomic Elution Buffer to the column.

19. Incubate at room temperature for 1 minute. Centrifuge the column at maximum speed for 1 minute at room temperature (In order to improve DNA extraction an additional 5-minute incubation step was added prior to elution).

Qiagen QIAamp DNA Micro Kit.

1. Homogenise the required number of specimens at 6000g for ten seconds twice through.

2. Immediately add 180μl Buffer ATL, and equilibrate to room temperature (15–25°C).

3. Add 20μl proteinase K and mix by pulse-vortexing for 15s.

4. Place the 1.5ml tube in a thermomixer or heated orbital incubator, and incubate at 56°C for 4-6 hours.

5. Add 200μl Buffer AL, close the lid, and mix by pulse-vortexing for 15s.

6. Add 200μl ethanol (96–100%), close the lid, and mix thoroughly by pulse-vortexing for 15s. Incubate for 5 min at room temperature (15–25°C).

7. Briefly centrifuge the 1.5ml tube to remove drops from inside the lid.

8. Carefully transfer the entire lysate from step 7 to the QIAamp MinElute column (in a 2ml collection tube) without wetting the rim. Close the lid, and centrifuge at 6000g (8000 rpm) for 1 min. Place the QIAamp MinElute column in a clean 2ml collection tube, and discard the collection tube containing the flow-through.

9. Carefully open the QIAamp MinElute column and add 500µl Buffer AW1 without wetting the rim. Close the lid, and centrifuge at 6000g (8000 rpm) for 1 min. Place the QIAamp MinElute column in a clean 2ml collection tube, and discard the collection tube containing the flow-through.

10. Carefully open the QIAamp MinElute column and add 500µl Buffer AW2 without wetting the rim. Close the lid, and centrifuge at 6000g (8000 rpm) for 1 min. Place the QIAamp MinElute column in a clean 2ml collection tube, and discard the collection tube containing the flow-through.

11. Centrifuge at full speed for 3 min to dry the membrane completely.

12. Place the QIAamp MinElute column in a clean 1.5ml microcentrifuge tube and discard the collection tube containing the flow-through. Carefully open the lid of the QIAamp MinElute column and apply 20–100µl Buffer AE or distilled water to the centre of the membrane.

13. Close the lid and incubate at room temperature (15–25°C) for 1 min. Centrifuge at full speed for 1 min (In order to improve DNA extraction an additional 5-minute incubation step was added prior to elution).

A finalised extraction protocol was devised using the Zymo kit which optimised DNA yield and purity with the tools and reagents available:

Optimised Zymo Quick-DNA Tissue/Insect Microprep Kit.
1. Add specimen(s) to a BashingBead^{TM} Lysis Tube (2.0 mm). Add 750µl BashingBead^{TM} Buffer to the tube and cap tightly.

2. Homogenise the required number of specimens at 6000g for ten seconds four times through.

3. Add 1,200μl of Genomic Lysis Buffer to the filtrate in the BashingBead™ Lysis Tube (2.0 mm). Mix well and incubate in a shaking apparatus at room temperature for 15 minutes.

4. Centrifuge the BashingBead™ Lysis Tube (2.0 mm) in a microcentrifuge at maximum speed for 1 minute twice through.

5. Transfer 800μl of the mixture from Step 4 to a Zymo-Spin™ IC Column in a collection Tube and centrifuge at 10,000g for 1 minute. Take care not to agitate the pellet.

6. Discard the flow through from the Collection Tube and repeat Step 5.

7. Add 200μl DNA Pre-Wash Buffer to the Zymo-Spin™ IC Column in a new Collection Tube and centrifuge at 10,000g for 1 minute.

8. Add 500μl g-DNA Wash Buffer to the Zymo-Spin™ IC Column and centrifuge at 10,000g for 1 minute.

9. Transfer the Zymo-Spin™ IC Column to a clean 1.5ml microcentrifuge tube and add 20μl DNA Elution Buffer for single flies or 50μl for multiple flies directly to the column matrix. Incubate at room temperature for 15 minutes in a shaking apparatus. Centrifuge at 10,000g for 30 seconds to elute the DNA.

Primers

Primer Title	Primer Structure (5' - 3')	Tm (Degrees)	GC Content
ND1 Forward	CCTTCAGCAAAATCAAAAGGAGTC	65.8	41.6
ND1 Reverse	ATAGTAGCTGGTTGGTCGTCT	59.3	47.6
Yui Forward	GCTGGAATTGCTCATGGTGGA	69.4	52.3
Yui Reverse	AGGGTGATTTGAGTGTGTAGAC	59.6	45.4
Yui Extended Forward	GGAATTGCTCATGGTGGAGCT	67.5	52.3
Yui Extended Reverse	GTGATTTGAGTGTGTAGACATT	55.6	36.3
Alternative Deletion Forward	CAGGAATTTCTTCAATTTTAGGAGC	72.0	36.0
Alternative Deletion Reverse	AAGATTGAATTATAGCTACAGCTGA	66.0	32.0
New Deletion Forward	CCGCTGGAATTGCTCATGGTGG	74.5	59.0
New Deletion Reverse	AGCTCCGATAGCTCCTGTTAATGGT	67.6	48.0
Optimal Deletion Forward	CTGTTTATCCACCTCTATCCGCT	68.0	47.8

Table 2.1. All primers were produced by Sigma-Aldrich at 100μM. All primers were stored at -20°C. Dilutions of each primer of 1 in 10 were made from stock primer solutions using sterile water. Diluted primer solutions were stored separately from stock primers at -20°C and were used for all QPCR reactions.

ND1 Primer Pair:
5' CCTTCAGCAAAATCAAAAGGAGTC <——216bp——> AGACGACCAACCAGCTACTAT 3'
3' GGAAGTCGTTTTAGTTTTCCTCAG   TCTGCTGGTTGGTCGATGATA 5'

           12063nt^   ^12279nt

Yui Primer Pair:
5' GCTGGAATTGCTCATGGTGGA <——2851bp ——> GTCTACACACTCAAATCACCCT 3'
3' CGACCTTAACGAGTACCACCT   CAGATGTGTGAGTTTAGTGGGA 5'

           1887nt^   ^4738nt

Yui Extended Primer Pair:
5' GGAATTGCTCATGGTGGAGCT <——2851bp——> AATGTCTACACACTCAAATCAC 3'
3' CCTTAACGAGTACCACCTCGA   TTACAGATGTGTGAGTTTAGTG 5'

           1890nt^   ^4741nt

Alternative Deletion Primer Pair:
5' CAGGAATTTCTTCAATTTTAGGAGC <——2716bp——> TCAGCTGTAGCTATAATTCAATCTT 3'
3' GTCCTTAAAGAAGTTAAAATCCTCG   AGTCGACATCGATATTAAGTTAGAA 5'

           1949nt^   ^4665nt

New Deletion Primer Pair:
5' CCGCTGGAATTGCTCATGGTGG <——2902bp——> ACCATTAACAGGAGCTATCGGAGCT 3'
3' GGCGACCTTAACGAGTACCACC   TGGTAATTGTCCTCGATAGCCTCGA 5'

           1886nt^   ^4788nt

Optimal Deletion Primer Pair:
5' CTGTTTATCCACCTCTATCCGCT <——2919bp——> ACCATTAACAGGAGCTATCGGAGCT 3'
3' GACAAATAGGTGGAGATAGGCGA   TGGTAATTGTCCTCGATAGCCTCGA 5'

           1869nt^   ^4788nt

Figure 2.2. Positions of each major mitochondrial primer pair listed in table 2.1 with primers shown in red. ND1 primer pair: forward position 12040nt-12063nt, reverse position 12279nt-12299nt. Yui primer pair: forward position 1867nt-1887nt, reverse position 4738nt-4759nt. Yui extended primer pair: forward position 1870nt-1890nt, reverse position 4741nt-4762nt. Alternative Deletion primer pair: forward 1925nt-1949nt, reverse position 4665nt-4689nt. New Deletion primer pair: forward position 1865nt-1886nt, reverse position 4788nt-4810nt. Optimal Deletion primer pair: forward position 1847nt-1869nt, reverse position 4788nt-4810nt.

QPCR

All QPCRs were performed using the Bio-Rad CFX96 Touch Real-Time PCR Detection System. All QPCRs were performed using SYBR mixes specified within figure legends. All QPCR conditions are specified within figure legends. All QPCR master mixes and reactions were set up on ice.

For Powerup (ThermoFisher/Applied Biosystems Powerup SYBR Green Master Mix (2x)) and Bio-Rad (BioRad SYBR Green Master Mix (2x)) QPCRs each master mix was made at a ratio of; SYBR (5µl at starting concentration of master mix), Forward Primer (1µl), Reverse Primer (1µl), Sterilised Water (2µl), and Template (1µl at concentration of extract) per 10µl reaction. All master mixes were pulse vortexed prior to pipetting.

Once all the reactions had been dispensed into a 96-well plate, the plate was sealed with a plastic film and pulse centrifuged up to 500g. The reactions were then transferred into the CFX96 Touch Real-Time PCR Detection System and programmed with a single initial 3:00 95°C denaturation step, then a repeating 30s 95°C denaturation step, varying annealing steps and reaction cycles (stated under each QPCR figure), and a 4°C 'holding' step once the reaction had finished until retrieved. Powerup reactions required an additional initial 50°C step for 120 seconds. All reaction conditions were set up taking into consideration manufacturers recommendations.

Agarose Gel Separation & Imaging

All agarose gels were made at 2% using 1x TBE at 60ml. To the gel 3μl of ThermoFisher SYBR Gold Nucleic Acid Gel Stain was added and mixed until dissolved. 1x TBE buffer was made by mixing; Tris Base 12.11g (1M), Boric Acid 6.18g (1M), EDTA 0.74g (0.02M) and made up to 1L with MilliQ water at pH 7. Gels were set in a 60ml mould with an 8 lane comb. Once the gel set it was transferred to a gel tank and submerged in 1x TBE. 5μl of 50-1500bp ladder (PCR Biosystems) and up to 30μl of all samples at a ratio of 5:1 of sample to PCR Biosystems 6x loading dye were then pipetted into their requisite wells. If necessary, samples were exposed to a speed vacuum to reduce their volume prior to the addition of loading dye.

All gels unless specified were ran at 90v for 60 minutes or until sufficient separation had occurred. Gels were viewed using both a fluorescent blue light and BioRad EcitaBlue Viewing Goggles. Images of the gels were taken using an overlaid BioRad EcitaBlue Viewing Goggle lens.

DNA Purification from Agarose Gel

Once a gel had been imaged any DNA bands requiring further examination were purified. DNA bands were excised using a surgical scalpel and EcitaBlue Viewing Goggles over a fluorescent blue light. Once a band was excised it was placed in a

preweighed Eppendorf ready for purification. The ThermoFisher GeneJET Gel Extraction Kit was used for all DNA purification and was followed to the manufacturer's instructions and recommendations. Eluted DNA was stored at -20°C.

Sequencing

Purified DNA bands that were to be used for sequencing reactions were first measured for purity and concentration. Sequencing reactions were performed by Source Bioscience and required reactions were set up according to their recommendations. If necessary, samples were exposed to a speed vacuum to reduce their overall volume.

Results

I aimed to quantify mtDNA deletions in single *Drosophila*, by first ageing *Drosophila* over a range of conditions in order to generate a large number of samples for DNA extraction. Total DNA extraction of *Drosophila* was performed to generate mtDNA template for subsequent QPCR experiments. QPCR was used to amplify both mtDNA deletions and a control region. Using data from the QPCR experiments both deletion and control reactions were optimised to improve amplification efficiency and replicability between repeats. Using this optimisation, an assessment of if accurate quantification of mtDNA deletions is viable from single *Drosophila* using the current assay was performed.

Drosophila Lifespan Data

Once *Drosophila* were aged for their required periods, they were processed and frozen at -20°C. The first set of *Drosophila* to be processed were aged in cages and vials at both 25°C and 17°C. Throughout ageing each death in cages and vials was recorded when their food was changed. After rapid deaths in the 25°C caged flies between days 14 to 21 (figure 3.1) the remaining healthy flies were frozen at day 35. At 60 days old 15 flies from each 17°C cage and 5 flies from each 25°C and 17°C vial

were frozen for DNA extraction. The remaining flies were left to age further until day 125 when all remaining flies from both cages and vials were frozen.
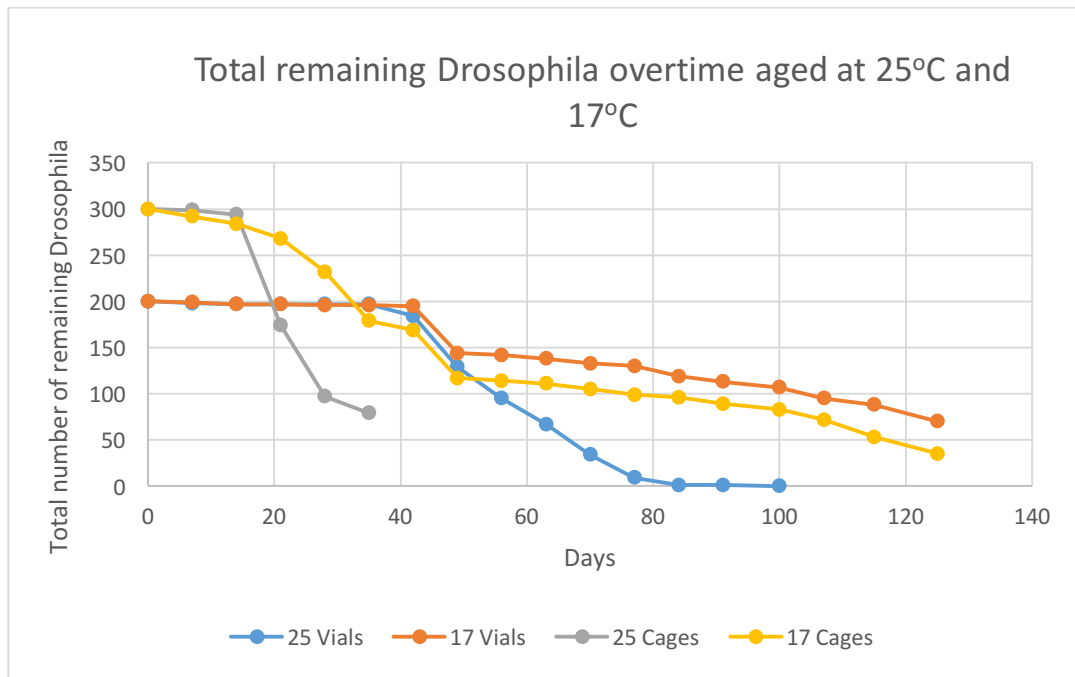
Figure 3.1. *Drosophila* **in cages and vials at 25°C and 17°C.**

The second set of *Drosophila* to be aged were virgin males, virgin females, mixed mated, and virgin males under shaking conditions (4.5 hours of gradual shaking 5 days per week, clashing against the side of the shaker for an average of 30 times per minute), all in vials at 25°C. At 60 days the remaining flies from all experimental conditions were processed and frozen. The average deaths per 20-fly vial after 60 days were then calculated across all experimental conditions: Virgin Males (13), Virgin Females (13.5), Mixed Mated (12.7), Shaker Virgin Males (11.4).

DNA Extraction

Comparing DNA Extraction Kits

Initial DNA extractions were performed using the Zymo Quick-DNA Tissue/Insect Microprep Kit and the Invitrogen Purelink Genomic DNA Kit. Comparison between these kits was used to determine which extraction kit produced the best extract for deletion amplification (Tables 3.2 and 3.3):

Extract	260/280	260/230	Concentration (ng/µl)
Zymo Young 1	1.46	0.01	1.00
Zymo Young 2	1.73	0.20	2.10
Zymo Young 3	1.80	0.01	3.30
Zymo Old 1	1.54	-0.01	0.30
Zymo Old 2	1.84	0.02	1.90
Zymo Old 3	2.08	0.01	1.80

Table 3.2. DNA extractions using the Zymo extraction kit. Young flies were aged at 25°C for 10 days, old flies at 25°C for 60 days.

Extract	260/280	260/230	Concentration (ng/µl)
Invitrogen Young 1	1.87	0.59	5.60
Invitrogen Young 2	2.02	0.47	2.50
Invitrogen Young 3	2.09	1.35	2.90
Invitrogen Old 1	1.80	1.15	2.80
Invitrogen Old 2	2.47	0.89	1.90
Invitrogen Old 3	2.47	0.52	1.80

Table 3.3. DNA extractions using the Invitrogen extraction kit. Young flies were aged at 25°C for 10 days, old flies at 25°C for 60 days.

Template generated from both extraction kits was tested using QPCR with the Yui primer pair. Template extracted by the Invitrogen kit failed to generate amplification in every reaction and so the Zymo extraction kit was selected for further use. After consistently low DNA yields when using the Zymo extraction kit, further study into other commercial DNA extraction kits aimed to identify which manufacturer would likely yield the highest quality and quantity per extraction. Overall, Qiagen extraction kits generally yield higher DNA quality and quantity over manufacturers such as Invitrogen and Genpoint (Persson et al., 2011). Template generated from Qiagen extraction kits also produce low levels of PCR inhibition (Stangegaard et al., 2013). From the information gathered the Qiagen QIAamp DNA Micro Kit was selected for further DNA extraction to try and increase the DNA yield per extract. Initial DNA extractions using the Qiagen kit produced more yield than the Zymo kit (Table 3.4):

Extract	260/280	260/230	Concentration (ng/μl)
Young 1	2.35	1.20	37.00
Young 2	1.94	0.57	32.10
Young 3	2.43	0.71	15.90
Young 4	1.95	0.64	12.00
Young 5	2.85	0.54	6.80
Old 1	2.18	0.52	8.30
Old 2	2.09	0.46	6.40
Old 3	2.39	0.56	11.30
Old 4	1.91	0.69	17.20
Old 5	2.29	0.50	10.00

Table 3.4. DNA extractions using the Qiagen extraction kit. Young flies were aged at 25°C for 10 days, old flies at 25°C for 60 days.

Qiagen Extraction Kit Contamination

Continued use of the Qiagen extraction kit generated higher yields per extract compared to Zymo extracts, which appeared to reduce the average Cq variability of triplicate reactions. This may have been due to the use of proteinase K over Guanidinium Thiocyanate to degrade proteins during extraction, where the Invitrogen kit also generated higher yields over the Zymo kit. However, higher yields using the Qiagen kit may be due to the quality of the protocol and kit components rather than one specific element. After initial success using the Qiagen kit, QPCR replicability began to deteriorate. Once this deterioration occurred each QPCR reaction component was replaced in turn in an attempt to identify the issue. This included new sterile MilliQ water, SYBR Green, primer dilutions, thermocyclers, extractions, and additional caution when preparing QPCR reactions. All changes produced no solution to the issue. After no positive impact was seen the Qiagen extraction kit was tested to see if contamination had occurred. If one of the extraction kits components had become contaminated, then the DNA extracted may be damaged. The concentrations of Qiagen extractions which produced poor replicability appeared to still yield similar quantity and quality of template. Further Qiagen extractions were performed taking additional care to avoid the possibility of shearing or damaging the template during the extraction process. Template from four Qiagen extractions were then run on an agarose gel to test for DNA presence (figure 3.5):
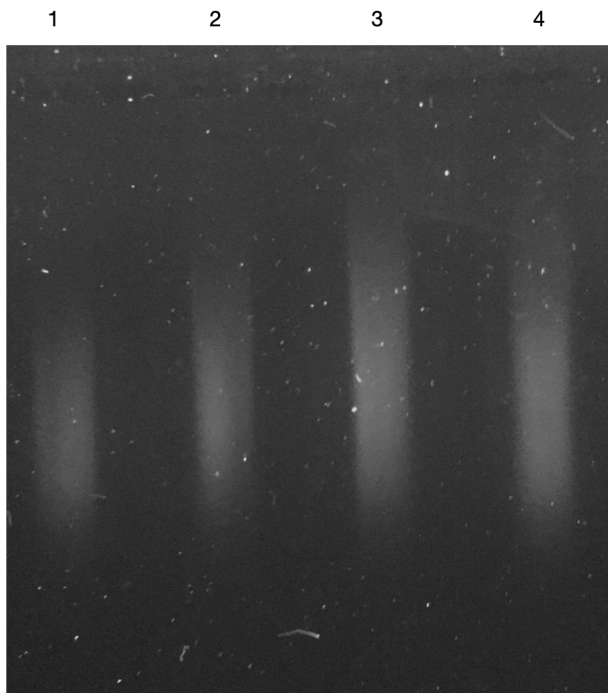
Figure 3.5. Agarose gel image of Qiagen DNA extractions. Gel was made at 2% using 1x TBE and run at 90V for 60 minutes.

All four Qiagen extractions run on the gel showed no evidence of intact DNA, instead showing a faint smear of what could be either RNA or fragmented DNA. The same extracts (20μL) were then incubated with 2μL of RNAse A (10mg/ml, Invitrogen) for 3 hours at 60°C to identify if these smears were the result of RNA. These extracts were then run on an agarose gel to see if the smear in figure 3.5 was RNA (figure 3.6).
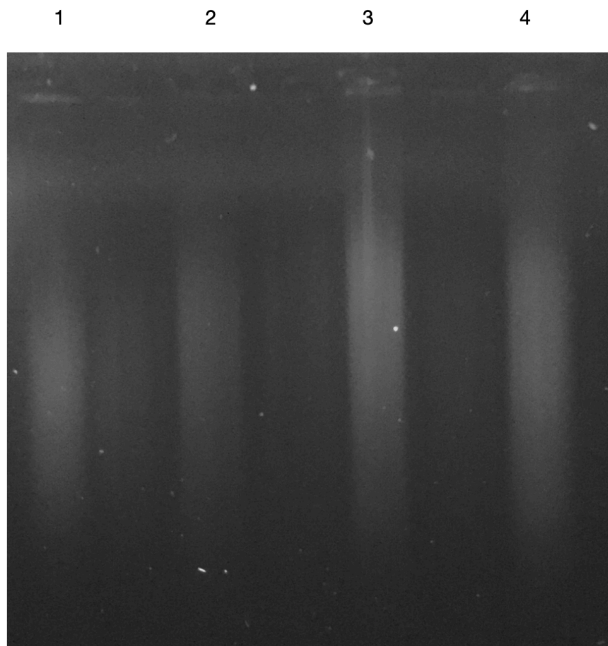
Figure 3.6. Agarose gel image of Qiagen DNA extractions after RNAse A treatment. Gel was made at 2% using 1x TBE and run at 90V for 60 minutes.

RNAse treatment appeared to have some impact in reducing the brightness of the smear, suggesting at least some of each smear was RNA. The remaining smear suggests that the DNA extracted had been degraded by a nuclease present in the Qiagen kit. As a result, an aliquot of each component of the Qiagen kit was heated at 60°C for six hours in an attempt to deactivate the nuclease. The following DNA extraction using these heated components produced no difference in the smear seen in figures 3.5 and 3.6. A further attempt to deactivate the nuclease by heating aliquots of each of the Qiagen kits components at 80°C for seven days produced no difference again, still producing a similar smear to figures 3.5 and 3.6. Because the specific component(s) harbouring the nuclease cannot be determined without replacing each component in turn and attempting DNA extraction, the Qiagen kit was ignored for further DNA extraction.

Optimisation of the Zymo Extraction Kit

Following the contamination of the Qiagen kit the Zymo kit was used for further DNA extraction. As the Zymo kit produces extractions with relatively low concentrations and 260/230 values (table 3.2), the protocol was optimised in an attempt to increase the DNA yield per extract. Optimisation mainly entailed increasing the duration of

homogenisation and the exposure of each homogenate to the lysis buffer in order to extract more DNA from each *Drosophila*. The optimised protocol (as stated in the methods) yields higher concentrations on average over the original Zymo protocol (table 3.7):

Extract	260/280	260/230	Conc (ng/µl)
Shaker 1	4.50	0.02	2.90
Shaker 2	2.63	0.12	1.80
Shaker 3	2.43	0.03	1.60
Shaker 4	1.83	0.20	3.80
Young 1	1.97	0.04	1.50
Young 2	1.95	0.09	4.90
Young 3	1.88	0.02	3.20
Young 4	4.83	0.04	1.40
Mixed 1	2.08	0.48	4.10
Mixed 2	4.06	0.09	7.40
Mixed 3	2.32	0.32	3.70
Mixed 4	1.95	0.02	2.80
Old 1	1.63	0.09	3.00
Old 2	1.21	0.02	4.60
Old 3	2.07	0.05	4.70
Old 4	2.48	0.02	1.90
25ºC 1	1.29	0.02	3.40
25ºC 2	1.24	0.02	3.50
17ºC 1	2.56	0.03	2.20
17ºC 2	1.54	0.01	2.10

Table 3.7. DNA extractions using the optimised Zymo extraction kit. All shaker flies were aged at 25°C for 60 days. All young flies were aged at 25°C for 10 days. All mixed flies (male) were aged at 25°C for 60 days. All old flies were aged at 17°C for 125 days. All 25°C flies (male) were aged for 60 days. All 17°C flies (male) were aged for 60 days. Experimental differences between all flies is described in the methods.

ND1 Primer Pair

The *ND1* primer pair was designed using primer blast as a control for mtDNA deletion quantification. From 5' to 3': Forward = CCTTCAGCAAAATCAAAAGGAGTC, Reverse = ATAGTAGCTGGTTGGTCGTCT. The *ND1* product is 260bp in length from 12030nt to 12290nt in mtDNA. The *ND1* primers were trialled across several temperature gradients and single temperature QPCRs, from 68°C to 57°C. Both gradient and single temperature QPCRs were trialled using 60s and 30s annealing steps. The *ND1* primers were used with template extracted using the Qiagen and Zymo extraction

kits. The quality of *ND1* amplification did not differ across the temperatures tested (68°C-57°C) and so an annealing temperature of 64°C was chosen for further amplification.

Optimisation of *ND1* Amplification

The *ND1* primer pair was initially tested using both BioRad and Powerup SYBR green with the same three templates extracted using the original Zymo kit (figures 3.8 – 3.11):

Figure 3.8. BioRad SYBR green QPCR amplification data of ND1 Primers. QPCR annealing temperature was set at 64°C for 30s for 50 cycles. Reactions used three single 60 day old Zymo extracts.

Figure 3.9. BioRad SYBR green QPCR melt peak data of ND1 Primers. QPCR annealing temperature was set at 64°C for 30s for 50 cycles. Reactions used three single 60 day old Zymo extracts.
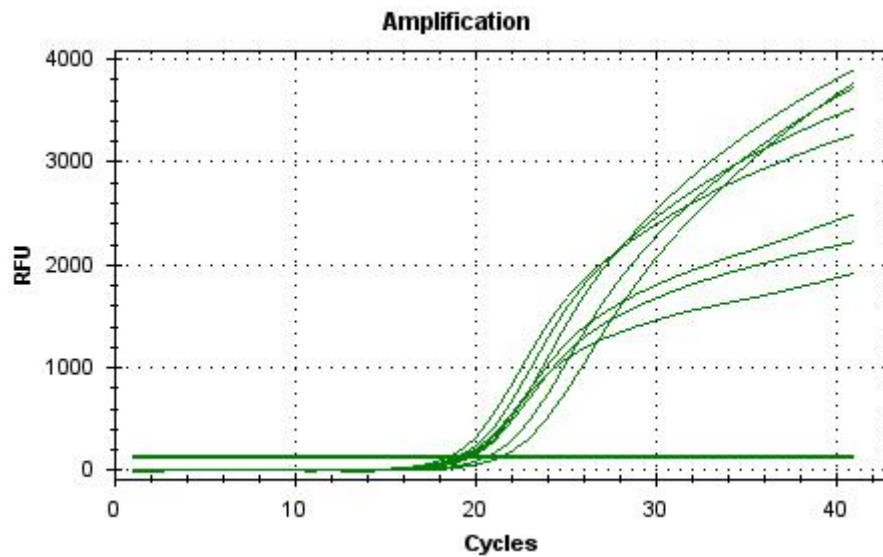
Figure 3.10. Powerup SYBR green QPCR amplification data of ND1 primer. QPCR annealing temperature was set at 64°C for 30s for 40 cycles. Reactions used three single 60 day old Zymo extracts.
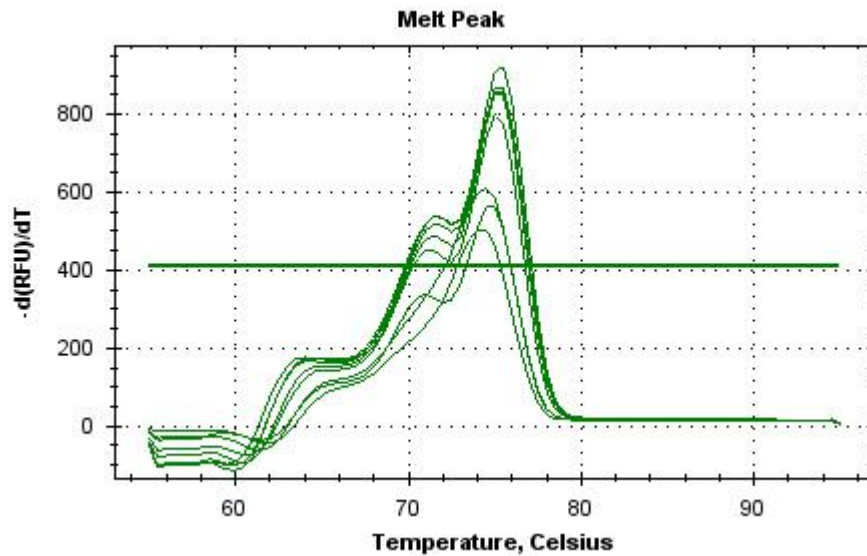
Figure 3.11. Powerup SYBR green QPCR melt peak data of ND1 primer. QPCR annealing temperature was set at 64°C for 30s for 40 cycles. Reactions used three single 60 day old Zymo extracts.

BioRad produced more similar Cq values and total working reactions when compared to Powerup, and Powerup appeared to have produced more than one product, seen as two melt peaks in figure 3.11. Because Powerup failed to produce amplification in every reaction and BioRad produced less Cq variation overall, BioRad was chosen as the optimal SYBR green for control amplification.

Following the optimisation of the Zymo extraction protocol, further testing of the *ND1* primer pair was done using three extracts from the optimised protocol (figures 3.12 and 3.13):
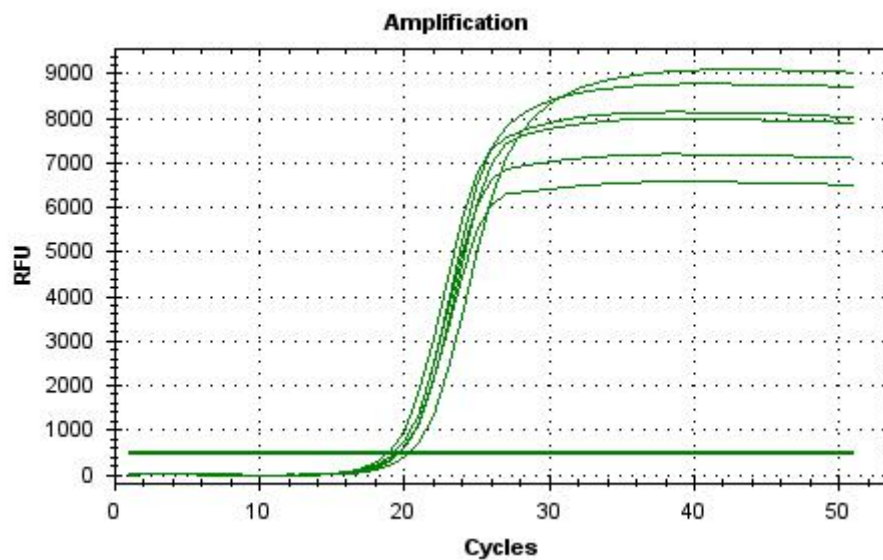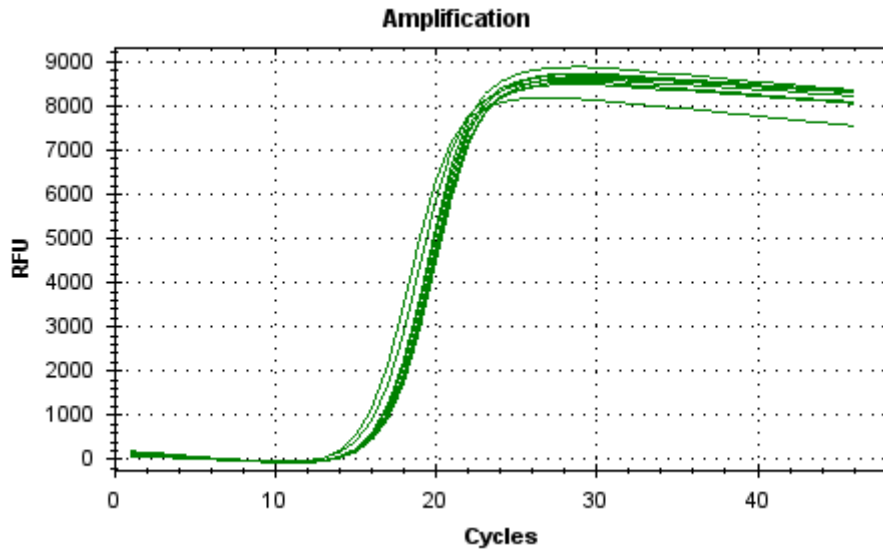
Figure 3.12. BioRad SYBR green QPCR amplification data of ND1 primers. QPCR annealing temperature was set at 64°C for 60s for 45 cycles. Reactions used three single 60 day old Zymo extracts.
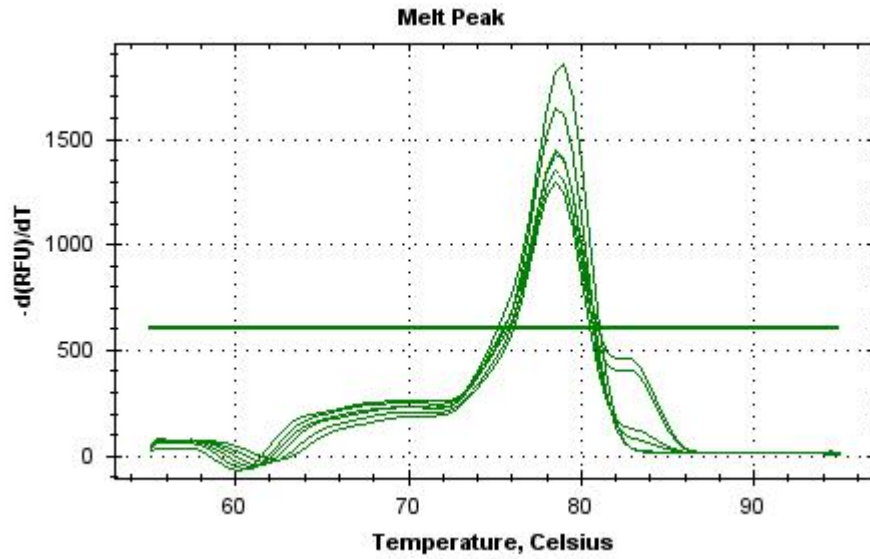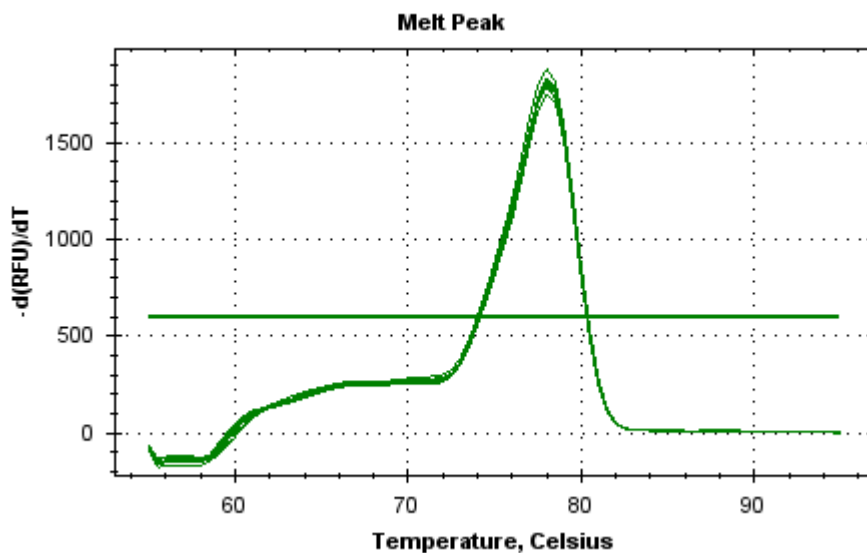

Figure 3.13. BioRad SYBR green QPCR melt peak data of ND1 primers. QPCR annealing temperature was set at 64°C for 60s for 45 cycles. Reactions used three single 60 day old Zymo extracts.

Compared to the amplification data in figure 3.8, figure 3.12 shows that the average Cq values have reduced by ~4 cycles when extending annealing time to 60s and using a more concentrated template. A 4 cycle reduction is equivalent to 16 times more template, however this likely indicates both more template and less inhibition. This is expected as the lower a Cq value of a reaction is the higher the initial target copy number within the sample. The similarities in melt peak height seen in figure 3.13 suggests that the optimised extract generates similar levels of mtDNA per extraction when compared to the original Zymo protocol (figure 3.9). No further attempts were

made to improve control amplification efficiency until reliable amplification of mtDNA deletions was established.

Yui Primer Pair

The first primer pair used to attempt to amplify mtDNA deletions was the same primer pair used by *Yui & Matsuura*, named Yui for reference (Yui and Matsuura, 2006). This primer pair was used with the goal of amplifying mtDNA deletions between 1866nt to 4737nt. From 5' to 3'; Forward = GCTGGAATTGCTCATGGTGGA, Reverse = AGGGTGATTTGAGTGTGTAGAC. The Yui primers were trialled across several temperature gradients and single temperature QPCRs, from 68°C to 57°C. Both gradient and single temperature QPCRs were trialled using 60s annealing steps. The Yui primers were used with template extracted using the Zymo extraction kit.

Optimisation of Yui Amplification

Initial QPCR attempts using the Yui primers were performed to gain understanding of which annealing temperature range produced the most optimal amplification. At this stage we simply expected amplified products to be deletions rather than off-target amplification. Multiple gradient QPCRs using the Yui primers were used to narrow the optimal annealing temperature range down to between 61.5^{o}C to 57°C. A final gradient QPCR between 61.5-57°C was done to try and identify which exact annealing temperature was optimal (figure 3.14 and 3.15):
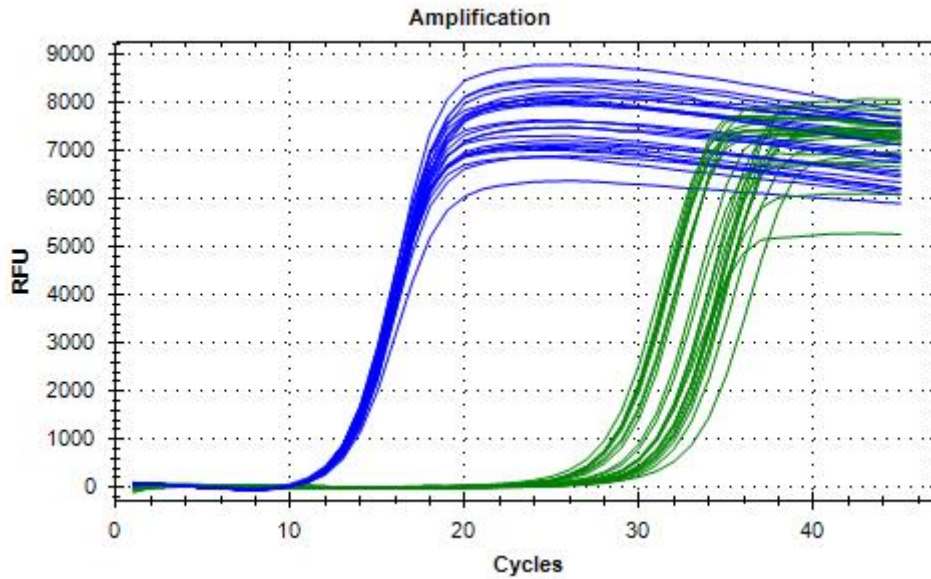
Figure 3.14. BioRad SYBR green QPCR amplification data of control (ND1 - blue) and deleted (Yui - green) mitochondrial DNA. Annealing temperature was set across a gradient of 61.5-57°C for 60s for 44 cycles. Reactions used a single 20 fly Zymo extract as template.
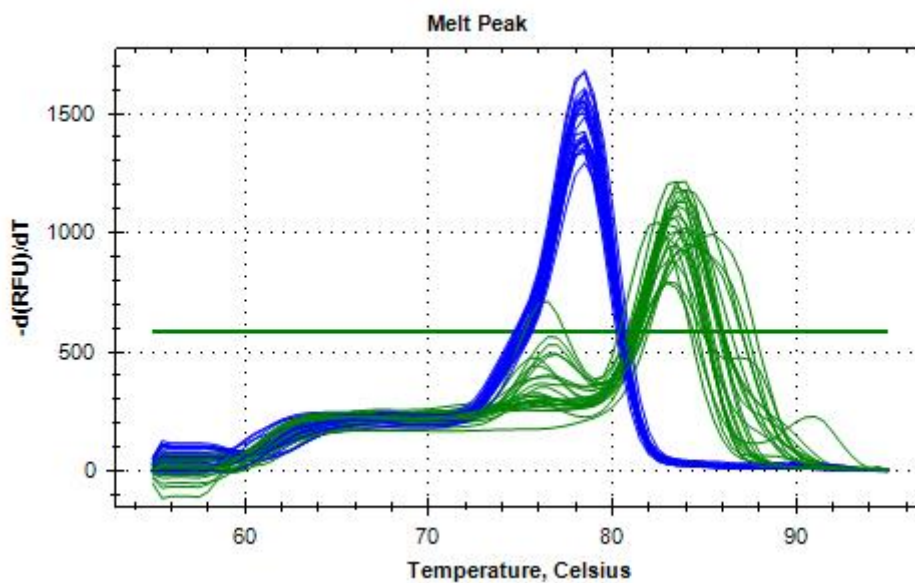
Figure 3.15. BioRad SYBR green QPCR melt peak data of control (ND1 - blue) and deleted (Yui - green) mitochondrial DNA. Annealing temperature was set across a gradient of 61.5-57°C for 60s for 44 cycles. Reactions used a single 20 fly Zymo extract as template.

There was no identifiable difference between 61.5°C and 57°C in Cq values (ranging from 33.84 to 25.94) or melt peak heights. This was because triplicate reactions were relatively dissimilar. Referring to figure 3.15, there appeared to be two separate products in most of the Yui reactions identified by two separate melt peaks. The minor green melt peak recorded at a lower temperature (74-78°C) was detected across the temperature range in most reactions in lower concentrations, with no

preference for annealing temperature. The low melting temperature of the minor product suggests that it could be a primer dimer, potentially resulting from excess primer being present in the reaction. The major second peak (81-86°C) appeared in every reaction in much higher concentrations.

Identification of the Yui Product

Following consistent amplification using the Yui primers across different extracts, all having relatively similar Cq values and melting temperatures, the decision was made to isolate and sequence the products amplified. So triplicates from the QPCR reaction corresponding to figures 3.14 and 3.15 were run on an agarose gel (figure 3.16):
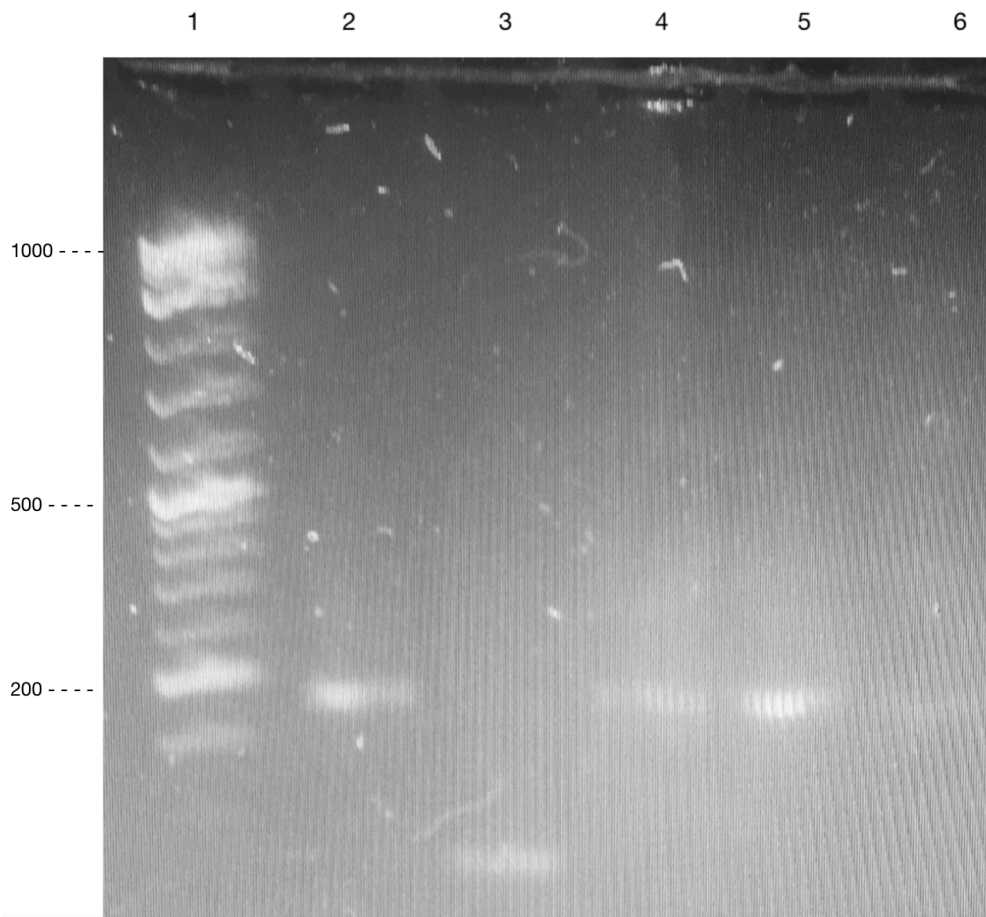
Figure 3.16. QPCR samples from figures 3.14/3.15. Reactions used a single 20 fly Zymo extract as template. Lane1 = 1kb Ladder, Lane2 = 61.5^{o}C Yui triplicate, Lane3 = 61.5^{o}C ND1 triplicate, Lane4 = 60°C Yui triplicate, Lane5 = 58.5^{o}C Yui triplicate, Lane6 = 57°C Yui triplicate. Gel was made at 2% using 1x TBE and run at 90V for 60 minutes.

Despite the detection of two products in figure 3.15, only a single band was identified on the gel. This single band was assumed to be the most abundant product. Due to the lower melting temperature and concentration of the minor product, it may have been either too short a product or not concentrated enough to be identified on agarose gel. The single band in lane 2 seen in figure 3.16 was excised, purified, and sent for sequencing.

The quality of the resulting sequence was poor with many bases being unidentifiable. As a result, the identity of each base was called individually using the sequencing data. Several base pairs either side of this product were unidentifiable and not included. The sequence of the isolated product was found to correspond similarly to a section of chromosome 2R from 19594485nt to 19594781nt, not mitochondrial DNA. High specificity blast search of the primers yields the *Drosophila* mitochondrial genome consistently; from 1867-1887nt to 4638-4759nt. Low specificity blast search of the primers does yield chromosomal mispriming, including chromosome 2R in multiple areas. Following this, the surrounding forward and reverse sequence of the misprimed product were analysed for any similarities to any combination of the Yui primer pair (figures 3.17 and 3.18):

GGTCGGACTCCACGCCCCATCATGACCTGCTGCGTAATATGAAACGCTTTCAGCAGATTAAC
CATTTTCCAGGCATGGTGGAGATATGCCGCAAGGATCTGCTGTCAAGAAATTTGAATCGCAT
GCTCAAAATGTTTCCCGGCGACTATCGCATATTCCCCAAAACCTGGCTAATGCCAACCGAGT
GAGTTTTCTTATTTTTGAAATTTGTCATAAATTCAGCTAAAAATATAATATAATAACCATTATT
TTCTGTCAGTGCCTACGATGTAGCCATTTATGCGAACAAACACAAGCGCACTTTTATCCTAAA
GCCTTATTCGGCGGGCCAAGGACGTGGCATCTGGATAACCACCGATCTTCGCACTGTGGGC
AAACGGGAGAAGCTCATCTGCCAAACTTACATAGAACGGGTAAGTCTGGAGAATGATACTA
ACGATCTATATGATCAACAATTTTCCCATTTGTAGCCCCTACTTATAGATGGCTA
CAAGTTT

Figure 3.17. A section of forward sequence from *Drosophila* chromosome 2R. Highlighted yellow is the exact sequence that the Yui product matches to, from 19594485nt to 19594781nt. Highlighted red is the exact match to the 3' end of the Yui forward primer indicating the likely mispriming site which generated the product. Sequence generated from reactions which used the Yui primer pair and a single 20 fly Zymo extract as a template.

AAACT**TGTAG**CCATCTATAAGTAGGGGCTACAAATGGGAAAATTGTTGATCATATAGATCGT
TA<mark>GTATCATTCTCCAGACTTACCCGTTCTATGTAAGTTTGGCAGATGAGCTTCTCCCGTTTGC</mark>
<mark>CCACAGTGCGAAGATCGGTGGTTATCCAGATGCCACGTCCTTGGCCCGCCGAATAAGGCTTT</mark>
<mark>AGGATAAAAGTGCGCTTGTGTTTGTTCGCATAAATGGCTACATCGTAGGCACTGACAGAAA</mark>
<mark>ATAATGGTTATTATATTATATTTTTAGCTGAATTTATGACAAATTTCAAAAATAAGAAAACTC</mark>
<mark>ACTCGGTTGGCATTAGCCAGGTTTTGGGGAATATGCGATAGTCGCCGGGAAACATTTTGAG</mark>
<mark>CATGCGATTCAAATTTCTTGACAGC</mark>AGATCCTTGCGGCATATCTCCACCATGCCTGGAAAAT
GGTTAATCTGCTGAAAGCGTTTCATATTACGCAGCAGGTCATGATGGGGCGTGGAGTCCGA
CC

Figure 3.18. A section of reverse sequence from *Drosophila* chromosome 2R. Highlighted yellow is the exact sequence that the Yui product matches to, from 19594485nt to 19594781nt. Highlighted red is the exact match to the 3' end of the Yui reverse primer indicating the likely mispriming site which generated the product. Sequence generated from reactions which used the Yui primer pair and a single 20 fly Zymo extract as a template.

Nine bases which match the final nine bases of the forward primer were identified close to the start of the misprimed product (figure 3.17). Six bases which match the final seven bases of the reverse primer were identified close to the end of the misprimed product (figure 3.18). The similarity between the 3' ends of both forward and reverse primers and the likely mispriming sites either side of the nonspecific product confirms the likelihood of the Yui primers mispriming to amplify the chromosomal sequence. As previous QPCR attempts using the Yui primer pair with different extracts and conditions generated almost identical Cq values and melt peaks, it was assumed to an extent that mispriming had occurred consistently throughout. Because the Yui primer pair has such a high potential for mispriming and failed to produce evidence of deleted sequence, this primer pair was ignored for further deletion amplification attempts.

Yui Extended Primer Pair

Due to the Yui primers possessing strong 3' mispriming the decision was made to extend each primer at the 3' end by 3 bases and shorten each primer at the 5' end by 3 bases. This was done with the goal of reducing/eliminating consistent nonspecific amplification, to strengthen mitochondrial binding, and to maintain most of the primer used by *Yui and Matsuura* (Yui and Matsuura, 2006). This primer pair was named Yui Extended. From 5' to 3': Forward = GGAATTGCTCATGGTGGAGCT, Reverse

= GTGATTTGAGTGTGTGTAGACATT. The Yui Extended primers were subject to annealing temperatures ranging from 68°C to 57°C in both gradient and single temperature QPCRs. Both gradient and single temperature QPCRs used annealing steps of 30s. The Yui extended primers were used with template extracted using the Qiagen and Zymo extraction kits.

Initial Mitochondrial Deletion Amplification

Due to previous issues with mispriming, attempts to optimise amplification efficiency would not be attempted until deletion amplification was achieved. Initial QPCRs using the Yui Extended primers were based on finding an optimal temperature for the reaction (figures 3.19 and 3.20):
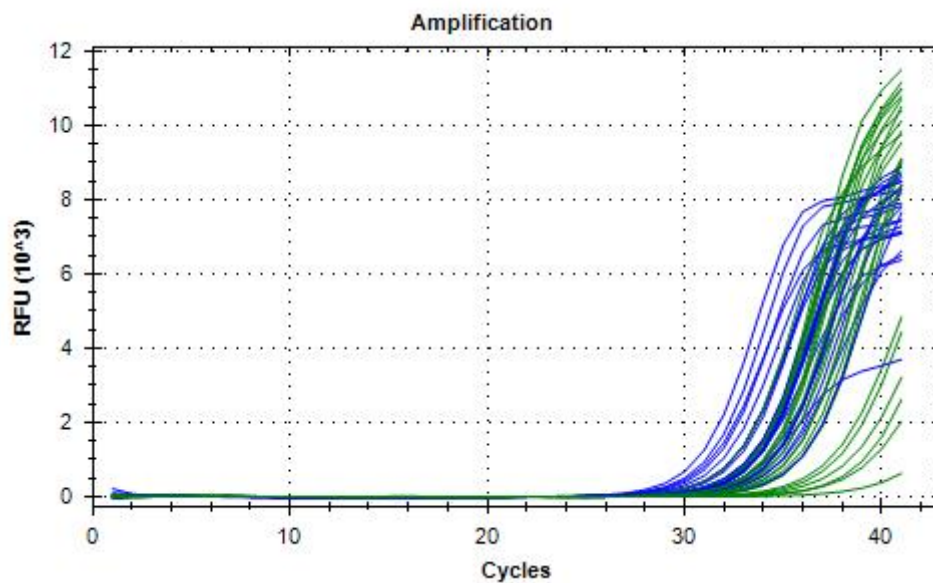
Figure 3.19. BioRad SYBR green QPCR amplification data of young (blue) and old (green) DNA. Annealing temperature was set across a gradient of 68-57°C for 30s for 40 cycles. Reactions used one young (10 days old) and one old (60 days old) Qiagen extraction.

Figure 3.20. BioRad SYBR green QPCR melt peak data of young (blue) and old (green) DNA. Annealing temperature was set across a gradient of 68-57°C for 30s for 40 cycles. Reactions used one young (10 days old) and one old (60 days old) Qiagen extraction.

The lowest Cq values and variation between Cq values was seen at 64°C, suggesting further QPCR attempts using these primers should be performed at this annealing temperature. The young extract (Young 1 from table 3.4) produced lower Cq values compared to the old extract (Old 4 from table 3.4), suggesting whatever was amplified was more abundant in the younger extract, likely due to the higher template concentration. If the primers were successful in amplifying mtDNA deletions, then more mtDNA deletions within the target region were present in the younger extract which is the opposite of what is expected. High Cq values using both extracts suggest whatever was amplified was present in a small concentration. Figure 3.20 shows consistent amplification of a one product (74-78°C) with random amplification of another product (82-87°C) in much smaller quantities, mainly in younger extracts. An agarose gel was run using product from 68-62.5^{o}C old fly reactions which amplified the major product between (74-78°C) to identify the origin of this amplification (figure 3.21):

Figure 3.21. QPCR samples from figures 3.19/3.20. Reactions used the Yui Extended primer pair and a single old fly (60 days) Qiagen extract as template. Lane1 = 50-500bp ladder, Lane 2 = 68-62.5^{o}C reactions from figures 3.19/3.20. Gel was made at 2% using 1x TBE and run at 90V for 60 minutes. Highlighted in the black box is the smear excised for sequencing.

When ran on agarose gel a smear was seen up to the bulk of the product. The bulk of the smear (highlighted in figure 3.21) was excised, purified, and sent for sequencing. The sequence retrieved was relatively clean, however some of the bases were called individually using the sequencing data. When blast searched the sequence yielded two separate mitochondrial hits between the two primers used, one close to each primer. This suggests that the short sequence amplified between the two primers is the sequence remaining after a deletion had occurred (. Using the end of each sequence as breakpoints of a potential deletion, the surrounding sequence was analysed for evidence of direct repeats (figure 3.22):

CCT**TTATTTGTTTG** (ATCAGTAGTTATTACT…AATC**TTAT**G**TGTTTG**) CTGTATTAA
     2025 < - - - - - - - - - - - - - - - - 2673bp - - - - - - - - - - - - - - - > 4698

Figure 3.22. Evidence of two direct repeats likely causing the deletion of mitochondrial sequence. Underlined are the direct repeats. In bold are all bases that identically match. Enclosed in brackets is the 2673bp deleted mitochondrial sequence from 2025nt to 4698nt. Sequence generated from reactions which used the Yui Extended primer pair and a single old fly (60 days) Qiagen extract as template.

Figure 3.22 shows the flanking direct repeats likely to have caused the deletion. Enclosed in brackets is the deleted mitochondrial sequence between the two

amplified products from 2025nt to 4968nt. This provided sufficient evidence for mitochondrial deletion amplification without major nonspecific amplification. Further amplification attempts would be focused on optimising amplification efficiency using the Yui Extended primers.

Yui Extended Nonspecific Amplification

Following the initial success of the Yui Extended primers, repeated attempts failed to generate mitochondrial amplification without additional nonspecific amplification. Successful deletion amplification with the two extracts used in figures 3.19 and 3.20 (Young 1 and Old 4 from figure 3.4), was partially associated with higher template concentration and thus higher mtDNA deletions levels within each extract. After several QPCR reactions producing additional nonspecific amplification a hot start QPCR was used to try and reduce nonspecific amplification (figures 3.23 and 3.24):
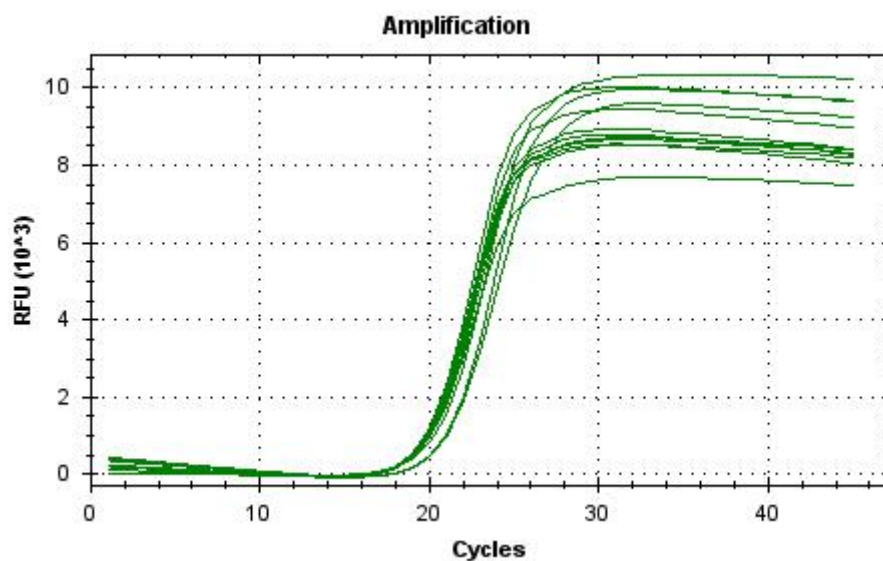
Figure 3.23. BioRad SYBR green QPCR amplification data of Yui Extended primers. QPCR annealing temperature was set at 64°C for 30s for 40 cycles with a hot start of 72°C for 20s. Reactions used one 60 day old Qiagen extraction.
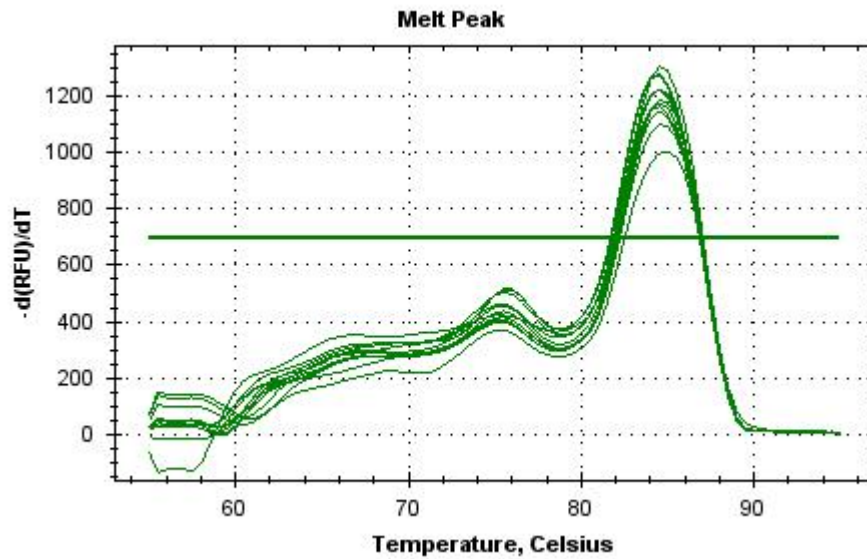
Figure 3.24. BioRad SYBR green QPCR melt peak data of Yui Extended primers. QPCR annealing temperature was set at 64°C for 30s for 40 cycles with a hot start of 72°C for 20s. Reactions used one 60 day old Qiagen extraction.

The low Cq values seen in figure 3.23 compared to the higher Cq values in figure 3.19 indicate that whatever major product was amplified in the hot start QPCR was in significantly higher abundance than in the previously successful QPCR (figure 3.19). As a mtDNA deletion within the target region is assumed to be rare, the resulting Cq value for an amplified deletion would be high. As the Cq values for the hot start QPCR were so high, it was assumed that whatever was amplified was unlikely to be a mtDNA deletion. The minor melt peak around 76°C seen in figure 3.24 is similar to the deletion amplified in figure 3.20, but in much smaller quantities. The major melt peak between 84-85°C in figure 3.24, seen sporadically and in low concentrations in figure 3.20, was likely the same sized product consistently amplified in all other Yui Extended QPCR attempts. As all reactions amplified equally, several reactions were run on agarose gel to identify what products were being amplified (figure 3.25):
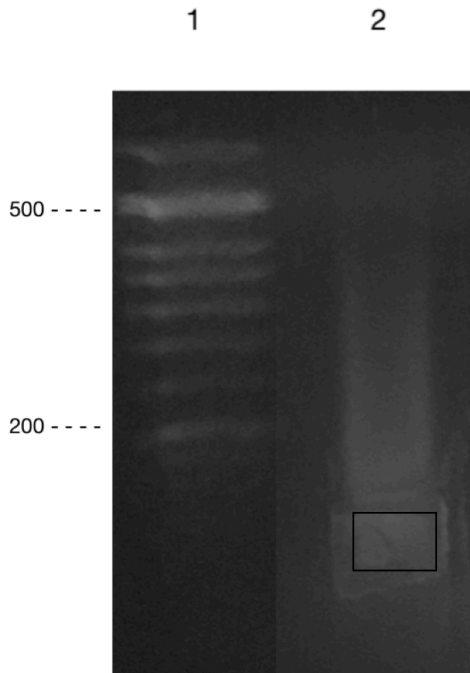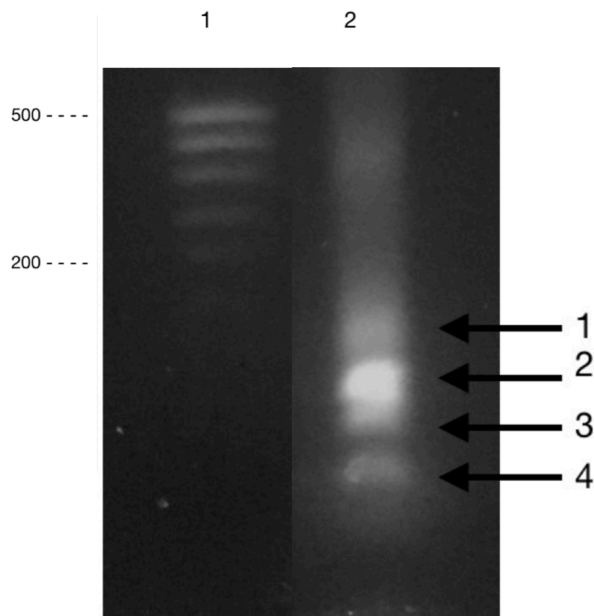
Figure 3.25. QPCR samples from figures 3.23/3.24. Reactions used the Yui Extended primer pair and a single old fly (60 days) Qiagen extract as a template. Lane1 = 50-500bp ladder, Lane2 = Triplicate from figures 3.23/3.24. Gel was made at 2% using 1x TBE and run at 90V for 60 minutes.

The sequencing retrieved for all four bands was generally poor, with many bases called individually using the sequencing data. Of the four products isolated on the gel, band 1 was identified as mitochondrial. The sequencing from this band only identified sequence close to the forward primer, with no identifiable sequence close to the reverse. This was assumed to be because of poor sequencing quality, resulting from the small quantity of product isolated from the gel. The identifiable sequence was analysed for presence of a direct repeat which may have caused the deletion of mtDNA, finding 'ATTAAT' close to the end of the product. Analysis of sequence close to the reverse primer identified an 'ATTAAT' sequence which was the closest match to the direct repeat potentially responsible for the amplified deletion (figure 3.26). Although target amplification will only occur if a deletion is present, the poor quality of sequencing meant the accurate identification of direct repeats was not possible. Figure 3.26 presents the likely pair of direct repeats responsible for causing the deletion amplified, but this cannot be confirmed without the whole sequence:

ACTGTA**ATTAAT** (ATACGATCACAACA…GTAA**ATTAAT**) GTCTACACA

   1978 < - - - - - - - - - - - - 2758bp - - - - - - - - - - - > 4736

Figure 3.26. Evidence of two direct repeats likely causing the deletion of mitochondrial sequence. Underlined are the direct repeats. In bold are all bases that identically match. Enclosed in brackets is the 2758bp deleted mitochondrial sequence from 1978nt to 4736nt. Sequence generated from reactions which used the Yui Extended primer pair and a single old fly (60 days) Qiagen extract as a template.

The three other bands isolated in figure 3.25 when blast searched were all found to correspond to areas of chromosome 3R. Of the three bands, band 2 was clearly the most abundant.

AGATGATACGTGGCCAGCAGAATAAGTCCAAAGTCCAAGCACTAACTGGTGGATCCAATCA
ATCGGAGGATCACAGCC<mark style="background:red">TGGT</mark>CA<mark style="background:red">AGCT</mark>GATCAACCAGAT<mark style="background:yellow">GATTATGGAGTTCCTCGATTGG</mark>
<mark style="background:yellow">TTCGGCTACAAGCACACCATGGAAACATTTCGCATGGAGACGGGTGAAAACGTGGCCAATC</mark>
<mark style="background:yellow">GCAGGGAGATGGAACAAAGTCTACACA</mark>TCACACCCGAGTCAAAGGATTTTCCGCTCCTGGC
TCAACTAGTTATGCGCGATTGGAAGTTCGGTGTGCAAAAAGGAGGTTCCAAAAAGTTGGTT
CAGCT

Figure 3.27. A section of forward sequence from *Drosophila* chromosome 3R. Highlighted yellow is the exact nonspecific sequence that the Yui Extended product matches to, from 15780137nt to 15780246nt. Highlighted red are the bases matching the forward primer indicating the likely mispriming site. Sequence generated from reactions which used the Yui Extended primer pair and a single old fly (60 days) Qiagen extract as a template.

AGCTGAACCAACTTTTTGGAACCTCCTTTTTGCACACCGAACTTCCAATCGCGCATAACTAGT
TGAGCCAGGAGCGGAAAATCCTTTGACTC<mark style="background:red">G</mark>G<mark style="background:red">GTGT</mark>GA<mark style="background:yellow">TGTGTAGACTTTGTTCCATCTCCCT</mark>
<mark style="background:yellow">GCGATTGGCCACGTTTTCACCCGTCTCCATGCGAAATGTTTCCATGGTGTGCTTGTAGCCGA</mark>
<mark style="background:yellow">ACCAATCGAGGAACTCCATAATC</mark>ATCTGGTTGATCAGCTTGACCAGGCTGTGATCCTCCGAT
TGATTGGATCCACCAGTTAGTGCTTGGACTTTGGACTTATTCTGCTGGCCACGTATCATCT

Figure 3.28. A section of reverse sequence from *Drosophila* chromosome 3R. Highlighted yellow is the exact nonspecific sequence that the Yui Extended product matches to, from 15780137nt to 15780246nt. Highlighted red are the bases matching the reverse primer indicating the likely mispriming site. Sequence generated from reactions which used the Yui Extended primer pair and a single old fly (60 days) Qiagen extract as a template.

The sequence of band 2 was found to correspond to a section of chromosome 3R from 15780137nt to 15780246nt. Following this, the surrounding forward and reverse sequence of the nonspecific product were analysed for any similarities to any combination of the Yui Extended primer pair to identify potential mispriming sites (figures 3.27 and 3.28). Figure 3.27 highlights in red, the 8 matching bases to the 3' end of the Yui Extended forward primer. Figure 3.28 highlights in red, the 5 matching bases to the middle of the Yui Extended reverse primer. Together this demonstrates the most likely mispriming sites causing nonspecific amplification. Note that the

quality of the sequencing was generally poor, so several unidentified bases at either end of the product were not presence when

As target amplification is still present in minor quantities, this suggests that nonspecific amplification is outcompeting deletion amplification for reaction components. The fewer target deletions there are within a template the later exponential amplification is achieved (Rudkjobing et al., 2014). With the QPCR reaction components unsaturated for a longer period of time, nonspecific amplification is more likely to occur. So when using the Yui Extended primer pair, sufficient target deletions must be present within a reaction for deletion amplification without nonspecific amplification to occur. Because accurate amplification and quantification requires a highly specific primer pair, the Yui Extended primers are not viable for mtDNA deletion amplification or quantification (Bustin and Huggett, 2017). From this conclusion, the Yui Extended primer pairs were ignored for further deletion amplification attempts.

Alternative Deletion Primer Pair

Further primer design was done with the goal of using different areas of the *COX* region to allow further flexibility in primer Tm, length, and location. New primer design was focused on reducing/eliminating the likelihood of mispriming. This was achieved by using primer blast to search for sequences similar to that of the newly designed primers where mispriming may occur. If two mismatched sites were within relatively close proximity ($\leq$300bp between the potential mispriming sites), then depending on the strength of mispriming the primer pair was ignored. The first primer pair designed was called Alternative Deletion. From 5' to 3': Forward = CAGGAATTTCTTCAATTTTAGGAGC, Reverse = AAGATTGAATTATAGCTACAGCTGA. The Alternative Deletion primers were subjected to annealing temperatures ranging from 68°C to 57°C in both gradient and single temperature QPCRs. Both gradient and single temperature QPCRs used annealing steps of 30s. The Alternative Deletion primers were used with template extracted using the Qiagen and Zymo extraction kits.

Initial Amplification Attempts

Gradient QPCR attempts using the Alternative Deletion primers failed to generate any amplification. Single temperature QPCRs also failed to generate any amplification. A final attempt at amplification was done using a hot start QPCR (figures 3.29 and 3.30):

Figure 3.29. BioRad SYBR green QPCR amplification data of Alternative Deletion primers. QPCR annealing temperature was set at 64°C for 30s for 40 cycles with a hot start of 72°C for 20s. Reactions used one 60 day old Qiagen extraction.
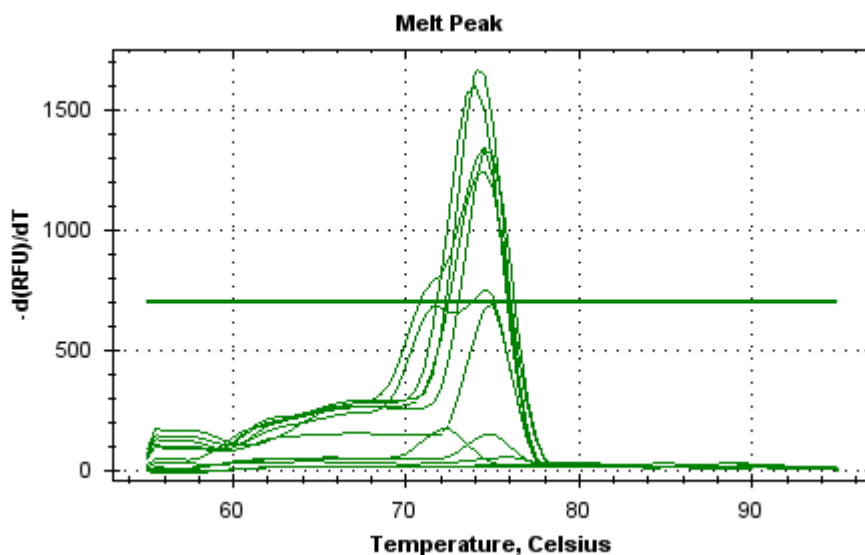
Figure 3.30. BioRad SYBR green QPCR melt peak data of Alternative Deletion primers. QPCR annealing temperature was set at 64°C for 30s for 40 cycles with a hot start of 72°C for 20s. Reactions used one 60 day old Qiagen extraction.

The amplification identified in figures 3.29 and 3.30 occurred in each reaction with very high Cq and low melt peak values. When ran on agarose gel no DNA band was seen, suggesting the product amplified was either smaller than the 50bp band of the ladder and run off the gel or was too small in concentration to be identified on the gel (the more likely explanation). From the lack of an identified DNA band, the low melting temperature of the product, and the high Cq values this amplification was assumed to be the result of primer dimers. At this stage in the project the Qiagen kit became contaminated as described previously. The DNA extraction method was then switched back to the Zymo kit.

Further Amplification Attempts

Attempts to repeat the results of the previous QPCR using Zymo extracts failed. The only Alternative Deletion QPCR which produced any amplification was when the cycle number was extended to 50 (figures 3.31 and 3.32):
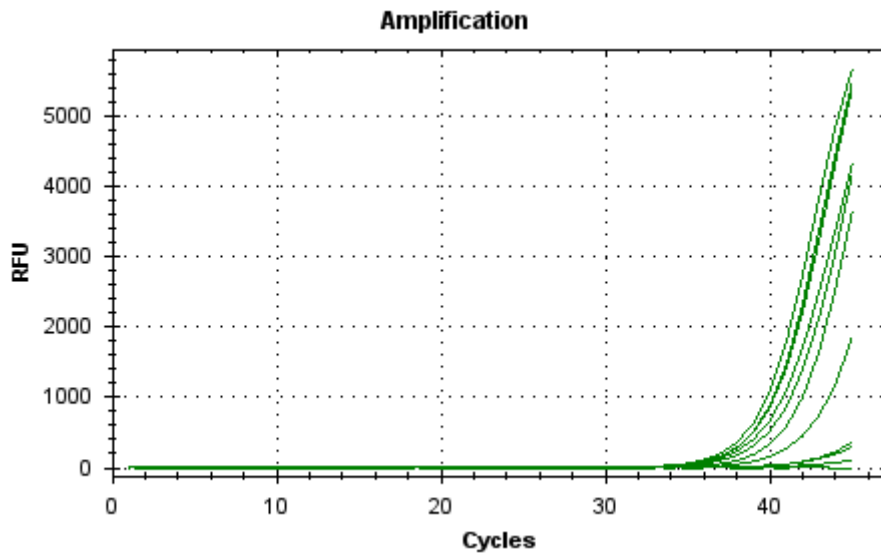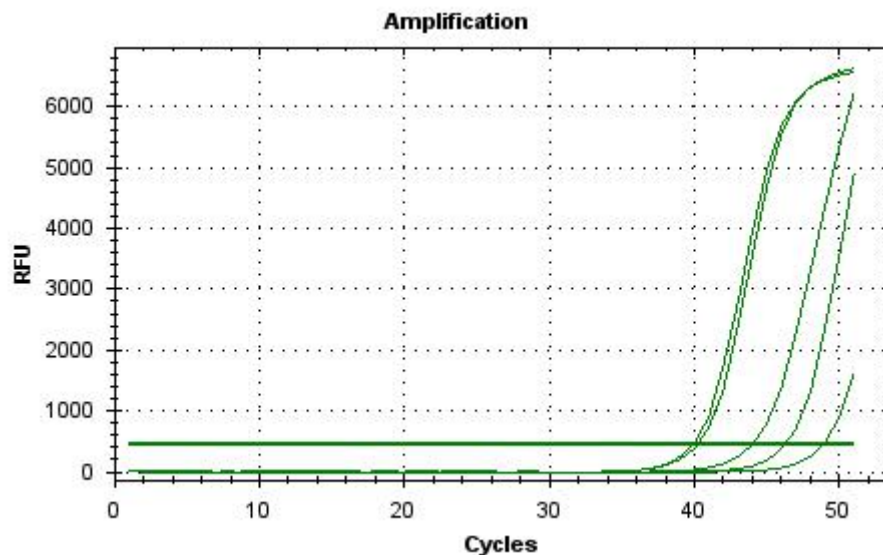

Figure 3.31. BioRad SYBR green QPCR amplification data of Alternative Deletion Primers. QPCR annealing temperature was set at 64°C for 30s for 50 cycles. Reactions used three 60 day old Zymo extracts.
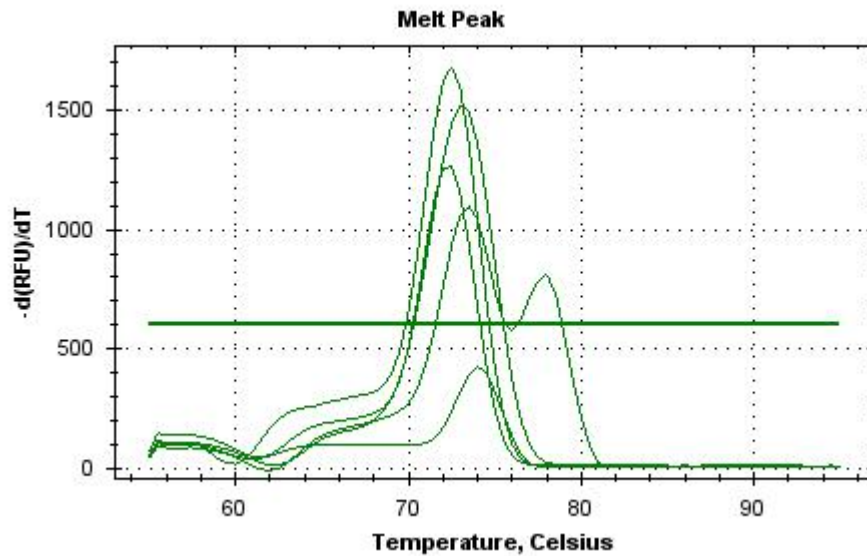
Figure 3.32. BioRad SYBR green QPCR melt peak data of Alternative Deletion Primers. QPCR annealing temperature was set at 64°C for 30s for 50 cycles. Reactions used three 60 day old Zymo extracts.

Amplification occurred randomly across all three Zymo extracts with very high Cq and low melt peak values. When all reactions possessing amplification were ran on agarose gel no DNA band was seen, again suggesting the product amplified was smaller than the 50bp band of the ladder and run off the gel or was too small in concentration to be identified on the gel. Because of the lack of any identifiable product, the lack of consistent amplification, and very high Cq values, the Alternative Deletion primers were ignored for further amplification attempts.

New Deletion Primer Pair

The second primer pair designed was called New Deletion. From 5' to 3': Forward = CCGCTGGAATTGCTCATGGTGG, Reverse = AGCTCCGATAGCTCCTGTTAATGGT. The New Deletion primers were subjected to annealing temperatures ranging from 68°C to 57°C in both gradient and single temperature QPCRs. Both gradient and single temperature QPCRs used annealing steps of 30s. The New Deletion primers were used with template extracted using the Qiagen and Zymo extraction kits. All QPCR attempts failed to produce any amplification, regardless of temperature or template used. Due to the lack of any amplification the New Deletion primers were ignored for further amplification attempts.

Optimal Deletion Forward Primer

After the previous four primer pairs failed to consistently amplify mtDNA deletions due to either no reaction, poor amplification, or mispriming, another forward primer was designed to be trialled with existing reverse primers. The decision to design just a forward primer was based on the strength of forward mispriming seen in the Yui and Yui Extended forward primers. The primer designed was the most optimal forward primer considering mispriming, dimerization, and target binding which still spanned the original set of deletions amplified by *Yui and Matsuura* (Yui and Matsuura, 2006). The new forward primer was called Optimal Deletion. From 5' to 3': CTGTTTATCCACCTCTATCCGCT. The Optimal Deletion primer was subjected to annealing temperatures of 64°C in single temperature QPCRs. The Optimal Deletion primer was used with template extracted using the Zymo extraction kit.

Finding the Best Primer Combination

The Optimal Deletion forward primer was trialled using the four reverse primers previously used in an attempt to identify which primer combination (if any) amplified mtDNA deletions with minimal/no mispriming (figures 3.33 and 3.34):
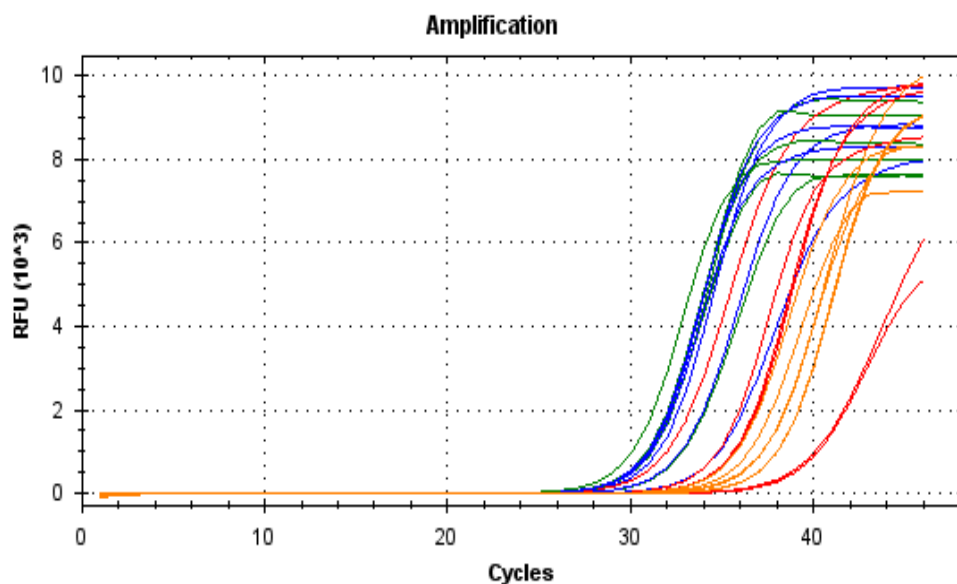
Figure 3.33. BioRad SYBR green QPCR amplification data of Optimal Deletion F primer with Yui R (Green), Yui Ext R (Blue), Alternative Deletion R (Red), and New Deletion R (Orange). QPCR annealing temperature was set at 64°C for 60s for 45 cycles. Reactions used two Zymo extracts consisting of 15 60 day old flies.
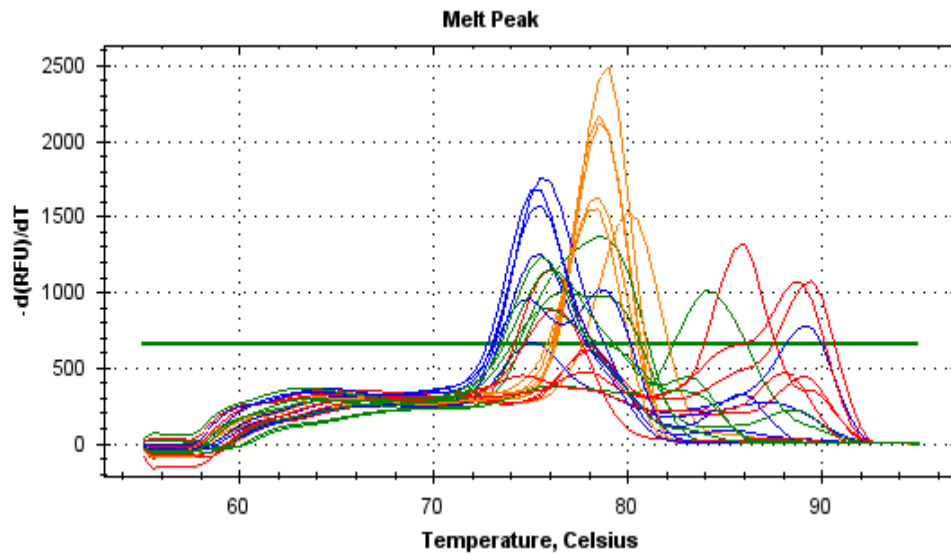
Figure 3.34. BioRad SYBR green QPCR melt peak data of Optimal Deletion F primer with Yui R (Green), Yui Ext R (Blue), Alternative Deletion R (Red), and New Deletion R (Orange). QPCR annealing temperature was set at 64°C for 60s for 45 cycles. Reactions used two Zymo extracts consisting of 15 60 day old flies.

From figures 3.33 and 3.34, each of the primer combinations appeared to amplify different products using the same extracts. As a result, all reactions for each of the primer combinations were combined and ran on agarose gel (figure 3.35):
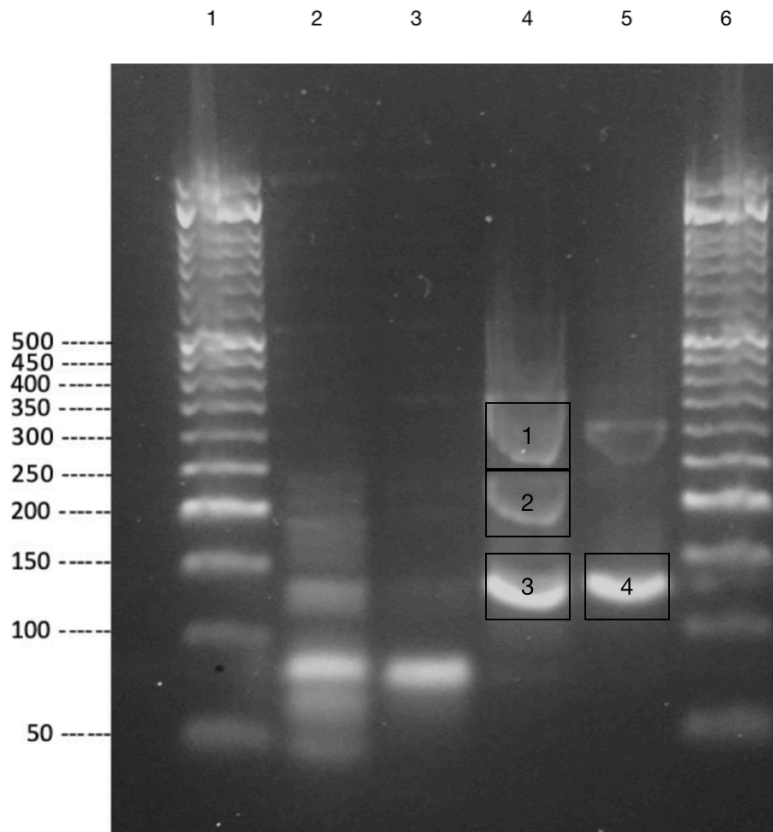
Figure 3.35. QPCR samples from the Optimal Deletion trial QPCR. Reactions used the Optimal Deletion forward primer, the reverse primer as stated with each lane description, and two Zymo extracts consisting of 15 60 day old flies each. Lane1 = 50-1500bp Ladder. Lane2 = Yui R, Lane3 = Yui Extended R, Lane4 = Alternative Deletion R, Lane5 = New Deletion R, Lane6 = 50-1500bp Ladder. Gel was made using at 2% using 1x TBE and run at 90V for 60 minutes.

Despite the larger number of different amplified products identified on the gel, only those highlighted in figure 3.35 were excised, purified, and sent for sequencing. Amplified products from lanes 2 and 3 were not chosen for sequencing due to the lack of clear, concentrated bands to excise without either excising multiple products or purifying too little product for accurate sequencing.

Referring to figure 3.35, band 1 retrieved no identifiable sequence and was ignored. Band 2 retrieved sequence corresponding to several different areas of chromosome X with low specificity. Quality of sequence was again an issue, with sections of sequence showing poor base identification. No evidence of mitochondrial sequence was retrieved and thus was assumed to be a product of mispriming, but the exact origins of this mispriming cannot be located. Band 3 retrieved sequence corresponding to chromosome 2R. This sequence was to an extent, of higher quality than the previous two and thus more accurately identified as a product of

mispriming. Band 4 retrieved clear mitochondrial sequence corresponding to two distinct areas of sequence close to each primer binding site. The surrounding sequence was analysed and the direct repeats which likely caused the amplified deletion were identified (figure 3.36):

ATTT**TATTACAA** (CTGTAATTAA…ATTAG**TATTA**G**AA**) TCAGCTGTAG
1967 < - - - - - - - - - - - 2697bp - - - - - - - - - - - - > 4664

Figure 3.36. Evidence of two direct repeats likely causing the deletion of mitochondrial sequence. Underlined are the direct repeats. In bold are all bases that identically match. Enclosed in brackets is the 2697bp deleted mitochondrial sequence from 1967nt to 4664nt. Sequence generated from reactions which used the Optimal Deletion forward primer, New Deletion reverse primer, and two Zymo extracts consisting of 15 60 day old flies each.

From analysis of the four sequences, New Deletion reverse appeared to be the best primer to use with the Optimal Deletion forward for deletion amplification. Referring to figure 2.1, both the Optimal Deletion forward and New Deletion reverse primers have near identical Tm (0.4^{o}C difference) and GC content (0.2% difference). With identical Tm's equal numbers of forward and reverse primers will theoretically be bound during the annealing phase of QPCR. Using this primer pair at its optimal annealing temperature, maximal numbers of both the forward and reverse primers will be bound to the target, maximising amplification efficiency of mtDNA deletions present (Bustin and Huggett, 2017). Following the primer pairs success and the above explanation, these primers were chosen as the optimal primer combination for deletion amplification.

Further Deletion Amplification

Following the success of the Optimal Deletion forward and New Deletion reverse primers, comparison between BioRad and Powerup SYBR green was done to identify which master mix was optimal for deletion amplification (figures 3.37 to 3.40):
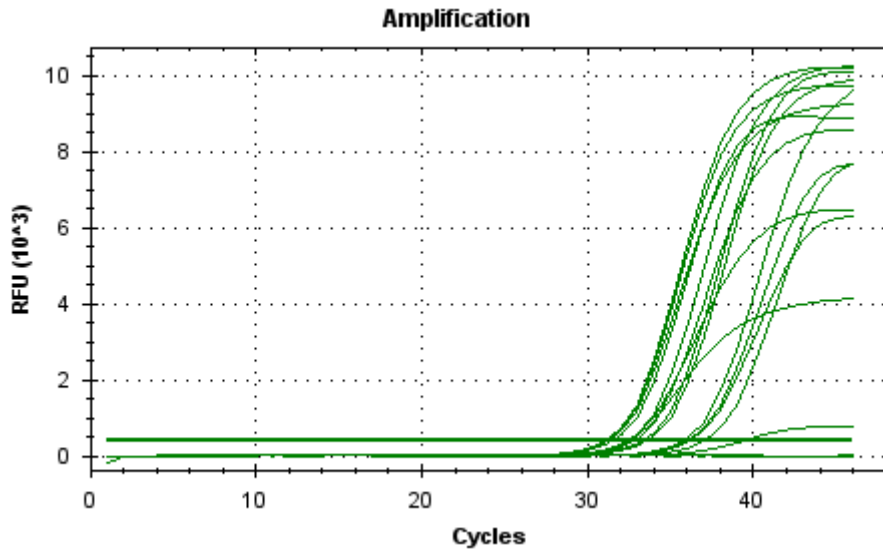
Figure 3.37. BioRad SYBR green QPCR amplification data of Optimal Deletion F primer with New Deletion R. QPCR annealing temperature was set at 64°C for 60s for 45 cycles. Reactions used three Zymo extracts.
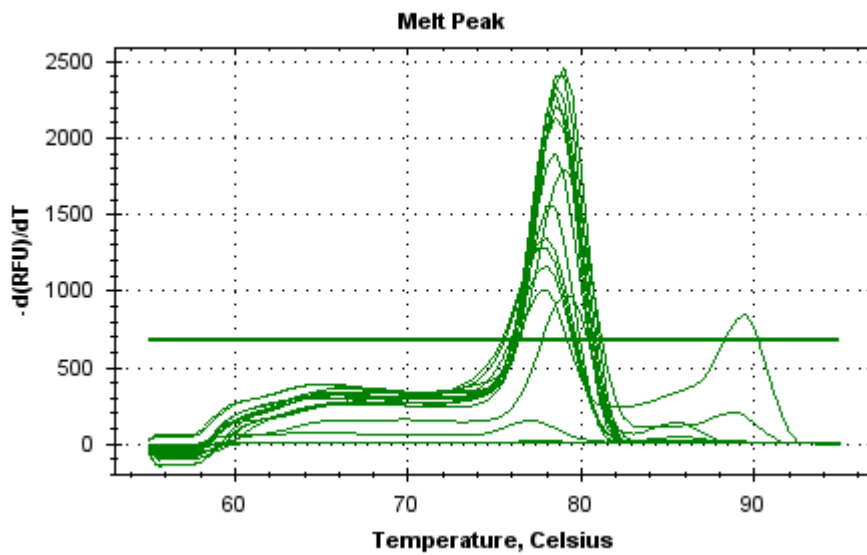
Figure 3.38. BioRad SYBR green QPCR melt peak data of Optimal Deletion F primer with New Deletion R. QPCR annealing temperature was set at 64°C for 60s for 45 cycles. Reactions used three Zymo extracts.
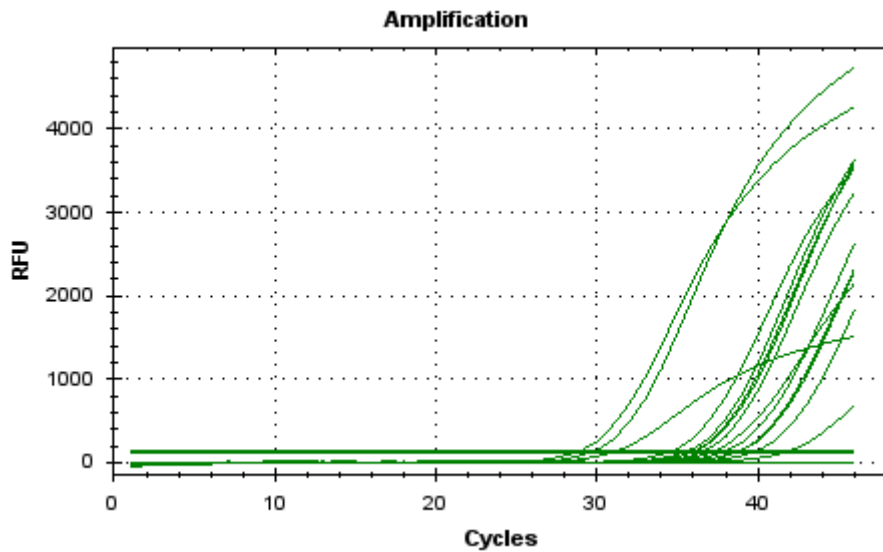
Figure 3.39. Powerup SYBR green QPCR amplification data of Optimal Deletion F primer with New Deletion R. QPCR annealing temperature was set at 64°C for 60s for 45 cycles. Reactions used three Zymo extracts.
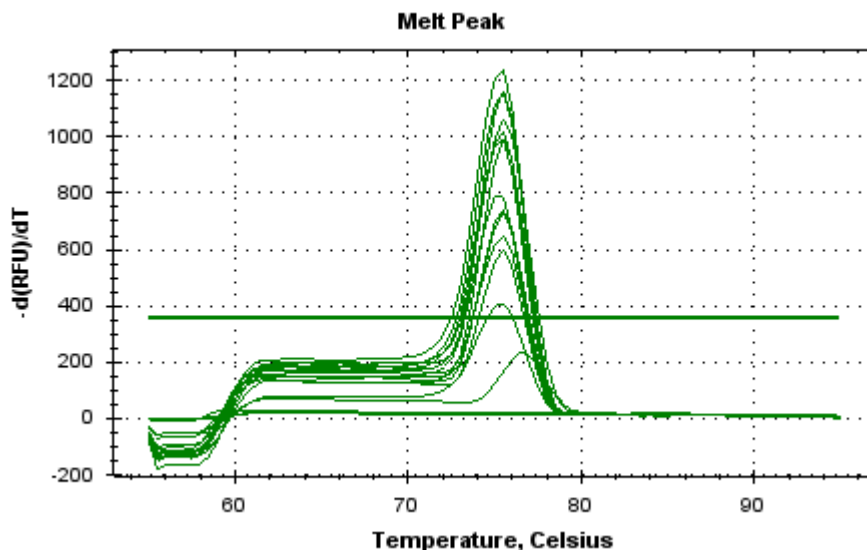
Figure 3.40. Powerup SYBR green QPCR melt peak data of Optimal Deletion F primer with New Deletion R. QPCR annealing temperature was set at 64°C for 60s for 45 cycles. Reactions used three Zymo extracts.

Both SYBR green mixes succeeded in producing amplification, with Powerup generating a wider range of Cq values compared to BioRad (figure 3.37 and 3.39). Note that the Cq values of both BioRad and Power amplification are still high, which is an issue for replicability and assay optimisation. Powerup however, failed to generate amplification in every reaction. Referring to the RFU scale in figures 3.37 and 3.39, BioRad appeared to amplify over double the product Powerup amplified once the reaction had finished. Finally, the product amplified using BioRad had a

melting temperature of 77-78°C whereas product amplified using Powerup had a melting temperature of 75-76°C. Successful triplicate reactions from both BioRad and Powerup QPCRs were run on agarose gel to identify how many products were amplified and their respective sizes (figure 3.41):
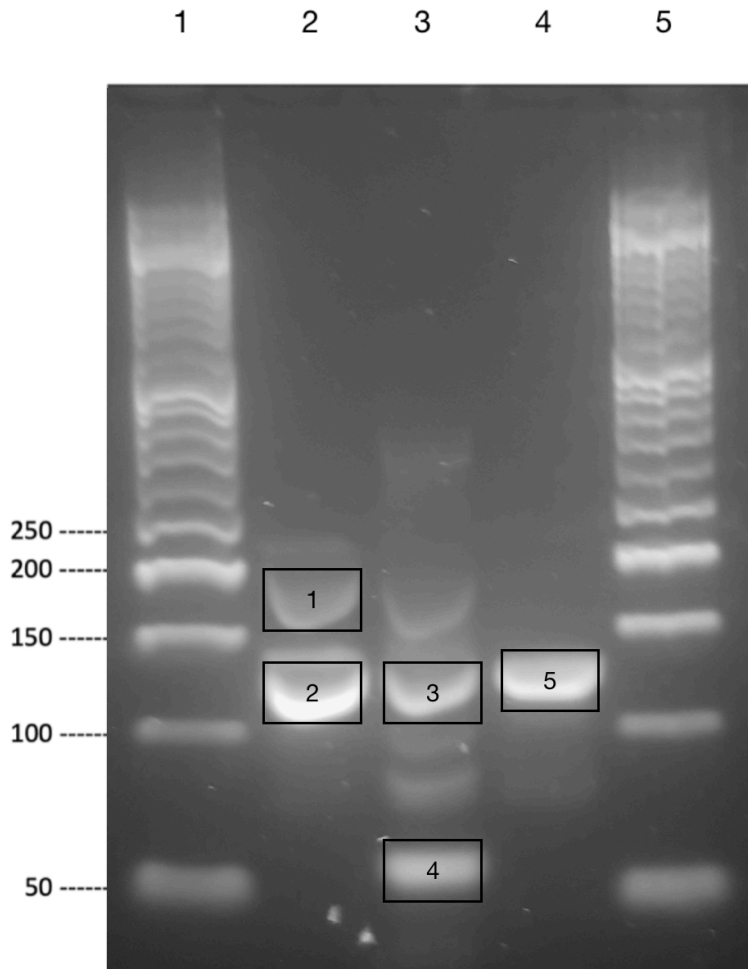
Figure 3.41. QPCR samples from figures 3.37-3.40. Reactions used the Optimal Deletion forward primer, New Deletion reverse primer, and three Zymo extracts as stated in the descriptions of each lane. Lane1 = Ladder, Lane2 = 10 x 60 day old single fly extract w/ BioRad, Lane3 = 60 day old single fly extract w/ BioRad, Lane4 = 10 day old single fly extract w/ Powerup, Lane5 = Ladder. Gel was made at 2% using 1x TBE and run at 90V for 60 minutes.

From figure 3.41, Powerup amplified a single product ~130bp in size (band 5). A similar sized product was also amplified in the BioRad reactions (bands 2 & 3). The five major bands highlighted in figure 3.41 were excised, purified, and sent for sequencing.

Band 1 sequencing produced a clear mitochondrial sequence close to the forward primer but lacked evidence of a sequence close to the reverse. Using the sequencing data, the product was analysed for presence of a repeat which may have caused the deletion of mtDNA, finding 'TTATTTGTTTG' close to the end of the product. Analysis of sequence close to the reverse primer identified 'TTATGTGTTTG' which was the closest match to the direct repeat potentially responsible for the amplified deletion (figure 3.42). Referring to figure 3.22, this appears to be the same deletion amplified using the Yui Extended primers. This however, cannot be used definitively to state where the second breakpoint occurred but can be used to identify the area within which the second breakpoint will have likely occurred.

CCT**TTATTTGTTTG** (ATCAGTAGTTATTACT…AATC**TTAT**G**TGTTTG**) CTGTATTAA
                     2025 < - - - - - - - - - - - - - - - - 2673bp - - - - - - - - - - - - - - - > 4698
Figure 3.42. Evidence of two direct repeats likely causing the deletion of mitochondrial sequence. Underlined are the direct repeats. In bold are all bases that identically match. Enclosed in brackets is the 2673bp deleted mitochondrial sequence from 2025nt to 4698nt. Sequence generated from reactions which used the Optimal Deletion forward primer, New Deletion reverse primer, and a single 10 x 60 day old fly Zymo extract w/ BioRad.

Band 2 sequencing produced two clear mitochondrial sequences close to the forward and reverse primers. This suggests that the short sequence amplified between the two primers is the sequence remaining after a deletion had occurred. Using the end of each sequence as breakpoints of a potential deletion, the surrounding sequence was analysed for evidence of direct repeats (figure 3.43):

GGAA**TTGCT** (CATGGTGGAG…TTATGTGT**TTGCT**) GTATTAAGAACT
                  1879 < - - - - - - - - - - - 2821bp - - - - - - - - - - - - > 4700
Figure 3.43. Evidence of two direct repeats likely causing the deletion of mitochondrial sequence. Underlined are the direct repeats. In bold are all bases that identically match. Enclosed in brackets is the 2821bp deleted mitochondrial sequence from 1879nt to 4700nt. Sequence generated from reactions which used the Optimal Deletion forward primer, New Deletion reverse primer, and a single 10 x 60 day old fly Zymo extract w/ BioRad.

An error by the sequencing company meant no forward sequence was supplied for Band 3. The product identified in the reverse sequence data exactly matched the product in band 2 close to the reverse primer, suggesting that band 3 and band 2 are the same mitochondrial deletion (figure 3.43). This is further supported because

bands 2 and 3 are the exact same size in figure 3.41, suggesting that they're potentially the same product.

Band 4 sequencing produced sequence with no clear origin even using low specificity search. As a result, the origin of this product was not identified and was assumed to be a product of nonspecific amplification.

Band 5 sequencing produced sequence which matched the same product in band 2 close to the reverse primer, suggesting that band 5 and band 2 are the same mitochondrial deletion (figure 3.43). This is further supported because bands 2 and 5 are similar in size in figure 3.41, suggesting that they're the same product.

The sequence of bands 3 and 5 were found to match to one half of the sequence retrieved for band 2. Together bands 2, 3, and 5 all appear to be the same mitochondrial product, present in all three extracts (figure 3.41). The identification of direct repeats likely to have caused the deletion amplified in band 2 (figure 3.43) suggest that the same mitochondrial product isolated in bands 2, 3, and 5 was from the same deletion. Referring to figure 3.41, the lack of complete sequence for bands 3 and 5 may be due to the lack of sufficiently concentrated product in the purified extracts of these bands compared to band 2. Note that bands 1 and 2 were amplified from an extract of 10 old flies, whereas bands 3, 4, and 5 were amplified from extracts of single flies. The same two deletions amplified using the 10 fly extract (bands 1 and 2) were also present when using the single fly extract but in smaller quantities (Lane 3 - figure 3.41). Because of this it could be assumed that more deleted mtDNA was present in the 10 fly extract over the single fly extract, so target amplification was more efficient when using the more concentrated extract.

Conclusion of the Results

The primary goal of these experiments was to develop an assay for mtDNA deletion amplification and quantification in single *Drosophila*. A summarisation of the progression of primer design can be seen in figure 3.44. With such high and variable

Cq values between triplicate repeats of successful deletion amplification attempts, accurate comparison and quantification is not viable using the current assay. So further attempts to amplify mtDNA deletions using the current assay will not progress quantification efforts and will only occasionally identify new deletions. This is likely due to the current DNA extraction approach failing to generate sufficiently concentrated mtDNA deletions per *Drosophila* for consistent and replicable amplification. So assay development cannot progress if insufficient mtDNA deletions are present per single *Drosophila* extract for replicable amplification to occur. Further review of QPCR assay design, mtDNA extraction, and the targeted amplification of specific mtDNA deletions will determine if quantification is possible using the current approach.

Figure 3.44. Summarisation of the troubleshooting steps and progression of primer design. Primers are shown in red.

Discussion

Deletion Amplification Attempts

The goal of this project was to develop an assay to quantify mtDNA deletions in single *Drosophila*. The current approach however, fails to consistently amplify mtDNA deletions without the potential for nonspecific amplification. Accurate quantification of mtDNA deletions from single *Drosophila* is not likely using the current protocol as the mtDNA content per extract is too small and variable. QPCR assay design, mtDNA extraction, and mtDNA deletion amplification should be reviewed to assess if the current approach is viable for mtDNA deletion quantification. Further review to assess which adaptations (if any) are required to make quantification viable will provide the direction that assay development should progress towards.

Yui Primers

It was assumed that the Yui primer pair, which worked well in amplifying mtDNA deletions in previous studies would also elicit similar results for this assay (Yui and Matsuura, 2006). Initial amplification attempts were thus focused on optimising conditions for replicability and efficiency. After consistent amplification regardless of annealing temperature (57°C to 68°C) and duration, the major amplified product was identified as a section of chromosome 2R rather than a deletion from the target region. The 3' half of both the Yui forward and reverse primers were found to match closely to areas either side of the misprimed product. This provided a likely explanation as to how the chromosomal product was amplified so consistently.

Consistent mispriming could be interpreted as a combination of strong enough mispriming to outcompete the desired reaction, an excess of nDNA which strengthened mispriming over deletion amplification, or a lack of sufficient deletions to be reliably amplified leaving mispriming as the next most efficient reaction (Ruiz-Villalba et al., 2017). Previous studies have suggested that mtDNA deletions within

this target region are present (Yui et al., 2003), and that QPCR can detect up to a single target copy in optimised reactions (Bustin and Huggett, 2017). This implies that the lack of deletion amplification is likely the result of strong 3' mispriming and a lack of sufficiently concentrated mtDNA deletions to outcompete nDNA binding. Also the way this assay is designed means primers will bind and extend on non-deleted mtDNA as well as deleted mtDNA, which will reduce the initial availability of primers for deletion amplification until sufficient target amplicons are present. The presence of minor amplification of an additional product in Yui QPCRs using 20 fly extracts could be interpreted as either amplification of mtDNA deletion(s) or amplification of the next most efficient nonspecific reaction. In hindsight the smaller peak (74-78°C) identified in these QPCRs was likely a deletion(s) amplified in small quantities, as any isolated deletion appeared in the same temperature range. If the additional product was deleted mtDNA then the only way this primer pair could work is if the template has a sufficiently high concentration of deleted mtDNA or the concentration of nDNA was substantially reduced. Overall the Yui primer pair demonstrated poor target binding, consistently mispriming to a chromosomal site with high replicability and thus rendering the primer pair useless for deletion amplification.

Yui Extended Primers

Yui extended primers were redesigned to reduce or eliminate 3' mispriming to the chromosomal mismatches and strengthen binding to the target mitochondrial region whilst maintaining most of the original primer sequence. Initially, Yui Extended primers produced one major melt peak for all reactions corresponding to a distinct mitochondrial sequence within the target gene, suggesting amplification of deleted mtDNA. Further Yui Extended QPCR reactions failed to amplify mitochondrial sequence as the major product, instead amplifying additional chromosomal products in higher concentrations. Generally, the lower concentrations of the extracts used for these QPCRs suggest that there was a lack of sufficient mtDNA deletions to reduce nonspecific amplification. Mispriming again appears to be the result of poor primer design, where shifting the Yui primers 3' by 3 bases increased the Tm difference between the primers to 12°C. By definition, when annealing temperature matches a

primers Tm ~50% of primer molecules are bound to the target. The lower the annealing temperature becomes relative to a primers Tm the higher the percentage of bound primers (Chuang et al., 2013). At too low an annealing temperature primer binding requires less specificity and amplification of nonspecific products may occur. At too high of an annealing temperature relative to a primers Tm, the primer will fail to bind to any sequence (Chuang et al., 2013). Generally, higher annealing temperatures are used as reducing the likelihood of nonspecific amplification is more important. A large Tm difference between a primer pair will fail to efficiently generate target product, increasing the likelihood of nonspecific amplification (Bustin and Huggett, 2017).

Since the Yui Extended Tm's differ so much, target binding and amplification will rely on a higher deletion concentration to be successful. Success of the initial Yui Extended QPCR may have been due to stronger presence of deleted mtDNA from a more concentrated extract (60-day old 25°C Qiagen extract), reducing the overall likelihood of mispriming. This will have reduced or prevented amplification of nonspecific products once sufficient target amplification had occurred. Use of both Zymo and Qiagen extracts produced similar mispriming, suggesting that mtDNA quantity may not have been the major cause. Review of the primer pair found strong self-dimerization of the forward primer, suggesting further disruption to target amplification. Consistent amplification of additional products other than target deleted mtDNA rendered this primer pair useless for deletion amplification.

Alternative Deletion Primers

The only successful reactions using the Alternative Deletion primer pair produced Cq values of 38-48 and melting peaks at 70°C-75°C with no replicability. Cq values above 35 tend to be reported as indeterminate and highly variable when replicated (Bolotin et al., 2015). Melt peak temperatures between 70°C-75°C are generally considered to be primer dimer structures (Ruijter et al., 2019). When ran on agarose gel the amplified band was too faint to accurately record, with faint fluorescence seen on the gel below 50bp. Since QPCR requires just a single copy of the target for a

successful reaction, this level of inefficiency suggests either no target was present or poor primer binding to the target sequence. Evidence of deletion detection using Yui Extended primers suggests that deletions will occur in at least some extracts and thus inefficient primer binding for the Alternative Deletion pair is likely the issue. With high Cq values, no replicability, and no visible band of DNA when ran on a gel the Alternative Deletion primer pair was ignored for further amplification attempts.

New Deletion Primers

QPCR reactions using the New Deletion primer pair produced no amplification, regardless of annealing temperature or duration. Further review of this primers design found it has the lowest potential for mispriming and dimerization across all four deletion primer pairs. The absence of amplification could be due to a lack of mtDNA deletions within the sample or a lack of primer binding to the target. The Tm values of this primer pair were equal to or higher than any annealing temperatures used (Forward Tm = 74.5^{o}C, Reverse Tm = 67.6^{o}C), so sufficient primers should have annealed for amplification to occur in each reaction. As most polymerases function best at 72°C, higher primer Tm is generally encouraged for QPCR reactions (Bustin and Huggett, 2017). Assuming this, amplification may have failed due a lack of deleted mtDNA, but previous studies highlighting the age-related accumulation of mtDNA deletions generally refutes this (Bua et al., 2006; Kennedy et al., 2013; Yui et al., 2003).

Since primer binding should have occurred and repeated trials produced no amplification, then either consistent instrumental failure, experimental failure, or significant inhibition in the reaction could have been the cause. Instrumental failure is unlikely given that positive results for other users were occurring. Total experimental failure is unlikely as non-specific and control amplification was achieved using the same reaction components with different primer pairs. Reaction inhibition could have occurred through contaminated template despite clear amplification with different primer pairs. Consistent presence of inhibitory components within extraction kits can reduce polymerase activity and amplification

efficiency (McCord et al., 2015). Regardless of minor inhibition, control amplification using the same templates occurred. Cq replicability of amplified products generally improved when using template from total extracts with higher concentrations and when template was diluted from higher concentrations. Failure of this primer pair despite the minimal potential for mispriming prompted primer design to be revisited.

Optimal Deletion Primers

Design of another forward primer was based on correcting the poor design choices of previous attempts. Across all four primer pairs either no amplification, nonspecific amplification, or primer structures produced the bulk of results. The only successful amplification of deleted mtDNA was when using the Yui Extended primer pair which had the largest difference between forward and reverse Tm and high potential for forward primer self-dimerization. Design of an optimal forward primer was thus focused on reducing mispriming and self-dimerization, encompassing the existing target region, having base pair length of 18 to 23, maintaining a GC content of ~50%, and a Tm of ~68°C.

The Optimal Deletion forward primer (Tm of 68°C and a GC content of 47.8%) was initially trialled with all other reverse deletion primers to find an optimal pair. The combination of Optimal Deletion Forward with New Deletion Reverse produced the most replicable result with a distinct mtDNA deletion isolated on the gel. As a result, this primer pair was selected for further deletion amplification efforts over all other combinations. The similarities in Tm and GC content, with a Tm difference of 0.4^{o}C, provides part of the explanation as to how this primer pair amplified target mtDNA more effectively than other combinations. At similar Tm values, near equal numbers of both forward and reverse primer molecules will be bound to the target sequence (Chuang et al., 2013). So the annealing temperatures where maximal forward and reverse primer molecules are bound to the target sequence is also near equal. Thus target amplification efficiency is most optimal when using this primer combination over all others. The higher target amplification efficiency becomes the faster target amplification surpasses any mispriming and reaches the detection threshold and

more accurately represents deletion copy number within the sample (Kralik and Ricchi, 2017).

Further analysis of this primer pair was performed using BioRad and Powerup SYBR Green to compare their effects on replicability and deleted product generation. Reactions from BioRad and Powerup were run on agarose gel and five bands were isolated across three different DNA extractions. Four of the five bands were found to be mitochondrial (with the other band unidentifiable), further supporting the use of this primer pair for deletion amplification. Three of these mitochondrial bands shared near identical sequences and identical flanking repeats. Collectively this suggested the amplification of the same sequence from three different samples. This amplification could be the result of a common deletion within the *COX* region or amplification of the most amplifiable sequence. Amplification of a common *COX* mtDNA deletion follows known deletion bias within the *COX* region (Yu-Wai-Man et al., 2010; Yui et al., 2003). During amplification, the shortest sequence will naturally amplify first as it requires the least nucleotides to be replicated (Cha and Thilly, 1993). The larger the deleted sequence the shorter the resulting amplified product as there are fewer base pairs between both primers. If multiple deleted products are competing for amplification components, then the deleted product with the highest concentration will saturate reaction components and surpass the detection threshold first, contributing to most of the Cq value for that reaction (Peng et al., 2015). If mtDNA deletions resulting from flanking repeats are at near equal levels, then the largest deletion (shortest sequence) will be amplified fastest and reach threshold concentrations first. In practice this means the final concentrations of each amplified deletion are uneven, favouring the largest deletion in this case. Previous results support this assumption as all sequenced bands were mitochondrial, the most concentrated mitochondrial bands were all the smallest, and the most concentrated deletions spanned the largest section of mtDNA.

The following attempts to amplify mtDNA deletions lead to further issues with nonspecific amplification and variable Cq values within triplicates, which tended to occur more at higher Cqs as expected. Greater variability between triplicates

generally occurred when using template from DNA extracts with low concentrations and/or poor purity. When performing an extraction of multiple *Drosophila*, QPCR reactions using this extract as a template produced more replicable Cq values regardless of the amplified product. Cq variation of more than 0.5 is generally considered untrustworthy and discarded (Nolan et al., 2006). Thus further amplification attempts using the current extraction methodology will likely fail to produce replicable and accurate amplification of mtDNA deletions within single *Drosophila* for quantification. Revision of the current assay with focus on optimising extraction of mtDNA to improve the quality of amplification would be the next clear step.

The Major Factors Influencing Target Amplification

Experimental Design & Optimisation in QPCR

For a precise and reliable QPCR assay, thorough optimisation of QPCR protocol, instrumentation, reagents, and analysis methods are vital. For QPCR assays detecting small differences in target presence, such as mtDNA deletions, precision is essential for reliable quantification (Bustin et al., 2009). A well optimised QPCR protocol will be able to amplify single target molecules within a sample, display consistency across replicate experiments, high amplification efficiency between 95% to 105%, be highly specific with minimal mispriming, and have a wide dynamic range (Forootan et al., 2017). A robust assay will generate usable data if conditions are not quite optimal, traces of inhibitor are present, or if the thermal cycler heats the block unevenly. Currently the low levels of mtDNA template extracted per fly means that although deletion amplification can occur, relative quantification is impossible. Amplification efficiency will unlikely reach the recommended 95% to 105% range as primers will also bind to non-deleted mtDNA.

Generally, assay optimisation is dependent on the combination of components, with the introduction of one different component requiring total re-optimisation of each reaction components concentration and the PCR conditions used (Nolan et al., 2006).

Attempts at assay optimisation were impeded by nonspecific amplification and an overall lack of consistent target amplification throughout the primer pairs trialled. So optimisation was repeatedly performed for each primer pair and SYBR Green used, exhausting valuable laboratory time on optimising an assay which failed to amplify mtDNA deletions with enough replicability. Optimisation mainly involved trialling different PCR conditions, template concentrations, and template from different flies. From the results and optimisation attempted, poor template quality and quantity hampered efforts to improve amplification efficiency using single *Drosophila* extracts. Using a consistent template consisting of extracts of multiple flies mixed and diluted to a standard concentration would've benefited optimisation to an extent, but still not been completely applicable to single *Drosophila* when using the current extraction protocol. The focus on developing a high throughput assay meant commercial extraction kits were initially preferred to much better and slower alternative extraction methods, in particular phenol-chloroform extraction. The exact issues of template quality and quantity will be discussed later in the dissertation.

Reproducibility of target amplification is influenced by template quality and quantity (Cankar et al., 2006), the reagents used in the reaction and their respective concentrations (Alemayehu et al., 2013), and the thermal cycler used to perform the reaction (Picard-Meyer et al., 2015). So an assay, regardless of quality and success, must be validated and optimised for each researcher's conditions and equipment. Optimising an assay prior to experimental use will avoid inconsistency and failure, saving time and money in the process. Multiple DNA lesions can block polymerase progression during the PCR reaction. If equal concentrations of template are used then the only variable impacting amplification (in an optimal assay) is the presence of lesions, including adducts, abasic sites, and single-stranded breaks (Ponti et al., 1991). So when using an optimal assay, minor variation in amplification replicability between extracts is expected.

Since empirical validation is so important, publication of QPCR data requires sufficient information (Bustin et al., 2009; Huggett et al., 2013). Multiple reports scoring the quality of QPCR studies generally found that the critical information used

to report QPCR data is insufficient for supporting the validity of conclusions made (Bustin and Nolan, 2017; Huggett and Bustin, 2011). The 2006 study by Yui and Matsuura for example, lacks sufficient information to exactly repeat the homogenisation and phenol-chloroform steps of DNA extraction and fails to explain if each *Drosophila* extraction used generated mtDNA deletion amplification (Yui and Matsuura, 2006). So the development of an assay with sufficient critical information to be validated and reproduced, means that a significant amount of optimisation across the whole assay would be required.

Deciding on which amplicon to use is important, as certain master mixes and amplification mechanisms function optimally with different sizes of amplicon. Probe-based assays for example, benefit from shorter amplicons (60-90bp) as the suboptimal elongation temperatures do not always double the target with each cycle (Debode et al., 2017). SYBR Green assays are optimised for amplicons of 80-150bp, with amplicons less than 80bp causing difficulties when differentiating between primer dimers and can result in high Cq values (Zipper et al., 2004). That said, an assay which amplifies longer amplicons will perform better than shorter amplicons, as long as the amplicon is not excessively longer than the recommended size (Bustin and Huggett, 2017). When attempting to amplify any mtDNA deletion present within the target region, the amplicons size may vary depending on which repeats the deletion resulted from. Generally, the size of all identified target amplicons was between 100bp to 200bp in length. As SYBR green QPCR assays are optimised for amplicons of 80-150bp in length, preferable amplification of larger deletions (smaller amplicons) may be the reason no smaller deletions (larger amplicons) were amplified.

Recommended primer concentration for SYBR Green assays is usually lower than for probe assays, but this is dependent on multiple other factors including varying forward and reverse concentrations as well as each primers optimal conditions (Bustin and Huggett, 2017). SYBR Green has an affinity for AT rich sequences over GC, causing AT rich amplicons to produce lower Cq values than GC rich ones. In SYBR Green assays the dye to base pair ratio is not consistent, rather it changes with cycle

number as dsDNA is generated and interacts with the minor groove of the melt curve (Bustin and Huggett, 2017). The following melt curve is thus influenced by cycle number and DNA quantity after amplification (Zipper et al., 2004). Amplicons should always be analysed for secondary structure, as the formation of secondary structures will reduce amplification efficiency. Kinetics of the annealing reaction will tend towards intramolecular binding over primer binding, reducing primer binding efficiency and thus amplification efficiency if secondary structure formation occurs (Gao et al., 2006). Additionally, the sequences either side of the amplicon should be reviewed, as they could impact primer binding and the initial PCR stages through secondary structures (Wilhelm et al., 2000). As this assay aimed to amplify mtDNA deletions from a range of sequence rather than just one specific deletion, amplicons could only be analysed for secondary structures once they were amplified, which defeats the overall purpose. Regardless of the suggestions for amplicon size and location, in practice the overall success of an assay depends on its specificity and optimisation.

Primer Design in QPCR

One of the major concerns when designing an assay is the unfamiliarity of primer design parameters and the lack of appropriate design tools. Primer design and optimisation generally follows four steps; target identification, primer design, primer characterisation, and assay optimisation. Primer pairs which are appropriately validated and optimised are essential in establishing the robustness, sensitivity, and specificity of any PCR reaction (Robertson and Walsh-Weller, 1998). A well designed primer pair will not dimerise, will be highly specific with minimal mispriming, and will be as close to 100% efficient as possible. Current primer design programs lack all the tools to design an optimal primer pair, so for mispriming to be completely avoided each primer must be assessed manually for mispriming. If primers generate useable results over a range of temperatures, the primer pair is generally considered to be robust, with target amplification over a very narrow range of temperatures considered to not be robust. When attempting to design a primer pair the amplicons

structure, location, and uniqueness should be considered to achieve accurate quantification (Chuang et al., 2013).

The critical value for primer design is the annealing temperature (Ta) rather than Tm, as Ta defines the temperature where maximal primer binding to the target occurs. Ta must be established experimentally because most primer design programs fail to calculate this for you (SantaLucia, 2007). Optimal annealing temperature differs with various buffers, so primer optimisation should be performed for each of the different buffers used (Nonis et al., 2011). Generally, the physical closeness of a primer pair at mismatched sites (where the nonspecific product is very short) may result in nonspecific amplification even at optimal reactions conditions. The BLAST program cannot guarantee optimal primer design since it fails to highlight thermodynamically favourable annealing and lacks accurate scoring of the gaps which can potentially loop out a base, creating a 'bulge' (SantaLucia, 2007).

Some consideration on the issues of mispriming should also be made for nDNA and the presence of Nuclear Mitochondria DNA or NUMTs. NUMTs are generated following the release of mtDNA to the cytoplasm after mitochondrial and morphological changes, where mtDNA is transferred to the nucleus and inserted into nDNA through double-stranded break repair (Gaziev and Shaikhaev, 2010; Hazkani-Covo et al., 2010). NUMTs have been identified across all studied eukaryotes differing in size and number across species, with the majority of mitochondrial genome regions reported as capable of being integrated into the nuclear genome (Hazkani-Covo et al., 2010; Qu et al., 2008). NUMTs also appear to have non-random distribution with an increased likelihood of insertion into certain locations (Tsuji et al., 2012). Notably, NUMTs have the potential to impact the function of whichever gene they are inserted into including the potential to influence various disorders and ageing (Dayama et al., 2014; Gaziev and Shaikhaev, 2010). So to an extent there is some potential for nDNA mispriming within a sample if a sufficient proportion of a mtDNA primer binding site has been transferred to nDNA. However, the lack of evidence of sufficient NUMTs possessing target primer sites to influence target

amplification to an impactful degree within a sample likely means NUMTs are not a major factor impacting amplification efficiency.

When using a primer pair used in a separate study, reliable QPCR requires validation and optimisation according to each laboratories equipment and conditions (Bustin and Huggett, 2017). The Yui primer pair when trialled across a wide temperature range appeared robust, replicable, and lacking any dimerization in the final product. However, after the amplified product was identified as nonspecific, further review of Yui and Matsuuras 2006 study found no information about nonspecific amplification (Yui and Matsuura, 2006). Further primer design attempts lead to difficulties due to the small useable area either side of the region containing the flanking repeats. Because the area for primer design was so small, many combinations produced mispriming, dimerization, and either very low or high Tm values. As nonspecific amplification was the issue with the Yui and Yui Extended primer pairs, further primer design was focused on preventing mispriming. This was achieved by manually assessing all potential mispriming sites and their closeness to one another. If two mispriming sites with sufficient 3' matches are within less than 300 bases, then the primer(s) would be further redesigned. The following Alternate and New Deletion primer pairs succeeded in avoiding nonspecific amplification but failed to amplify any product (other than potential dimerization). The design of an 'optimal' forward deletion primer took the previously discussed points of optimal primer design into question. The success of the Optimal Deletion forward primer and New Deletion reverse primer reflected the quality of the primers combination. Together this primer pair has the lowest mispriming and dimerization potential with the closest Tm values of any primer combination. This final primer design exhausted the viable options for *COX* deletion detection without losing some of the encompassed flanking repeats or extending the length of potential products.

DNA Quantity in QPCR

Further use of the Optimal Deletion primer pair still leads to variable Cq values and potential for nonspecific amplification within the current assay. Optimisation of both primer design and assay conditions still produced nonspecific amplification, dependant on the template used. Replicability was relatively random between extracts, but extracts with higher concentrations generally produced more replicable reactions and were more likely to amplify target product. A primer pair will not generate identical results under different conditions as assay performance varies depending on what extraction and purification methods were used to generate the required template (Cankar et al., 2006). Thus the DNA extraction methodology and resulting template is the likely cause of nonspecific amplification and lack of target amplification.

Total *Drosophila* DNA extraction using commercial kits produces variable concentrations of DNA, with generally low DNA concentrations from the Zymo and Invitrogen extraction kits. DNA extracts from the Qiagen extraction kit produced significantly higher concentrations overall, but still largely variable. Regardless, consistently poor replicability and target amplification plagued assay development. Following the contamination of the Qiagen extraction kit, attempts to optimise the Zymo extraction kit still failed to generate high enough concentrations of DNA and were still largely variable. The use of multiple fly extracts was useful to generate sufficiently concentrated mtDNA to amplify deletions but not to quantify deletions in individual flies. An issue with extracting maximal mtDNA per fly is the small overall quantity of starting mtDNA molecules in *Drosophila* compared to mammalian tissue samples. Commercial DNA extraction kits often rely on silica-based extraction, where DNA is expected to bind to the column and remain there throughout repeated washing steps until elution. If DNA is unable to bind it is simply washed away and discarded. When extracting DNA from smaller starting quantities this minor DNA loss may become more pronounced (Katevatis et al., 2017). Commercial kits often require a high starting input of DNA to produce usable extracts, meaning mtDNA extraction from single flies likely fails to produce sufficient template in the final extract. Since

the cellular ratio of deleted to non-deleted mtDNA varies widely, a high quantity of mtDNA molecules will be required so that sufficient deleted mtDNA is present within the sample for replicable amplification. In this assays case this must account for the deletion of just one region of mtDNA, so the minimum mtDNA concentration for replicable deletion amplification will be high.

Amplification of nonspecific products is frequently seen in QPCR assays and is generally unrelated to the resulting PCR efficiency and Cq values. Amplification of nonspecific products and accurate quantification of target products is partly dependent on the quantity of 'non-template' DNA (Ruiz-Villalba et al., 2017). Presence of nDNA when attempting to amplify and quantify mtDNA deletions will impact accurate quantification and as previously seen, lead to the amplification of nonspecific products. The lack of specific mtDNA extraction or isolation means that total *Drosophila* DNA extraction contained excess nuclear DNA which contributed significantly to nonspecific amplification and reducing target amplification efficiency (Ruiz-Villalba et al., 2017). Due to the small quantity of template pipetted into each reaction, variation may occur due to pipetting error. Cq variation of more than 0.5 is generally considered untrustworthy and discarded (Nolan et al., 2006). At low target concentrations the variation due to template differences becomes even larger than variation caused by pipetting error. This variation causes a relatively large range of Cq values regardless of pipetting quality (De Ronde et al., 2017). The small concentration of extracted mtDNA from single *Drosophila* compared to mammalian tissue, will thus have contributed significantly to the Cq variation across both nonspecific and target amplification. At lower concentrations of DNA reaction inhibitors present within the extract can have a more pronounced effect on amplification efficiency and Cq variation (Lance and Guan, 2020).

Overall, commercial DNA extraction kits fail to generate sufficient mtDNA template for consistent and replicable deletion amplification. With such low and variable concentrations of mtDNA extracted from single *Drosophila*, accurate quantification is near impossible. Without a method of mtDNA extraction which can generate sufficient mtDNA molecules assay development cannot progress.

DNA Quality in QPCR

Template quality is an important factor in QPCR and is essential for accurate quantification and optimal amplification efficiency. Template quality is generally affected by the duration and conditions of storage, the presence of a nuclease, the presence of an inhibitor, and the presence of any substance which interacts with detection (Dang et al., 2016). Template purity is essential in this assay as single *Drosophila* extracts have limited mtDNA quantity and amplification efficiency is more sensitive when target quantity within a sample is low (Huggett and Bustin, 2011). Due to the small quantity of template pipetted into each reaction, variation due to pipetting error may also lead to further amplification differences with varying inhibitor presence within the template (De Ronde et al., 2017).

The lack of target amplification within the current assay could in part, be associated with the presence of reaction inhibitors within the final extract (El Bali et al., 2014). When using undiluted single fly extracts from the Zymo kit Cq replicability was generally poor, when diluted down by 1/2 using Zymo elution buffer amplification replicability increases to near total. This effect is the same under 1/4 and 1/8 dilutions. When reviewing the Zymo and Qiagen kits there is one component which contains a known inhibitor able to impact the templates performance when present during PCR, guanidinium isothiocyanate (GIT) (Suffys et al., 2001). When reviewing the 260/230 values of Zymo extracts which were used in QPCR reactions they were much lower than the optimal value (~2.0). GIT is added to lysis buffer to inhibit RNAse's & DNase's but mainly to act as a protein denaturant (McCord et al., 2015).

The impacts of GIT inhibition in the PCR reaction are twofold; GIT facilitates hydrogen bonding of complementary base pairs keeping dsDNA intact and binds to Taq polymerase reducing its affinity for DNA (McCord et al., 2015). GIT has been identified to shift melt curves by up to 3°C and in increasing concentrations raises melting temperature of affected DNA (McCord et al., 2015). Assuming GIT is responsible for inhibiting the QPCR reaction, its dilution drastically improved amplification efficiency. Inhibitor presence within the final extract of commercial kits

is likely due to residual components used earlier in the extraction process remaining in the column until elution (El Bali et al., 2014). Additionally, total *Drosophila* extraction introduces a wide range of compounds alongside DNA which may not be washed away during extraction when using a commercial kit, leaving potential inhibitors present in the final extract. Depending on the extraction protocol used, purification of the final extract using ethanol precipitation or phenol chloroform for example, may be required if accurate amplification and quantification is the goal.

DNA Extraction Methodology

The focus on designing a high throughput assay impacted DNA quantity and quality to the point where QPCR inefficiency plagued assay development. Use of high throughput DNA extraction kits provided a simple, direct approach to generating template. This approach however, is not optimal for the amplification and quantification of mtDNA deletions from individual *Drosophila*. So the design and optimisation of a mtDNA extraction protocol to generate maximal mtDNA per *Drosophila* is essential for deletion amplification and further assay development.

Most DNA extraction methods first require homogenisation of tissues before isolating DNA from cellular components. Typically, homogenisation is left to the user in commercial extraction kits and thus the quality and quantity of separated DNA within the homogenised solution is largely variable based on the method used. Generally, homogenisation of insects is performed in buffer solution and tissues are broken apart either by hand using a pestle-like tool or by automated homogenisation using a sterile disruptor (Denno et al., 2015; Nebbak et al., 2016; Yuan et al., 2012). The homogenisation of single *Drosophila* using Zymo Bashing Beads, centrifugation, and transfer of the total suspended extract to a column can result in variable template loss if DNA remains around the pellet and beads. A homogenisation protocol which consistently separates maximal mtDNA from each *Drosophila* into solution and minimises mtDNA loss from transfer between containers is important for accurate mtDNA deletion quantification (Yuan et al., 2012). Sufficient disruption for mtDNA quantification can be achieved using automated homogenisation with

inactive beads and incubation with proteinase K (Peinnequin et al., 2011). Following this, further efforts to obtain maximal mtDNA from the homogenate should be performed if necessary. The suspended mtDNA can then be isolated using whichever protocol causes minimal mtDNA loss during extraction.

Automated extraction is likely not a viable alternative despite the speed and control it provides as mtDNA is often supercoiled in the final extract. Primers cannot completely access supercoiled mtDNA during the PCR reaction, rendering mtDNA amplification inefficient (Furda et al., 2012). This issue can however be circumvented by using a restriction enzyme to linearize mtDNA in an area away from the target region. Considering the expense of automated extraction and the volume of extracts required for any viable comparison or quantification attempts, automated extraction is not a realistic option. Previous mtDNA deletion studies on *Drosophila* have used buffer homogenisation, ethanol precipitation, and phenol chloroform to extract template for PCR (Yui and Matsuura, 2006). Phenol-chloroform extractions allow the separation of DNA from homogenised tissue. Equal volumes of phenol and chloroform are thoroughly mixed and centrifuged to form two distinct phases, an upper aqueous phase and a lower organic phase. Hydrophobic lipids will be held in the organic phase with proteins held in the interface. Nucleic acids will be isolated in the upper aqueous phase and can be pipetted off for further extraction and purification if required (Chomczynski and Sacchi, 1987).

The decision to not use phenol-chloroform extraction was based on the high throughput focus of assay design. Phenol-chloroform extractions generally take longer to perform than when using commercial kits and the reagents are not supplied in their required states. Phenol-chloroform extraction can be more susceptible to contamination and the components used for extraction can have significant impacts on downstream applications such as QPCR (Toni et al., 2018). That said, phenol-chloroform extraction is cheaper overall than commercial kits and generates higher DNA quality and yield (Toni et al., 2018). Phenol-chloroform extraction does not expose the target DNA to repeated washing and centrifugation steps through a silica column where minor DNA loss and extract contamination may

occur. Finally, phenol-chloroform extraction protocols can be optimally designed to benefit whatever purpose the final extract has, including concentrating the extract in a chosen buffer solution (Chen et al., 2010). Despite the additional time and effort phenol-chloroform extraction requires, the improved purity and yield would be essential in extracting sufficient mtDNA for consistent deletion amplification.

Despite using an optimal homogenisation and extraction protocol, excess nuclear DNA would still present within the extract, impacting mtDNA deletion amplification efficiency through mispriming and nonspecific amplification (Ruiz-Villalba et al., 2017). Total DNA extraction and purification from tissue leads to quantification errors due to the size and structural variation of genomic DNA and mtDNA, which results in discrepancies within DNA extraction yields (Nicklas et al., 2004). Extraction methods which isolate mitochondria tend to run into difficulties when recovering mitochondria of varying densities and sizes without nDNA present in the final extract (Kang et al., 1998). Peinnequin and colleagues in 2011 described a QPCR protocol using a tissue lysate to accurately quantify deleted and total mtDNA and genomic DNA without DNA extraction. The lysate-based method resulted in more reliable and replicable measurements of the deleted and total mtDNA ratio (Peinnequin et al., 2011). This method eliminates the potential for minor mtDNA loss in between transfer and wash steps by keeping all genetic material together throughout the protocol. Using this approach when designing an optimal extraction protocol should assist in keeping extract concentrations more consistent.

Considering the consistent nonspecific amplification of nuclear products within the current assay, total DNA extraction may not be sufficient for quantifying mtDNA deletions in *Drosophila*. This cannot be confirmed until an optimised extraction protocol is devised and trialled with the current assay to assess target amplification, amplification efficiency, and replicability. If an extraction protocol cannot generate sufficient mtDNA content alone, then efforts to enrich and purify mtDNA should be taken. Previous mtDNA studies however, appear to produce sufficient mtDNA content for deletion amplification without purification or enrichment by using

proteinase k and either phenol chloroform or tissue lysate extraction (Bai and Wong, 2005; Peinnequin et al., 2011; Yui and Matsuura, 2006).

Further Work

Optimisation of Mitochondrial DNA Extraction

From previous QPCR attempts it is clear that poor template quality and quantity is a major factor in the consistent nonspecific amplification of nuclear products. Optimisation of the current assay cannot be performed if the template used fails to amplify deleted mtDNA in a replicable manner. Total DNA extraction using a commercial kit failed to generate the required mtDNA quality and quantity for consistent deletion amplification without the potential for nonspecific amplification. The limited mtDNA content of individual *Drosophila* and the high DNA input requirement for commercial extraction kits means further optimisation of an extraction kit may still fail to provide consistent useable template (Katevatis et al., 2017). Previous *Drosophila* mtDNA deletion amplification using template generated by phenol-chloroform extraction and ethanol precipitation may provide the answer to the current template problems (Yui and Matsuura, 2006). That said, Yui and Matsuura fail to explain if their extracts provided consistent target amplification, only showing the sequences and flanking repeats of mtDNA deletions they amplified. So phenol-chloroform extraction may still fail to provide the quality and quantity of mtDNA per single *Drosophila* extraction required for consistent mtDNA deletion quantification. Regardless, this method will likely generate more consistently concentrated mtDNA over any commercial extraction kit and eliminate the potential presence of an inhibitor in the final extract (Guo et al., 2009; Nacheva et al., 2017).

Tissue lysate methods such as one described by Peinnequin and colleagues specifically focus on producing template optimised for QPCR and accurate quantification. The tissue lysate method eliminates mtDNA loss from repeated wash steps by keeping all the material in the same vials throughout extraction processes. The use of inactive zirconium beads for homogenisation also means that this

protocol can be used with the available machinery (Peinnequin et al., 2011). The protocol was designed to extract DNA and mtDNA from 30mg rat brain and liver samples (an average fly weighs ~0.5mg) but could be redesigned to use smaller volumes of lysis buffer to concentrate the mtDNA content per microliter. The inclusion of sonication to improve QPCR efficiency in the tissue lysate protocol however, will damage mtDNA deletion amplification attempts as excessive sonication can shear DNA down to less than ~150bp in size (Wang and Son, 2013). If mtDNA was excessively sheared, then the likelihood of a complete target sequence still present in each sample would be poor. Even mild sonication of an extract will increase the Cq values of any amplification attempt, since a proportion of target sequence will have been sheared and cannot be amplified (Fykse et al., 2003). So for this method to be a viable option for deletion amplification and quantification sonication cannot be used. The major difficulty in using this protocol however, would be the lack of any step which concentrates the extract down to an optimal level for mtDNA deletion amplification attempts. Within the protocol further dilution is still required to obtain reproducible QPCR efficiency (Peinnequin et al., 2011). Considering this, an adaptation of the tissue lysate protocol may still fail to produce sufficiently concentrated mtDNA for replicable deletion amplification without the inclusion of steps to isolate and concentrate the extract.

Collectively, both the phenol-chloroform and tissue lysate extraction methods will likely generate better quality mtDNA over a commercial extraction kit. The concentration of this extract will need to be improved for replicable mtDNA deletion amplification however, and the quality of this concentrated extract will determine if these protocols are viable for single *Drosophila* extraction. As the lysis buffer used by the tissue lysate protocol apparently impacts QPCR efficiency, additional isolation or purification efforts using a sterile buffer solution would be required to make this protocol viable for quantification (Peinnequin et al., 2011). As significant adaptation of the tissue lysate method would be required for any amplification attempts, a standard phenol-chloroform and ethanol precipitation extraction which includes some initial aspects of the tissue lysate method may generate the best extract overall.

Enrichment for Mitochondrial DNA

Enriching extractions for mtDNA can assist in accurate detection of deleted sequence by reducing the overall nDNA content, decreasing the potential for nonspecific amplification (Devall et al., 2015; Gould et al., 2016; Ruiz-Villalba et al., 2017). Studies which isolate mtDNA from *Drosophila* often use very basic hand or automated homogenisation followed by two separate centrifugation steps. The first (~300g) is to isolate the suspended cellular contents from the remaining tissues and the second (~6000g) is to pellet mitochondria, separating them from the cytosolic fraction which is then discarded and the mitochondria re-suspended (Holmbeck et al., 2015; Villa-Cuesta and Rand, 2015). This method of enrichment however, often fails to recover mitochondria of various sizes and densities without also recovering minor levels of nDNA (Peinnequin et al., 2011). Gould and colleagues trialled multiple protocols which aimed to isolate and enrich mtDNA for QPCR to assist in reducing nonspecific amplification from nDNA. Mitochondria were isolated from human blood and cell lines using differential centrifugation and magnetic bead binding. Following mtDNA extraction using a commercial extraction kit (Qiagen), mtDNA was further enriched using exonuclease digest (exonuclease V) (Gould et al., 2016). Exonuclease digestion of linear DNA was performed using the Plasmid Safe ATP-dependent DNase (EpiBio) which aimed to deplete nDNA content because the digest cleaves nucleotides off of the ends of DNA strands. They identified that differential centrifugation followed by exonuclease digest generated the most optimal extract, with digestion drastically improving mtDNA yield over centrifugation alone (Gould et al., 2016). If any direct attempts to extract sufficient mtDNA for deletion amplification fail, then the isolation of mtDNA prior to extraction would likely solve any issues regarding nonspecific amplification.

Prior to any attempt to enrich extracted mtDNA, an optimal extraction protocol should first be established. The quantity of mtDNA molecules extracted by this optimal protocol may be sufficient for deletion presence within each sample and replicable deletion amplification in each QPCR. If template from an optimal extraction protocol still produces nonspecific amplification of nDNA then mtDNA

enrichment is required. Considering the mtDNA enrichment protocols described previously, the additional work required to enrich each extract and to what extent enrichment improves the assay could be explored. Enrichment may be required for accurate quantification of mtDNA if target amplification efficiency is too variable (outside of the 95-105% range) (Huggett et al., 2013). Enrichment can be used to reduce the extract concentration required for replicable amplification (Gould et al., 2016). However, repeated QPCR reactions using the same template is unlikely to produce further useful data for that individual fly, so enrichment to reduce the required template concentration for a successful reaction is not beneficial. Overall, mtDNA enrichment would only be beneficial if total DNA extractions fail to provide consistent and efficient target amplification without nonspecific amplification of nDNA. If all this is achieved, then mtDNA deletion quantification may be attempted.

Optimisation of QPCR Methodology

As the current assay fails to consistently and accurately amplify deleted mtDNA, the optimisation of reaction component concentrations and QPCR parameters cannot be viably trialled until an optimal mtDNA extraction protocol is developed. Reproduction of QPCR amplification is influenced by the duration of pipetting, with longer overall bench times correlating with increased artefact generation (Ruiz-Villalba et al., 2017). Reactions which were not set up on ice and/or not kept on ice throughout until the QPCR was initiated were more prone to mispriming and nonspecific amplification in Yui Extended QPCRs. This strict control also applies to long durations on ice; even if a reaction mix was kept on ice, mispriming would likely occur if enough time was allowed to pass before QPCR was initiated. When a reaction is held at higher temperatures more molecules within the reaction possess the required energy to react with one another. In the context of this project this can be related to primer molecules reacting with one another, nDNA, and mtDNA. Even on ice some reaction components may still possess sufficient energy to interact. The longer a reaction is held for the more of these interactions occur, depending on the temperature (Nikolaev, 1978). When a PCR reaction mix is made the reaction components may interact with one another to varying degrees depending on the

temperature and duration the reaction is held for prior to PCR (Lorenz, 2012). The polymerase acts as a catalyst to this interaction, where a temperature of 72°C often maximises the polymerases activity (Lorenz, 2012). This interaction includes primer binding and given enough time may lead to nonspecific primer binding and initial amplification of nonspecific products prior to and during PCR (Ruiz-Villalba et al., 2017). These interactions may decrease the overall efficiency of the reaction and potentially lead to nonspecific amplification during PCR, which almost certainly impacted assay development (Booth et al., 2010).

So despite the correct precautions in place, amplification efficiency and the likelihood of nonspecific amplification may still be affected by the duration of reaction set up. Long reaction set up only happens when large numbers of replicates using different extracts are made on the same QPCR plate. When producing so many separate reactions, each triplicate is often set up separate to others so template is not mixed. Nonspecific amplification occurs more often on these larger QPCR plates, but this may be due to the larger number of extracts used rather than minor interactions. For future amplification attempts, setting up QPCR reactions on ice in a temperature controlled cold room will reduce the temperature all components are held at throughout set up. Additionally, performing more targeted QPCR reactions using fewer samples per reaction will reduce the duration the reaction is kept at temperatures where nonspecific amplification may begin. That said, optimisation of mtDNA extraction may make the effects of these steps redundant if sufficiently concentrated mtDNA is present in each reaction.

The target and control primer pairs have different optimal reaction temperatures. As a result, running both target and control reactions at the same temperature reduces the amplification efficiency of at least one set of the reactions. Quantification requires amplification efficiencies of both target and control primers to be as close to 100% as possible for an accurate estimation (Bustin and Huggett, 2017). So further QPCR reactions should be performed separately for the target and control primers at their respective optimal temperatures. This is not ideal in QPCR, so this assay may benefit from a new pair of control primers with Tm's closer to the optimal deletion

primer pairs. Comparable reactions should be performed using the same template origin, template concentration, thermocycler, reaction composition, and optimal reaction conditions to make quantification as accurate as possible (Huggett et al., 2013).

Theoretically only one target copy is required for PCR amplification (Dang et al., 2016). The amplification of mtDNA deletions however, relies on the generation of a sufficient number of deletions throughout the lifespan of the organism to be detected in an aliquot of the final extract. As this assay aims to quantify deleted mtDNA within one section of the mtDNA genome, the rarity of this target deletion is further increased. The exact quantity of mtDNA deletions per cell depends entirely on the duration of lifespan, exposure of mtDNA to damage during lifespan, pre-existing mutations within replication and/or repair machinery, and deletions established prior to the genetic bottleneck (Nissanka et al., 2019). Considering this, each extract will hold a limited number of target deleted mtDNA molecules. If total DNA extracts are used for mtDNA deletion amplification, then the minimal concentration of genetic material required for replicable amplification within each reaction will be high. mtDNA enrichment will lower the required concentration but may still be relatively higher than the minimal concentration required for replicable control amplification (Andreu et al., 2009). With this reiterated, for accurate and replicable mtDNA deletion amplification and quantification the minimal template concentration required will be much higher than for the amplification of the control. Estimation of the minimal concentration of template required for replicable target amplification again relies on the optimisation of mtDNA extraction prior to any amplification attempts.

Further Mitochondrial DNA Deletion Amplification Attempts

Once the extraction methodology and amplification using both deletion and control primers have been improved, further mtDNA deletion amplification and quantification can be attempted. Since mtDNA deletion amplification lacking nonspecific amplification has already been achieved, an optimised protocol will likely

ensure at least consistent presence of target amplification in each reaction. If repeated mtDNA deletion amplification without mispriming is established over multiple extracts, then serial dilutions of a successful extract for both deletion and control primer pairs can be used to calculate amplification efficiency. With efficiencies estimated, further attempts to optimised reaction composition will likely develop a useable assay for mtDNA deletion amplification. Minor variability of mtDNA deletion copy number within each sample may still have a pronounced effect on amplification replicability depending on the rarity of target deleted mtDNA relative to the measured concentration of total DNA/mtDNA (Grady et al., 2014).

Depending on the assay quality, further investigation into the presence of a potential 'common deletion' may be attempted. Current evidence for a common deleted sequence within the *COX* region can be seen in figure 3.41. and the subsequent sequencing data. The same deletion was isolated from three different extracts; one young (10 days aged at 17°C), one old (60 days aged at 17°C), and one containing multiple ten old flies (60 days aged at 17°C). However, from the quality of this sequencing all breakpoints were not clearly defined. To what degree this deletion is 'common' and why should be a focus of following work. Considering that different deletions have been amplified by the current assay and that only three different extracts generated the same deletion, this common deletion may not be common at all. As previously stated, this common deletion may simply be the amplification of the most amplifiable deletion rather than a deletion which is most common (Peng et al., 2015).

If repeated amplification of a specific deletion is identified, then this assay may benefit from the inclusion of a probe designed to amplify just this deletion. The effects of experimental conditions on deletion generation by measuring the frequency of an individual deletion will be more accurate than measuring multiple deletions across a gene or area (Grady et al., 2014; He et al., 2002). This is due to differential amplification of deletions depending on size, which renders any comparison inaccurate. For quantification to be considered accurate, Cq variation between triplicates should generally be less than 0.5 (Nolan et al., 2006). The quality

of mtDNA deletion quantification using this assay will thus be dependent on the concentration and quality of mtDNA per reaction as well as the optimisation of reaction conditions. If an optimal assay cannot amplify deleted mtDNA with enough efficiency and replicability, then the assay cannot accurately quantify mtDNA deletions from single *Drosophila*, only amplify them. If accurate quantification is achieved, then these conclusions would still only be applicable to the Dahomey strain. Repeating this work across various *Drosophila* species would solidify any conclusions drawn. Once similar conclusions are drawn across multiple *Drosophila* species then an overall conclusion on the effects of various conditions on deletion frequency in *Drosophila* could be made.

Final Conclusions

The Likelihood of Quantifying Mitochondrial DNA Deletions in *Drosophila*

Amplification of multiple mtDNA deletions within one QPCR reaction may not accurately represent deletion frequency. If several deletions begin to compete for reaction components, the most abundant or most amplifiable deletion will amplify fastest. This deletion will achieve exponential amplification first and saturate the majority of reaction components (Grady et al., 2014; Kralik and Ricchi, 2017). So the total quantity of each amplicon in the final reaction will be less than if each deletion was amplified individually. Crucially, the resulting Cq value would be from a combination of all amplified sequences but mainly indicative of the most abundant or most amplifiable deletion since it will make up the majority of amplicons present. So any conclusions drawn from experimental effects on mtDNA deletion frequency would not be accurate and quantification using this method is not viable.

Quantification of specific deletions appears the most viable direction for this assay. Identification of more frequent deletions through further deletion amplification experiments will define which deletion(s) would be best suited for quantification. Following this, the design of a probe specific for the most frequently amplified/common deletion should allow for the most accurate method of

quantification possible using this protocol. The efficient amplification of one target sequence should provide a quantifiable measure of mtDNA deletion frequency which can be measured across different conditions. This however, requires sufficient deletion generation per *Drosophila* for this specific deletion to be present in each extract. Moreover, this specific deletion must be present in a high enough concentration for it to be amplified when using an aliquot of that extract. The limited number of mtDNA molecules in an average *Drosophila* may not be enough for this method of quantification and so using more concentrated extracts of multiple *Drosophila* may be required for accurately measuring experimental effects on mtDNA deletion frequency. If this is the case then accurate quantification of mtDNA deletions within *Drosophila* is possible, but not from individual flies.

What Might a Working Protocol Look Like

Without enough mtDNA content per extract, optimisation of mtDNA deletion amplification and quantification cannot be attempted. So a working protocol requires a method of mtDNA extraction (and if required enrichment) which generates enough mtDNA for this purpose. Attempts should still be made to make this extraction protocol as high throughput as possible without sacrificing mtDNA content. Considering the previously described extraction methods, phenol-chloroform followed by ethanol precipitation would likely produce the best quality extract and allow the most control over the components, repetition, and duration of various steps (Guo et al., 2009; Nacheva et al., 2017).

Described below is a general phenol-chloroform and ethanol precipitation extraction protocol for single *Drosophila*. The homogenisation technique was based off of previous optimisation efforts and *Drosophila* homogenisation in previous studies (Jensen et al., 2013; Tennessen et al., 2014). The lysis buffer's components and their concentrations were based off of previous use in various quantification studies (Coutlee and Voyer, 1998; Le et al., 2015; Peinnequin et al., 2011; Peper et al., 2014; Wang et al., 2019). This protocol has been streamlined to attempt to extract mtDNA in the shortest time possible without sacrificing any major steps. Comparison

between this extraction protocol and the current commercial extraction kit data would likely provide a conclusion on whether this protocol is worth using prior to any optimisation. Considerable optimisation of this protocols steps will likely be required to extract maximal mtDNA per *Drosophila*:

1. Homogenise the required specimen(s) using an automated homogeniser in a lysis tube (2.0 mm) with inert bashing beads (6000g for 10s four times) in 180μL of lysis buffer (0.05% (v/v) Tween 20 (Sigma Aldrich), 0.05% (v/v) Nonidet p40 (Sigma Aldrich), 10mM Tris HCL, pH 8.0) and 20μL Proteinase K. Ensure any pelleted tissue is re-suspended between each homogenisation step.

2. Re-suspend any pelleted tissue and incubate at 56°C for 2 hours in a shaking incubator.

3. Incubate at 95°C for 15 minutes (to deactivate the Proteinase K).

4. Add 200μL of phenol:chloroform:isoamyl alcohol (25:24:1) to the extract and vortex thoroughly for 20s. Leave to stand for 1 minute.

5. Centrifuge at maximum RPM at room temperature for 5 minutes and transfer the upper aqueous phase to a clean 1.5ml Eppendorf. Take care not to agitate the interphase layer.

6. Add 0.1x volume of 3M Sodium Acetate and 2.5x volume of 100% ethanol (chilled at -20°C) to the extract. Leave to precipitate at -80°C for 1 hour or -20°C overnight.

7. Centrifuge at maximum RPM at 4°C for 30 minutes.

8. Remove as much supernatant as possible without agitating the pelleted DNA.

9. Add 200μL of 70% ethanol (diluted using sterile H$_2$O and chilled at -20°C) to wash the pellet (avoid dislodging the pellet).

10. Centrifuge at maximum RPM at 4°C for 10 minutes

11. Repeat steps 8 through 10.

12. Remove as much supernatant as possible without agitating the pelleted DNA and evaporate residual ethanol using a speed-vac or 37°C heat block.

13. Re-suspend the pelleted DNA in sterile H$_2$O or buffer of choice to the appropriate concentration and test for DNA presence.

If nonspecific nDNA amplification is still present using an optimal extraction protocol, then altering the protocol for mtDNA enrichment would be the next step. Although mtDNA enrichment techniques fail to eliminate all presence of nDNA, the reduction of nDNA concentration would be hugely beneficial in reducing the possibility of nonspecific amplification. Performing mitochondrial enrichment prior to the protocol would be the simplest adaptation and may sufficiently reduce nDNA concentration to prevent nonspecific amplification (Holmbeck et al., 2015; Villa-Cuesta and Rand, 2015). If amplification efficiency is still too variable for accurate quantification then more targeted efforts to isolate mtDNA would be the only option left for quantification (Devall et al., 2015; Gould et al., 2016).

The Value of Quantifying Deletions Within *Drosophila*

The difficulty in comparing mtDNA deletion quantification within model organisms such as *Drosophila* to humans is the effects of a short lifespan on mtDNA deletion accumulation. Although in most cases this allows the effects of conditions to be manipulated and recorded in a controlled environment, deletion generation relies on time (Lakshmanan et al., 2018). With enough exposure to time and stress the mitochondrial genome will undergo sufficient cycles of replication so that deletions may be generated and clonally expanded. With sufficient expansion the impacts of these deletions on the organism's function and lifespan will be measurable. However, clonal expansion of mtDNA deletions is a private mechanism reserved for long-lived species. Simply put, most model organisms do not live long enough to see these effects build naturally and those under sufficient stresses to cause mtDNA deletions will likely die well before the desired effects are seen (Kauppila et al., 2018). As previously stated, with sufficient quality mtDNA extracted from *Drosophila* so that replicable deletion amplification is established, targeted quantification could then be reliably achieved. However, the question to then ask is if quantification is really required when the impacts of mtDNA deletions are mostly felt in organisms with longer lifespans? In conclusion, the quantification of deletions within *Drosophila* appears most useful when understanding the impacts of various stresses on deletion generation. The ability to manipulate and monitor stresses across so many individual

organisms at one time and then rapidly quantify these effects in terms of mtDNA deletion generation is an important tool. Using this tool, we would further understand if stresses can impact mtDNA deletion levels within *Drosophila*, which can translate across to all relevant organisms.

References

Ahlqvist, K. J., Hamalainen, R. H., Yatsuga, S., Uutela, M., Terzioglu, M., Gotz, A., Forsstrom, S., Salven, P., Angers-Loustau, A., Kopra, O. H., Tyynismaa, H., Larsson, N. G., Wartiovaara, K., Prolla, T., Trifunovic, A. & Suomalainen, A. (2012) Somatic Progenitor Cell Vulnerability to Mitochondrial DNA Mutagenesis Underlies Progeroid Phenotypes in Polg Mutator Mice. *Cell Metabolism,* 15(1)**,** 100-109.

Ahmed, N., Ronchi, D. & Comi, G. P. (2015) Genes and Pathways Involved in Adult Onset Disorders Featuring Muscle Mitochondrial DNA Instability. *International Journal of Molecular Sciences,* 16(8)**,** 18054-18076.

Alemayehu, S., Feghali, K. C., Cowden, J., Komisar, J., Ockenhouse, C. F. & Kamau, E. (2013) Comparative evaluation of published real-time PCR assays for the detection of malaria following MIQE guidelines. *Malaria Journal,* 12.

Alpatov, W. W. & Pearl, R. (1929) Experimental Studies on the Duration of Life. XII. Influence of Temperature during the Larval Period and Adult Life on the Duration of the Life of the Imago of Drosophila melanogaster.: The American Naturalist.

Ameur, A., Stewart, J. B., Freyer, C., Hagstrom, E., Ingman, M., Larsson, N. G. & Gyllensten, U. (2011) Ultra-Deep Sequencing of Mouse Mitochondrial DNA: Mutational Patterns and Their Origins. *Plos Genetics,* 7(3).

Andreu, A. L., Martinez, R., Marti, R. & Garcia-Arumi, E. (2009) Quantification of mitochondrial DNA copy number: Pre-analytical factors. *Mitochondrion,* 9(4)**,** 242-246.

Bai, R. K. & Wong, L. J. C. (2005) Simultaneous detection and quantification of mitochondrial DNA deletion(s), depletion, and over-replication in patients with mitochondrial disease. *Journal of Molecular Diagnostics,* 7(5)**,** 613-622.

Baker, D. J., Wijshake, T., Tchkonia, T., Lebrasseur, N. K., Childs, B. G., Van De Sluis, B., Kirkland, J. L. & Van Deursen, J. M. (2011) Clearance of p16(Ink4a)-positive senescent cells delays ageing-associated disorders. *Nature,* 479(7372)**,** 232-U112.

Balaban, R. S., Nemoto, S. & Finkel, T. (2005) Mitochondria, oxidants, and aging. *Cell,* 120(4)**,** 483-495.

Ballard, J. W. O. (2000) Comparative genomics of mitochondrial DNA in members of the Drosophila melanogaster subgroup. *Journal of Molecular Evolution,* 51(1)**,** 48-63.

Barnes, A. I., Wigby, S., Boone, J. M., Partridge, L. & Chapman, T. (2008) Feeding, fecundity and lifespan in female Drosophila melanogaster. *Proceedings of the Royal Society B-Biological Sciences,* 275(1643)**,** 1675-1683.

Bayona-Bafaluy, M. P., Blits, B., Battersby, B. J., Shoubridge, E. A. & Moraes, C. T. (2005) Rapid directional shift of mitochondrial DNA heteroplasmy in animal tissues by a mitochondrially targeted restriction endonuclease. *Proceedings of the National Academy of Sciences of the United States of America,* 102(40)**,** 14392-14397.

Beckman, K. B. & Ames, B. N. (1998) The free radical theory of aging matures. *Physiological Reviews,* 78(2)**,** 547-581.

Bender, A., Krishnan, K. J., Morris, C. M., Taylor, G. A., Reeve, A. K., Perry, R. H., Jaros, E., Hersheson, J. S., Betts, J., Klopstock, T., Taylor, R. W. & Turnbull, D. M. (2006) High levels of mitochondrial DNA deletions in substantia nigra neurons in aging and Parkinson disease. *Nature Genetics,* 38(5)**,** 515-517.

Bjelakovic, G., Nikolova, D., Gluud, L. L., Simonetti, R. G. & Gluud, C. (2007) Mortality in randomized trials of antioxidant supplements for primary and secondary prevention - Systematic review and meta-analysis. *Jama-Journal of the American Medical Association,* 297(8)**,** 842-857.

Bjelakovic, G., Nikolova, D., Gluud, L. L., Simonetti, R. G. & Gluud, C. (2012) Antioxidant supplements for prevention of mortality in healthy participants and patients with various diseases. *Cochrane Database of Systematic Reviews*(3).

Boczonadi, V. & Horvath, R. (2014) Mitochondria: Impaired mitochondrial translation in human disease. *International Journal of Biochemistry & Cell Biology,* 48**,** 77-84.

Bolotin, S., Deeks, S. L., Marchand-Austin, A., Rilkoff, H., Dang, V., Walton, R., Hashim, A., Farrell, D. & Crowcroft, N. S. (2015) Correlation of Real Time PCR Cycle Threshold Cut-Off with Bordetella pertussis Clinical Severity. *Plos One,* 10(7).

Boore, J. L. (1999) Animal mitochondrial genomes. *Nucleic Acids Research,* 27(8)**,** 1767-1780.

Booth, C. S., Pienaar, E., Termaat, J. R., Whitney, S. E., Louw, T. M. & Viljoen, H. J. (2010) Efficiency of the polymerase chain reaction. *Chemical Engineering Science,* 65(17)**,** 4996-5006.

Boveris, A. & Chance, B. (1973) MITOCHONDRIAL GENERATION OF HYDROGEN-PEROXIDE - GENERAL PROPERTIES AND EFFECT OF HYPERBARIC-OXYGEN. *Biochemical Journal,* 134(3)**,** 707-716.

Bratic, A., Kauppila, T. E. S., Macao, B., Gronke, S., Siibak, T., Stewart, J. B., Baggio, F., Dols, J., Partridge, L., Falkenberg, M., Wredenberg, A. & Larsson, N. G. (2015) Complementation between polymerase- and exonuclease-deficient mitochondrial DNA polymerase mutants in genomically engineered flies. *Nature Communications,* 6.

Bratic, A. & Larsson, N. G. (2013) The role of mitochondria in aging. *Journal of Clinical Investigation,* 123(3)**,** 951-957.

Brierley, E. J., Johnson, M. A., James, O. F. W. & Turnbull, D. M. (1997) Mitochondrial involvement in the ageing process. Facts and controversies. *Molecular and Cellular Biochemistry,* 174(1-2)**,** 325-328.

Bua, E., Johnson, J., Herbst, A., Delong, B., Mckenzie, D., Salamat, S. & Aiken, J. M. (2006) Mitochondrial DNA-deletion mutations accumulate intracellularly to

detrimental levels in aged human skeletal muscle fibers. *American Journal of Human Genetics,* 79(3)**,** 469-480.

Bustin, S. & Huggett, J. (2017) QPCR primer design revisited. *Biomolecular detection and quantification.*

Bustin, S. & Nolan, T. (2017) Talking the talk, but not walking the walk: RT-qPCR as a paradigm for the lack of reproducibility in molecular research. *European Journal of Clinical Investigation,* 47(10)**,** 756-774.

Bustin, S. A. (2002) Quantification of mRNA using real-time reverse transcription PCR (RT-PCR): trends and problems. *Journal of Molecular Endocrinology,* 29(1).

Bustin, S. A., Benes, V., Garson, J. A., Hellemans, J., Huggett, J., Kubista, M., Mueller, R., Nolan, T., Pfaffl, M. W., Shipley, G. L., Vandesompele, J. & Wittwer, C. T. (2009) The MIQE Guidelines: Minimum Information for Publication of Quantitative Real-Time PCR Experiments. *Clinical Chemistry,* 55(4)**,** 611-622.

Campisi, J. (2013) Aging, Cellular Senescence, and Cancer. *Annual Review of Physiology, Vol 75,* 75**,** 685-705.

Cankar, K., Stebih, D., Dreo, T., Zel, J. & Gruden, K. (2006) Critical points of DNA quantification by real-time PCR - effects of DNA extraction method and sample matrix on quantification of genetically modified organisms. *Bmc Biotechnology,* 6.

Cha, R. S. & Thilly, W. G. (1993) SPECIFICITY, EFFICIENCY, AND FIDELITY OF PCR. *Pcr-Methods and Applications,* 3(3)**,** S18-S29.

Chandrasekaran, A., Idelchik, M. D. S. & Melendez, J. A. (2017) Redox control of senescence and age-related disease. *Redox Biology,* 11**,** 91-102.

Charlesworth, B. & Partridge, L. (1997) Ageing: Levelling of the grim reaper. *Current Biology,* 7(7)**,** R440-R442.

Chen, H., Rangasamy, M., Tan, S. Y., Wang, H. C. & Siegfried, B. D. (2010) Evaluation of Five Methods for Total DNA Extraction from Western Corn Rootworm Beetles. *Plos One,* 5(8).

Chen, J. Q., Cammarata, P. P., Baines, C. P. & Yager, J. D. (2009) Regulation of mitochondrial respiratory chain biogenesis by estrogens/estrogen receptors and physiological, pathological and pharmacological implications. *Biochimica Et Biophysica Acta-Molecular Cell Research,* 1793(10)**,** 1540-1570.

Chen, T. B., Xun, Z., Lin, J. P., Liu, C., Fu, Y., Wu, W. N., Fu, X. C., Hu, Y. H. & Ou, Q. S. (2017) Real-time PCR for quantitative detection of mitochondrial DNA from peripheral blood mononuclear cell in patients with HBV-related hepatocellular carcinoma. *International Journal of Clinical and Experimental Medicine,* 10(3)**,** 5629-5636.

Chen, X. J. & Butow, R. A. (2005) The organization and inheritance of the mitochondrial genome. *Nature Reviews Genetics,* 6(11)**,** 815-825.

Chen, Y. C., Umanah, G. K. E., Dephoure, N., Andrabi, S. A., Gygi, S. P., Dawson, T. M., Dawson, V. L. & Rutter, J. (2014) Msp1/ATAD1 maintains mitochondrial function by facilitating the degradation of mislocalized tail-anchored proteins. *Embo Journal,* 33(14)**,** 1548-1564.

Chinnery, P. F., Johnson, M. A., Wardell, T. M., Singh-Kler, R., Hayes, C., Brown, D. T., Taylor, R. W., Bindoff, L. A. & Turnbull, D. M. (2000) The epidemiology of pathogenic mitochondrial DNA mutations. *Annals of Neurology,* 48(2)**,** 188-193.

Choi, J. S., Choi, K. M. & Lee, C. K. (2011) Caloric restriction improves efficiency and capacity of the mitochondrial electron transport chain in Saccharomyces cerevisiae. *Biochemical and Biophysical Research Communications,* 409(2)**,** 308-314.

Chomczynski, P. & Sacchi, N. (1987) SINGLE-STEP METHOD OF RNA ISOLATION BY ACID GUANIDINIUM THIOCYANATE PHENOL CHLOROFORM EXTRACTION. *Analytical Biochemistry,* 162(1)**,** 156-159.

Chuang, L. Y., Cheng, Y. H. & Yang, C. H. (2013) Specific primer design for the polymerase chain reaction. *Biotechnology Letters,* 35(10)**,** 1541-1549.

Circu, M. L. & Aw, T. Y. (2010) Reactive oxygen species, cellular redox systems, and apoptosis. *Free Radical Biology and Medicine,* 48(6)**,** 749-762.

Clayton, D. A. (1982) REPLICATION OF ANIMAL MITOCHONDRIAL-DNA. *Cell,* 28(4)**,** 693-705.

Cocheme, H. M., Quin, C., Mcquaker, S. J., Cabreiro, F., Logan, A., Prime, T. A., Abakumova, I., Patel, J. V., Fearnley, I. M., James, A. M., Porteous, C. M., Smith, R. A. J., Saeed, S., Carre, J. E., Singer, M., Gems, D., Hartley, R. C., Partridge, L. & Murphy, M. P. (2011) Measurement of H2O2 within Living Drosophila during Aging Using a Ratiometric Mass Spectrometry Probe Targeted to the Mitochondrial Matrix. *Cell Metabolism,* 13(3)**,** 340-350.

Colman, R. J., Anderson, R. M., Johnson, S. C., Kastman, E. K., Kosmatka, K. J., Beasley, T. M., Allison, D. B., Cruzen, C., Simmons, H. A., Kemnitz, J. W. & Weindruch, R. (2009) Caloric Restriction Delays Disease Onset and Mortality in Rhesus Monkeys. *Science,* 325(5937)**,** 201-204.

Copeland, W. C. (2012) Defects in mitochondrial DNA replication and human disease. *Critical Reviews in Biochemistry and Molecular Biology,* 47(1)**,** 64-74.

Corraldebrinski, M., Horton, T., Lott, M. T., Shoffner, J. M., Mckee, A. C., Beal, M. F., Graham, B. H. & Wallace, D. C. (1994) MARKED CHANGES IN MITOCHONDRIAL-DNA DELETION LEVELS IN ALZHEIMER BRAINS. *Genomics,* 23(2)**,** 471-476.

Correa, C. C., Aw, W., Melvin, R. G., Pichaud, N. & Ballard, J. W. O. (2012) Mitochondrial DNA variants influence mitochondrial bioenergetics in Drosophila melanogaster. *Mitochondrion,* 12(4)**,** 459-464.

Coutlee, F. & Voyer, H. (1998) Effect of nonionic detergents on amplification of human papillomavirus DNA with consensus primers MY09 and MY11. *Journal of Clinical Microbiology,* 36(4)**,** 1164-1164.

Cree, L. M., Samuels, D. C., Lopes, S., Rajasimha, H. K., Wonnapinij, P., Mann, J. R., Dahl, H. H. M. & Chinnery, P. F. (2008) A reduction of mitochondrial DNA molecules during embryogenesis explains the rapid segregation of genotypes. *Nature Genetics,* 40(2)**,** 249-254.

Dai, D. F., Rabinovitch, P. S. & Ungvari, Z. (2012) Mitochondria and Cardiovascular Aging. *Circulation Research,* 110(8)**,** 1109-1124.

Dang, J., Mendez, P., Lee, S., Kim, J. W., Yoon, J. H., Kim, T. W., Sailey, C. J., Jablons, D. M. & Kim, I. J. (2016) Development of a robust DNA quality and quantity assessment qPCR assay for targeted next-generation sequencing library preparation. *International Journal of Oncology,* 49(4)**,** 1755-1765.

Dani, M. A. C., Dani, S. U., Lima, S. P. G., Martinez, A., Rossi, B. M., Soares, F., Zago, M. A. & Simpson, A. J. G. (2004) Less DeltamtDNA4977 than normal in various

types of tumors suggests that cancer cells are essentially free of this mutation. *Genetics and molecular research : GMR,* 3(3)**,** 395-409.

Dayama, G., Emery, S. B., Kidd, J. M. & Mills, R. E. (2014) The genomic landscape of polymorphic human nuclear mitochondrial insertions. *Nucleic Acids Research,* 42(20)**,** 12640-12649.

De Bont, R. & Van Larebeke, N. (2004) Endogenous DNA damage in humans: a review of quantitative data. *Mutagenesis,* 19(3)**,** 169-185.

De Ronde, M. W. J., Ruijter, J. M., Lanfear, D., Bayes-Genis, A., Kok, M. G. M., Creemers, E. E., Pinto, Y. M. & Pinto-Sietsma, S. J. (2017) Practical data handling pipeline improves performance of qPCR-based circulating miRNA measurements. *Rna,* 23(5)**,** 811-821.

Debode, F., Marien, A., Janssen, E., Bragard, C. & Berben, G. (2017) The influence of amplicon length on real-time PCR results. *Biotechnologie Agronomie Societe Et Environnement,* 21(1)**,** 3-11.

Denno, M. E., Privman, E. & Venton, B. J. (2015) Analysis of Neurotransmitter Tissue Content of Drosophila melanogaster in Different Life Stages. *Acs Chemical Neuroscience,* 6(1)**,** 117-123.

Devall, M., Burrage, J., Caswell, R., Johnson, M., Troakes, C., Al-Sarraj, S., Jeffries, A. R., Mill, J. & Lunnon, K. (2015) A comparison of mitochondrial DNA isolation methods in frozen post-mortem human brain tissue-applications for studies of mitochondrial genetics in brain disorders. *Biotechniques,* 59(4)**,** 241-246.

Doonan, R., Mcelwee, J. J., Matthijssens, F., Walker, G. A., Houthoofd, K., Back, P., Matscheski, A., Vanfleteren, J. R. & Gems, D. (2008) Against the oxidative damage theory of aging: superoxide dismutases protect against oxidative stress but have little or no effect on life span in Caenorhabditis elegans. *Genes & Development,* 22(23)**,** 3236-3241.

Droge, W. (2002) Free radicals in the physiological control of cell function. *Physiological Reviews,* 82(1)**,** 47-95.

Du, Z. D., Hu, Y. J., Yang, Y., Sun, Y., Zhang, S. L., Zhou, T., Zeng, L. L., Zhang, W. J., Huang, X., Kong, W. J. & Zhang, H. L. (2012) NADPH oxidase-dependent oxidative stress and mitochondrial damage in hippocampus of D-galactose-induced aging rats. *Journal of Huazhong University of Science and Technology-Medical Sciences,* 32(4)**,** 466-472.

Durham, S. E., Samuels, D. C. & Chinnery, P. F. (2006) Is selection required for the accumulation of somatic mitochondrial DNA mutations in post-mitotic cells? *Neuromuscular Disorders,* 16(6)**,** 381-386.

Edgar, D., Shabalina, I., Camara, Y., Wredenberg, A., Calvaruso, M. A., Nijtmans, L., Nedergaard, J., Cannon, B., Larsson, N. G. & Trifunovic, A. (2009) Random Point Mutations with Major Effects on Protein-Coding Genes Are the Driving Force behind Premature Aging in mtDNA Mutator Mice. *Cell Metabolism,* 10(2)**,** 131-138.

El Bali, L., Diman, A., Bernard, A., Roosens, N. H. C. & De Keersmaecker, S. C. J. (2014) Comparative study of seven commercial kits for human DNA extraction from urine samples suitable for DNA biomarker-based public health studies. *Journal of biomolecular techniques : JBT,* 25(4)**,** 96-110.

Ernster, L. & Schatz, G. (1981) MITOCHONDRIA - A HISTORICAL REVIEW. *Journal of Cell Biology,* 91(3)**,** S227-S255.

Fahlstrom, A., Yu, Q. & Ulfahke, B. (2011) Behavioral changes in aging female C57BL/6 mice. *Neurobiology of Aging,* 32(10)**,** 1868-1880.

Falkenberg, M. (2018) Mitochondrial DNA replication in mammalian cells: overview of the pathway. *Mitochondrial Diseases,* 62(3)**,** 287-296.

Farr, C. L., Wang, Y. X. & Kaguni, L. S. (1999) Functional interactions of mitochondrial DNA polymerase and single-stranded DNA-binding protein - Template-primer DNA binding and initiation and elongation of DNA strand synthesis. *Journal of Biological Chemistry,* 274(21)**,** 14779-14785.

Fayet, G., Jansson, M., Sternberg, D., Moslemi, A. R., Blondy, P., Lombes, A., Fardeau, M. & Oldfors, A. (2002) Ageing muscle: clonal expansions of mitochondrial DNA point mutations and deletions cause focal impairment of mitochondrial function. *Neuromuscular Disorders,* 12(5)**,** 484-493.

Feleciano, D. R. & Kirstein, J. (2016) Collapse of redox homeostasis during aging and stress. *Molecular & Cellular Oncology,* 3(2).

Flatt, T. (2011) Survival costs of reproduction in Drosophila. *Experimental Gerontology,* 46(5)**,** 369-375.

Forootan, A., Sjoback, R., Bjorkman, J., Sjogreen, B., Linz, L. & Kubista, M. (2017) Methods to determine limit of detection and limit of quantification in quantitative real-time PCR (qPCR). *Biomolecular detection and quantification,* 12**,** 1-6.

Fukui, H. & Moraes, C. T. (2009) Mechanisms of formation and accumulation of mitochondrial DNA deletions in aging neurons. *Human Molecular Genetics,* 18(6)**,** 1028-1036.

Furda, A. M., Bess, A. S., Meyer, J. N. & Van Houten, B. (2012) Analysis of DNA damage and repair in nuclear and mitochondrial DNA of animal cells using quantitative PCR. *Methods in molecular biology (Clifton, N.J.),* 920**,** 111-32.

Fykse, E. M., Olsen, J. S. & Skogan, G. (2003) Application of sonication to release DNA from Bacillus cereus for quantitative detection by real-time PCR. *Journal of Microbiological Methods,* 55(1)**,** 1-10.

Gabaldon, T. & Huynen, M. A. (2007) From endosymbiont to host-controlled organelle: The hijacking of mitochondrial protein synthesis and metabolism. *Plos Computational Biology,* 3(11)**,** 2209-2218.

Gao, Y., Wolf, L. K. & Georgiadis, R. M. (2006) Secondary structure effects on DNA hybridization kinetics: a solution versus surface comparison. *Nucleic Acids Research,* 34(11)**,** 3370-3377.

Gardner, A. & Welch, J. J. (2011) A formal theory of the selfish gene. *Journal of Evolutionary Biology,* 24(8)**,** 1801-1813.

Gates, K. S. (2009) An Overview of Chemical Processes That Damage Cellular DNA: Spontaneous Hydrolysis, Alkylation, and Reactions with Radicals. *Chemical Research in Toxicology,* 22(11)**,** 1747-1760.

Gaziev, A. I. & Shaikhaev, G. O. (2010) Nuclear mitochondrial pseudogenes. *Molecular Biology,* 44(3)**,** 358-368.

Giordano, C., Montopoli, M., Perli, E., Orlandi, M., Fantin, M., Ross-Cisneros, F. N., Caparrotta, L., Martinuzzi, A., Ragazzi, E., Ghelli, A., Sadun, A. A., D'amati, G. & Carelli, V. (2011) Oestrogens ameliorate mitochondrial dysfunction in Leber's hereditary optic neuropathy. *Brain,* 134**,** 220-234.

Goffart, S., Cooper, H. M., Tyynismaa, H., Wanrooij, S., Suomalainen, A. & Spelbrink, J. N. (2009) Twinkle mutations associated with autosomal dominant progressive external ophthalmoplegia lead to impaired helicase function and in vivo mtDNA replication stalling. *Human Molecular Genetics,* 18(2)**,** 328-340.

Gomez, L. A. & Hagen, T. M. (2012) Age-related decline in mitochondrial bioenergetics: Does supercomplex destabilization determine lower oxidative capacity and higher superoxide production? *Seminars in Cell & Developmental Biology,* 23(7)**,** 758-767.

Gould, M. P., Bosworth, C. M., Mcmahon, S., Grandhi, S., Grimberg, B. T. & Laframboise, T. (2016) PCR-Free Enrichment of Mitochondrial DNA from Human Blood and Cell Lines for High Quality Next-Generation DNA Sequencing (vol 10, e0139253, 2015). *Plos One,* 11(5).

Grady, J. P., Murphy, J. L., Blakely, E. L., Haller, R. G., Taylor, R. W., Turnbull, D. M. & Tuppen, H. A. L. (2014) Accurate Measurement of Mitochondrial DNA Deletion Level and Copy Number Differences in Human Skeletal Muscle. *Plos One,* 9(12).

Gray, M. W. (2012) Mitochondrial Evolution. *Cold Spring Harbor Perspectives in Biology,* 4(9).

Graziewicz, M. A., Longley, M. J. & Copeland, W. C. (2006) DNA polymerase gamma in mitochondrial DNA replication and repair. *Chemical Reviews,* 106(2)**,** 383-405.

Grotewiel, M. S., Martin, I., Bhandari, P. & Cook-Wiens, E. (2005) Functional senescence in Drosophila melanogaster. *Ageing Research Reviews,* 4(3)**,** 372-397.

Gruber, J., Chen, C. B., Fong, S., Ng, L. F., Teo, E. & Halliwell, B. (2015) Caenorhabditis elegans: What We Can and Cannot Learn from Aging Worms. *Antioxidants & Redox Signaling,* 23(3)**,** 256-279.

Guo, W., Jiang, L., Bhasin, S., Khan, S. M. & Swerdlow, R. H. (2009) DNA extraction procedures meaningfully influence qPCR-based mtDNA copy number determination. *Mitochondrion,* 9(4)**,** 261-265.

Guo, X. H., Kudryavtseva, E., Bodyak, N., Nicholas, A., Dombrovsky, I., Yang, D. Y., Kraytsberg, Y., Simon, D. K. & Khrapko, K. (2010) Mitochondrial DNA deletions in mice in men: Substantia nigra is much less affected in the mouse. *Biochimica Et Biophysica Acta-Bioenergetics,* 1797(6-7)**,** 1159-1162.

Haag-Liautard, C., Coffey, N., Houle, D., Lynch, M., Charlesworth, B. & Keightley, P. D. (2008) Direct estimation of the mitochondrial DNA mutation rate in Drosophila melanogaster. *Plos Biology,* 6(8)**,** 1706-1714.

Haigis, M. C. & Yankner, B. A. (2010) The Aging Stress Response. *Molecular Cell,* 40(2)**,** 333-344.

Harbottle, A., Krishnan, K. J. & Birch-Machin, M. A. (2004) Implications of using the ND1 gene as a control region for real-time PCR analysis of mitochondrial DNA deletions in human skin. *Journal of Investigative Dermatology,* 122(6)**,** 1518-1521.

Harman, D. (1956) AGING - A THEORY BASED ON FREE-RADICAL AND RADIATION-CHEMISTRY. *Journals of Gerontology,* 11(3)**,** 298-300.

Harman, D. (1972) The biologic clock: the mitochondria? 4 ed.: *Journal of the American Geriatrics Society.*

Harman, D. (2006) Free Radical Theory of Aging: An Update Increasing the Functional Life Span. *Understanding and Modulating Aging,* 1067**,** 10-21.

Hayflick, L. (1965) LIMITED IN VITRO LIFETIME OF HUMAN DIPLOID CELL STRAINS. *Experimental Cell Research,* 37(3)**,** 614-&.

Hazkani-Covo, E., Zeller, R. M. & Martin, W. (2010) Molecular Poltergeists: Mitochondrial DNA Copies (numts) in Sequenced Nuclear Genomes. *Plos Genetics,* 6(2).

He, L. P., Chinnery, P. F., Durham, S. E., Blakely, E. L., Wardell, T. M., Borthwick, G. M., Taylor, R. W. & Turnbull, D. M. (2002) Detection and quantification of mitochondrial DNA deletions in individual cells by real-time PCR. *Nucleic Acids Research,* 30(14).

Helbock, H. J., Beckman, K. B. & Ames, B. N. (1999) 8-hydroxydeoxyguanosine and 8-hydroxyguanine as biomarkers of oxidative DNA damage. *Oxidants and Antioxidants, Pt B,* 300**,** 156-166.

Herbener, G. H. (1976) MORPHOMETRIC STUDY OF AGE-DEPENDENT CHANGES IN MITOCHONDRIAL POPULATIONS OF MOUSE-LIVER AND HEART. *Journals of Gerontology,* 31(1)**,** 8-12.

Herbst, A., Pak, J. W., Mckenzie, D., Bua, E., Bassiouni, M. & Aiken, J. M. (2007) Accumulation of mitochondrial DNA deletion mutations in aged muscle fibers: Evidence for a causal role in muscle fiber loss. *Journals of Gerontology Series a-Biological Sciences and Medical Sciences,* 62(3)**,** 235-245.

Holmbeck, M. A., Donner, J. R., Villa-Cuesta, E. & Rand, D. M. (2015) A Drosophila model for mito-nuclear diseases generated by an incompatible interaction between tRNA and tRNA synthetase. *Disease Models & Mechanisms,* 8(8)**,** 843-U530.

Holt, I. J., Harding, A. E., Cooper, J. M., Schapira, A. H. V., Toscano, A., Clark, J. B. & Morganhughes, J. A. (1989) MITOCHONDRIAL MYOPATHIES - CLINICAL AND BIOCHEMICAL FEATURES OF 30 PATIENTS WITH MAJOR DELETIONS OF MUSCLE MITOCHONDRIAL-DNA. *Annals of Neurology,* 26(6)**,** 699-708.

Holt, I. J., Lorimer, H. E. & Jacobs, H. T. (2000) Coupled leading- and lagging-strand synthesis of mammalian mitochondrial DNA. *Cell,* 100(5)**,** 515-524.

Holt, I. J. & Reyes, A. (2012) Human Mitochondrial DNA Replication. *Cold Spring Harbor Perspectives in Biology,* 4(12).

Holzenberger, M., Dupont, J., Ducos, B., Leneuve, P., Geloen, A., Even, P. C., Cervera, P. & Le Bouc, Y. (2003) IGF-1 receptor regulates lifespan and resistance to oxidative stress in mice. *Nature,* 421(6919)**,** 182-187.

Huggett, J. & Bustin, S. A. (2011) Standardisation and reporting for nucleic acid quantification. *Accreditation and Quality Assurance,* 16(8-9)**,** 399-405.

Huggett, J. F., Foy, C. A., Benes, V., Emslie, K., Garson, J. A., Haynes, R., Hellemans, J., Kubista, M., Nolan, R., Pfaffl, M. W., Shipley, G. L., Vandesompele, J., Wittwer, C. T. & Bustin, S. A. (2013) The Digital MIQE Guidelines: Minimum Information for Publication of Quantitative Digital PCR Experiments. *Clinical Chemistry,* 59(6)**,** 892-902.

Humble, M. M., Young, M. J., Foley, J. F., Pandiri, A. R., Travlos, G. S. & Copeland, W. C. (2013) Polg2 is essential for mammalian embryogenesis and is required for mtDNA maintenance. *Human Molecular Genetics,* 22(5)**,** 1017-1025.

Iliadi, K. G. & Boulianne, G. L. (2010) Age-related behavioral changes in Drosophila. *Aging, Cancer, and Age-Related Diseases: Common Mechanism?,* 1197**,** 9-18.

Iwai, K., Miyao, M., Wadano, Y. & Iwamura, Y. (2003) Dynamic changes of deleted mitochondrial DNA in human leucocytes after endurance exercise. *European Journal of Applied Physiology,* 88(6)**,** 515-519.

Jackson, M. J. & Mcardle, A. (2016) Role of reactive oxygen species in age-related neuromuscular deficits. *Journal of Physiology-London,* 594(8)**,** 1979-1988.

Jensen, K., Sanchez-Garcia, J., Williams, C., Khare, S., Mathur, K., Graze, R. M., Hahn, D. A., Mcintyre, L. M., Rincon-Limas, D. E. & Fernandez-Funez, P. (2013) Purification of Transcripts and Metabolites from Drosophila Heads. *Jove-Journal of Visualized Experiments*(73).

Jezierska-Drutel, A., Rosenzweig, S. A. & Neumann, C. A. (2013) Role of Oxidative Stress and the Microenvironment in Breast Cancer Development and Progression. *Advances in Cancer Research, Vol 119,* 119**,** 107-125.

Johnson, T. E. (2006) Recent results: Biomarkers of aging. *Experimental Gerontology,* 41(12)**,** 1243-1246.

Johnston, I. G., Burgstaller, J. P., Havlicek, V., Kolbe, T., Rulicke, T., Brem, G., Poulton, J. & Jones, N. S. (2015) Stochastic modelling, Bayesian inference, and new in vivo measurements elucidate the debated mtDNA bottleneck mechanism. *Elife,* 4.

Kamenisch, Y., Fousteri, M., Knoch, J., Von Thaler, A. K., Fehrenbacher, B., Kato, H., Becker, T., Dolle, M. E. T., Kuiper, R., Majora, M., Schaller, M., Van Der Horst, G. T. J., Van Steeg, H., Rocken, M., Rapaport, D., Krutmann, J., Mullenders, L. H. & Berneburg, M. (2010) Proteins of nucleotide and base excision repair pathways interact in mitochondria to protect from loss of subcutaneous fat, a hallmark of aging. *Journal of Experimental Medicine,* 207(2)**,** 379-390.

Kang, C. M., Kristal, B. S. & Yu, B. P. (1998) Age-related mitochondrial DNA deletions: Effect of dietary restriction. *Free Radical Biology and Medicine,* 24(1)**,** 148-154.

Kao, S. H., Chao, H. T. & Wei, Y. H. (1995) MITOCHONDRIAL DEOXYRIBONUCLEIC-ACID 4977-BP DELETION IS ASSOCIATED WITH DIMINISHED FERTILITY AND MOTILITY OF HUMAN SPERM. *Biology of Reproduction,* 52(4)**,** 729-736.

Kapahi, P., Zid, B. M., Harper, T., Koslover, D., Sapin, V. & Benzer, S. (2004) Regulation of lifespan in Drosophila by modulation of genes in the TOR signaling pathway. *Current Biology,* 14(10)**,** 885-890.

Katevatis, C., Fan, A. & Klapperich, C. M. (2017) Low concentration DNA extraction and recovery using a silica solid phase. *Plos One,* 12(5).

Kauppila, T. E. S., Bratic, A., Jensen, M. B., Baggio, F., Partridge, L., Jasper, H., Gronke, S. & Larsson, N. G. (2018) Mutations of mitochondrial DNA are not major contributors to aging of fruit flies. *Proceedings of the National Academy of Sciences of the United States of America,* 115(41), E9620-E9629.

Kauppila, T. E. S., Kauppila, J. H. K. & Larsson, N. G. (2017) Mammalian Mitochondria and Aging: An Update. *Cell Metabolism,* 25(1)**,** 57-71.

Kazachkova, N., Ramos, A., Santos, C. & Lima, M. (2013) Mitochondrial DNA Damage Patterns and Aging: Revising the Evidences for Humans and Mice. *Aging and Disease,* 4(6)**,** 337-350.

Kazak, L., Reyes, A. & Holt, I. J. (2012) Minimizing the damage: repair pathways keep mitochondrial DNA intact. *Nature Reviews Molecular Cell Biology,* 13(10)**,** 659-671.

Kennedy, S. R., Salk, J. J., Schmitt, M. W. & Loeb, L. A. (2013) Ultra-Sensitive Sequencing Reveals an Age-Related Increase in Somatic Mitochondrial Mutations That Are Inconsistent with Oxidative Damage. *Plos Genetics,* 9(9).

Kirkwood, T. B. L. & Holliday, R. (1979) EVOLUTION OF AGING AND LONGEVITY. *Proceedings of the Royal Society Series B-Biological Sciences,* 205(1161)**,** 531-546.

Knuever, J., Poeggeler, B., Gaspar, E., Klinger, M., Hellwig-Burgel, T., Hardenbicker, C., Toth, B. I., Biro, T. & Paus, R. (2012) Thyrotropin-Releasing Hormone Controls Mitochondrial Biology in Human Epidermis. *Journal of Clinical Endocrinology & Metabolism,* 97(3)**,** 978-986.

Koonin, E. V. (2010) The origin and early evolution of eukaryotes in the light of phylogenomics. *Genome Biology,* 11(5).

Koopman, R. & Van Loon, L. J. C. (2009) Aging, exercise, and muscle protein metabolism. *Journal of Applied Physiology,* 106(6)**,** 2040-2048.

Korhonen, J. A., Gaspari, M. & Falkenberg, M. (2003) TWINKLE has 5 '-> 3 ' DNA helicase activity and is specifically stimulated by mitochondrial single-stranded DNA-binding protein. *Journal of Biological Chemistry,* 278(49)**,** 48627-48632.

Kralik, P. & Ricchi, M. (2017) A Basic Guide to Real Time PCR in Microbial Diagnostics: Definitions, Parameters, and Everything. *Frontiers in Microbiology,* 8.

Krishnan, K. J., Reeve, A. K., Samuels, D. C., Chinnery, P. F., Blackwood, J. K., Taylor, R. W., Wanrooij, S., Spelbrink, J. N., Lightowlers, R. N. & Turnbull, D. M. (2008) What causes mitochondrial DNA deletions in human cells? *Nature Genetics,* 40(3)**,** 275-279.

Krizhanovsky, V., Yon, M., Dickins, R. A., Hearn, S., Simon, J., Miething, C., Yee, H., Zender, L. & Lowe, S. W. (2008) Senescence of activated stellate cells limits liver fibrosis. *Cell,* 134(4)**,** 657-667.

Kuilman, T., Michaloglou, C., Mooi, W. J. & Peeper, D. S. (2010) The essence of senescence. *Genes & Development,* 24(22)**,** 2463-2479.

Lakshmanan, L. N., Yee, Z., Ng, L. F., Gunawan, R., Halliwell, B. & Gruber, J. (2018) Clonal expansion of mitochondrial DNA deletions is a private mechanism of aging in long-lived animals. *Aging Cell,* 17(5).

Lance, R. F. & Guan, X. (2020) Variation in inhibitor effects on qPCR assays and implications for eDNA surveys. *Canadian Journal of Fisheries and Aquatic Sciences,* 77(1)**,** 23-33.

Larsson, N. G. (2010) Somatic Mitochondrial DNA Mutations in Mammalian Aging. *Annual Review of Biochemistry, Vol 79,* 79**,** 683-706.

Le, A. V. P., Huang, D. X., Blick, T., Thompson, E. W. & Dobrovic, A. (2015) An optimised direct lysis method for gene expression studies on low cell numbers. *Scientific Reports,* 5.

Lee, D. Y. & Clayton, D. A. (1998) Initiation of mitochondrial DNA replication by transcription and R-loop processing. *Journal of Biological Chemistry,* 273(46)**,** 30614-30621.

Lee, H. C. & Wei, Y. H. (2007) Oxidative stress, mitoichondrial DNA mutation, and apoptosis in aging. *Experimental Biology and Medicine,* 232(5)**,** 592-606.

Lee, H. F., Lee, H. J., Chi, C. S., Tsai, C. R., Chang, T. K. & Wang, C. J. (2007) The neurological evolution of Pearson syndrome: Case report and literature review. *European Journal of Paediatric Neurology,* 11(4)**,** 208-214.

Lee, H. R. & Johnson, K. A. (2006) Fidelity of the human mitochondrial DNA polymerase. *Journal of Biological Chemistry,* 281(47)**,** 36236-36240.

Lewis, K. N., Andziak, B., Yang, T. & Buffenstein, R. (2013) The Naked Mole-Rat Response to Oxidative Stress: Just Deal with It. *Antioxidants & Redox Signaling,* 19(12)**,** 1388-1399.

Li, X. Y., Fang, P., Mai, J. T., Choi, E. T., Wang, H. & Yang, X. F. (2013) Targeting mitochondrial reactive oxygen species as novel therapy for inflammatory diseases and cancers. *Journal of Hematology & Oncology,* 6.

Lisanti, M. P., Martinez-Outschoorn, U. E., Pavlides, S., Whitaker-Menezes, D., Pestell, R. G., Howell, A. & Sotgia, F. (2011) Accelerated aging in the tumor microenvironment Connecting aging, inflammation and cancer metabolism with personalized medicine. *Cell Cycle,* 10(13)**,** 2059-2063.

Livak, K. J. & Schmittgen, T. D. (2001) Analysis of relative gene expression data using real-time quantitative PCR and the 2(T)(-Delta Delta C) method. *Methods,* 25(4)**,** 402-408.

Lopez-Gallardo, E., Lopez-Perez, M. J., Montoya, J. & Ruiz-Pesini, E. (2009) CPEO and KSS differ in the percentage and location of the mtDNA deletion. *Mitochondrion,* 9(5)**,** 314-317.

Lopez-Otin, C., Blasco, M. A., Partridge, L., Serrano, M. & Kroemer, G. (2013) The Hallmarks of Aging. *Cell,* 153(6)**,** 1194-1217.

Lorenz, T. C. (2012) Polymerase Chain Reaction: Basic Protocol Plus Troubleshooting and Optimization Strategies. *Jove-Journal of Visualized Experiments*(63).

Lott, M. T., Leipzig, J. N., Derbeneva, O., Xie, H. M., Chalkia, D., Sarmady, M., Procaccio, V. & Wallace, D. C. (2013) mtDNA Variation and Analysis Using Mitomap and Mitomaster. *Current protocols in bioinformatics,* 44**,** 1.23.1-26.

Madreiter-Sokolowski, C. T., Sokolowski, A. A., Waldeck-Weiermair, M., Malli, R. & Graier, W. F. (2018) Targeting Mitochondria to Counteract Age-Related Cellular Dysfunction. *Genes,* 9(3).

Manczak, M., Jung, Y. S., Park, B. S., Partovi, D. & Reddy, P. H. (2005) Time-course of mitochondrial gene expressions in mice brains: implications for mitochondrial dysfunction, oxidative damage, and cytochrome c in aging. *Journal of Neurochemistry,* 92(3)**,** 494-504.

Mangialasche, F., Polidori, M. C., Monastero, R., Ercolani, S., Camarda, C., Cecchetti, R. & Mecocci, P. (2009) Biomarkers of oxidative and nitrosative damage in Alzheimer's disease and mild cognitive impairment. *Ageing Research Reviews,* 8(4)**,** 285-305.

Mao, P. Z., Gallagher, P., Nedungadi, S., Manczak, M., Shirendeb, U. P., Kohama, S. G., Ferguson, B., Park, B. S. & Reddy, P. H. (2012) Mitochondrial DNA deletions and differential mitochondrial DNA content in Rhesus monkeys: Implications for aging. *Biochimica Et Biophysica Acta-Molecular Basis of Disease,* 1822(2)**,** 111-119.

Margulis, L. & Sagan, D. (2000) Origin of eukaryotic cells (Reprinted). *Recherche*(331)**,** 81-84.

Martin, L. J. (2012) Biology of Mitochondria in Neurodegenerative Diseases. *Molecular Biology of Neurodegenerative Diseases,* 107**,** 355-415.

Masoro, E. J. (2005) Overview of caloric restriction and ageing. *Mechanisms of Ageing and Development,* 126(9)**,** 913-922.

Massudi, H., Grant, R., Braidy, N., Guest, J., Farnsworth, B. & Guillemin, G. J. (2012) Age-Associated Changes In Oxidative Stress and NAD(+) Metabolism In Human Tissue. *Plos One,* 7(7).

Mccord, B., Pionzio, A. & Thompson, R. (2015) Analysis of the Effect of a Variety of PCR Inhibitors on the Amplification of DNA using Real Time PCR, Melt Curves and STR Analysis.

Mccord, J. M. & Fridovic.I (1969) SUPEROXIDE DISMUTASE AN ENZYMIC FUNCTION FOR ERYTHROCUPREIN (HEMOCUPREIN). *Journal of Biological Chemistry,* 244(22)**,** 6049-&.

Mckinney, E. A. & Oliveira, M. T. (2013) Replicating animal mitochondrial DNA. *Genetics and Molecular Biology,* 36(3)**,** 308-315.

Medawar, P. B. (1952) *An unsolved problem of Biology*.

Meissner, C., Bruse, P., Mohamed, S. A., Schulz, A., Warnk, H., Storm, T. & Oehmichen, M. (2008) The 4977 bp deletion of mitochondrial DNA in human skeletal muscle, heart and different areas of the brain: A useful biomarker or more? *Experimental Gerontology,* 43(7)**,** 645-652.

Melov, S., Lithgow, G. J., Fischer, D. R., Tedesco, P. M. & Johnson, T. E. (1995) INCREASED FREQUENCY OF DELETIONS IN THE MITOCHONDRIAL GENOME WITH AGE OF CAENORHABDITIS-ELEGANS. *Nucleic Acids Research,* 23(8)**,** 1419-1425.

Melov, S., Schneider, J. A., Coskun, P. E., Bennett, D. A. & Wallace, D. C. (1999) Mitochondrial DNA rearrangements in aging human brain and in situ PCR of mtDNA. *Neurobiology of Aging,* 20(5)**,** 565-571.

Melvin, R. G. & Ballard, J. W. O. (2011) Females With a Mutation in a Nuclear-Encoded Mitochondrial Protein Pay a Higher Cost of Survival Than Do Males in Drosophila. *Journals of Gerontology Series a-Biological Sciences and Medical Sciences,* 66(7)**,** 765-770.

Mena, N. P., Urrutia, P. J., Lourido, F., Carrasco, C. M. & Nunez, M. T. (2015) Mitochondrial iron homeostasis and its dysfunctions in neurodegenerative disorders. *Mitochondrion,* 21**,** 92-105.

Mockett, R. J., Sohal, B. H. & Sohal, R. S. (2010) Expression of multiple copies of mitochondrially targeted catalase or genomic Mn superoxide dismutase transgenes does not extend the life span of Drosophila melanogaster. *Free Radical Biology and Medicine,* 49(12)**,** 2028-2031.

Muller, F. L., Lustgarten, M. S., Jang, Y., Richardson, A. & Van Remmen, H. (2007) Trends in oxidative aging theories. *Free Radical Biology and Medicine,* 43(4)**,** 477-503.

Murphy, M. P. (2009) How mitochondria produce reactive oxygen species. *Biochemical Journal,* 417**,** 1-13.

Murray, D. B., Beckmann, M. & Kitano, H. (2007) Regulation of yeast oscillatory dynamics. *Proceedings of the National Academy of Sciences of the United States of America,* 104(7)**,** 2241-2246.

Nacheva, E., Mokretar, K., Soenmez, A., Pittman, A. M., Grace, C., Valli, R., Ejaz, A., Vattathil, S., Maserati, E., Houlden, H., Taanman, J. W., Schapira, A. H. & Proukakis, C. (2017) DNA isolation protocol effects on nuclear DNA analysis by microarrays, droplet digital PCR, and whole genome sequencing, and on mitochondrial DNA copy number estimation. *Plos One,* 12(7).

Navarro, A. & Boveris, A. (2007) The mitochondrial energy transduction system and the aging process. *American Journal of Physiology-Cell Physiology,* 292(2)**,** C670-C686.

Nebbak, A., Willcox, A. C., Bitam, I., Raoult, D., Parola, P. & Almeras, L. (2016) Standardization of sample homogenization for mosquito identification using an innovative proteomic tool based on protein profiling. *Proteomics,* 16(24)**,** 3148-3160.

Neiman, M. & Taylor, D. R. (2009) The causes of mutation accumulation in mitochondrial genomes. *Proceedings of the Royal Society B-Biological Sciences,* 276(1660)**,** 1201-1209.

Nicholls, T. J., Zsurka, G., Peeva, V., Scholer, S., Szczesny, R. J., Cysewski, D., Reyes, A., Kornblum, C., Sciacco, M., Moggio, M., Dziembowski, A., Kunz, W. S. & Minczuk, M. (2014) Linear mtDNA fragments and unusual mtDNA rearrangements associated with pathological deficiency of MGME1 exonuclease. *Human Molecular Genetics,* 23(23)**,** 6147-6162.

Nicklas, J. A., Brooks, E. M., Hunter, T. C., Single, R. & Branda, R. F. (2004) Development of a quantitative PCR (TaqMan) assay for relative mitochondrial DNA copy number and the common mitochondrial DNA deletion in the rat. *Environmental and Molecular Mutagenesis,* 44(4)**,** 313-320.

Nie, H. R., Shu, H. Y., Vartak, R., Milstein, A. C., Mo, Y. L., Hu, X. Q., Fang, H. Z., Shen, L. J., Ding, Z. N., Lu, J. X. & Bai, Y. D. (2013) Mitochondrial Common Deletion, a Potential Biomarker for Cancer Occurrence, Is Selected against in Cancer Background: A Meta-Analysis of 38 Studies. *Plos One,* 8(7).

Nikolaev, Y. A. (1978) MODEL OF THE KINETICS OF CHEMICAL-REACTIONS AT HIGH-TEMPERATURES. *Combustion Explosion and Shock Waves,* 14(4)**,** 468-471.

Nissanka, N., Bacman, S. R., Plastini, M. J. & Moraes, C. T. (2018) The mitochondrial DNA polymerase gamma degrades linear DNA fragments precluding the formation of deletions. *Nature Communications,* 9.

Nissanka, N., Minczuk, M. & Moraes, C. T. (2019) Mechanisms of Mitochondrial DNA Deletion Formation. *Trends in Genetics,* 35(3)**,** 235-244.

Nissanka, N. & Moraes, C. T. (2018) Mitochondrial DNA damage and reactive oxygen species in neurodegenerative disease. *Febs Letters,* 592(5)**,** 728-742.

Nolan, T., Hands, R. E. & Bustin, S. A. (2006) Quantification of mRNA using real-time RT-PCR. *Nature Protocols,* 1(3)**,** 1559-1582.

Nonis, A., Scortegagna, M. & Ruperti, B. (2011) PRaTo: A web-tool to select optimal primer pairs for qPCR. *Biochemical and Biophysical Research Communications,* 415(4)**,** 707-708.

Odom, D. T., Dowell, R. D., Jacobsen, E. S., Gordon, W., Danford, T. W., Macisaac, K. D., Rolfe, P. A., Conboy, C. M., Gifford, D. K. & Fraenkel, E. (2007) Tissue-

specific transcriptional regulation has diverged significantly between human and mouse. *Nature Genetics,* 39(6)**,** 730-732.

Ojaimi, J., Masters, C. L., Opeskin, K., Mckelvie, P. & Byrne, E. (1999) Mitochondrial respiratory chain activity in the human brain as a function of age. *Mechanisms of Ageing and Development,* 111(1)**,** 39-47.

Oliveira, M. T., Garesse, R. & Kaguni, L. S. (2010) Animal models of mitochondrial DNA transactions in disease and ageing. *Experimental Gerontology,* 45(7-8)**,** 489-502.

Olovnikov, A. M. (1973) THEORY OF MARGINOTOMY - INCOMPLETE COPYING OF TEMPLATE MARGIN IN ENZYMIC-SYNTHESIS OF POLYNUCLEOTIDES AND BIOLOGICAL SIGNIFICANCE OF PHENOMENON. *Journal of Theoretical Biology,* 41(1)**,** 181-190.

Park, C. B. & Larsson, N. G. (2011) Mitochondrial DNA mutations in disease and aging. *Journal of Cell Biology,* 193(5)**,** 809-818.

Peeva, V., Blei, D., Trombly, G., Corsi, S., Szukszto, M. J., Rebelo-Guiomar, P., Gammage, P. A., Kudin, A. P., Becker, C., Altmuller, J., Minczuk, M., Zsurka, G. & Kunz, W. S. (2018) Linear mitochondrial DNA is rapidly degraded by components of the replication machinery. *Nature Communications,* 9.

Peinnequin, A., Poyot, T., Dib, A., Aubourg, A., Mouret, C. & Demeilliers, C. (2011) Direct quantification of mitochondrial DNA and its 4.9-kb common deletion without DNA purification. *Analytical Biochemistry,* 409(2)**,** 298-300.

Peng, Q., Satya, R. V., Lewis, M., Randad, P. & Wang, Y. X. (2015) Reducing amplification artifacts in high multiplex amplicon sequencing by using molecular barcodes. *Bmc Genomics,* 16.

Peper, G., Fankhauser, A., Merlin, T., Roscic, A., Hofmann, M. & Obrdlik, P. (2014) Direct real-time quantitative PCR for measurement of host-cell residual DNA in therapeutic proteins. *Journal of Pharmaceutical and Biomedical Analysis,* 100**,** 123-130.

Persson, O., Muthukumar, Y., Basu, S., Jenninger, L., Uhler, J. P., Berglund, A. K., Mcfarland, R., Taylor, R. W., Gustafsson, C. M., Larsson, E. & Falkenberg, M. (2019) Copy-choice recombination during mitochondrial L-strand synthesis causes DNA deletions. *Nature Communications,* 10.

Persson, S., De Boer, R. F., Kooistra-Smid, A. M. D. & Olsen, K. E. P. (2011) Five commercial DNA extraction systems tested and compared on a stool sample collection. *Diagnostic Microbiology and Infectious Disease,* 69(3)**,** 240-244.

Phillips, A. F., Millet, A. R., Tigano, M., Dubois, S. M., Crimmins, H., Babin, L., Charpentier, M., Piganeau, M., Brunet, E. & Sfeir, A. (2017) Single-Molecule Analysis of mtDNA Replication Uncovers the Basis of the Common Deletion. *Molecular Cell,* 65(3)**,** 527-+.

Phillips, N. R., Sprouse, M. L. & Roby, R. K. (2014) Simultaneous quantification of mitochondrial DNA copy number and deletion ratio: A multiplex real-time PCR assay. *Scientific Reports,* 4.

Picard, M., Taivassalo, T., Ritchie, D., Wright, K. J., Thomas, M. M., Romestaing, C. & Hepple, R. T. (2011) Mitochondrial Structure and Function Are Disrupted by Standard Isolation Methods. *Plos One,* 6(3).

Picard-Meyer, E., De Garam, C. P., Schereffer, J. L., Marchal, C., Robardet, E. & Cliquet, F. (2015) Cross-Platform Evaluation of Commercial Real-Time SYBR

Green RT-PCR Kits for Sensitive and Rapid Detection of European Bat Lyssavirus Type 1. *Biomed Research International*.

Pisoschi, A. M. & Pop, A. (2015) The role of antioxidants in the chemistry of oxidative stress: A review. *European Journal of Medicinal Chemistry,* 97**,** 55-74.

Pitceathly, R. D. S., Rahman, S. & Hanna, M. G. (2012) Single deletions in mitochondrial DNA - Molecular mechanisms and disease phenotypes in clinical practice. *Neuromuscular Disorders,* 22(7)**,** 577-586.

Ponti, M., Forrow, S. M., Souhami, R. L., Dincalci, M. & Hartley, J. A. (1991) MEASUREMENT OF THE SEQUENCE SPECIFICITY OF COVALENT DNA MODIFICATION BY ANTINEOPLASTIC AGENTS USING TAQ DNA-POLYMERASE. *Nucleic Acids Research,* 19(11)**,** 2929-2933.

Prakash, A. & Doublié, S. (August 2015) Base Excision Repair in the Mitochondria. Journal of Cellular Biochemistry.

Qi, Y., Liu, H., Daniels, M. P., Zhang, G. & Xu, H. (2016) Loss of Drosophila i-AAA protease, dYME1L, causes abnormal mitochondria and apoptotic degeneration. *Cell Death and Differentiation,* 23(2)**,** 291-302.

Qu, H. Y., Ma, F. & Li, Q. W. (2008) Comparative analysis of mitochondrial fragments transferred to the nucleus in vertebrate. *Journal of Genetics and Genomics,* 35(8)**,** 485-490.

Radak, Z., Zhao, Z. F., Koltai, E., Ohno, H. & Atalay, M. (2013) Oxygen Consumption and Usage During Physical Exercise: The Balance Between Oxidative Stress and ROS-Dependent Adaptive Signaling. *Antioxidants & Redox Signaling,* 18(10)**,** 1208-1246.

Rattan, S. I. S. (2008) Principles and practice of hormetic treatment of ageing and age-related diseases. *Human & Experimental Toxicology,* 27(2)**,** 151-154.

Robberson, D. L., Vinograd, J. & Kasamatsu, H. (1972) REPLICATION OF MITOCHONDRIAL-DNA - CIRCULAR REPLICATIVE INTERMEDIATES IN MOUSE L CELLS. *Proceedings of the National Academy of Sciences of the United States of America,* 69(3)**,** 737-+.

Robertson, J. M. & Walsh-Weller, J. (1998) An introduction to PCR primer design and optimization of amplification reactions. *Methods in molecular biology (Clifton, N.J.),* 98**,** 121-54.

Roos, S., Sofou, K., Hedberg-Oldfors, C., Kollberg, G., Lindgren, U., Thomsen, C., Tulinius, M. & Oldfors, A. (2019) Mitochondrial complex IV deficiency caused by a novel frameshift variant in MT-CO2 associated with myopathy and perturbed acylcarnitine profile. *European Journal of Human Genetics,* 27(2)**,** 331-335.

Roth, L. W. & Polotsky, A. J. (2012) Can we live longer by eating less? A review of caloric restriction and longevity. *Maturitas,* 71(4)**,** 315-319.

Rudkjobing, V. B., Wolff, T. Y. & Skovhus, T. L. (2014) Quantitative Real-time Polymerase Chain Reaction (qPCR) Methods for Abundance and Activity Measures. *Applications of Molecular Microbiological Methods***,** 193-201.

Ruijter, J. M., Ruiz-Villalba, A., Van Den Hoff, A. J. J., Gunst, Q. D., Wittwer, C. T. & Van Den Hoff, M. J. B. (2019) Removal of artifact bias from qPCR results using DNA melting curve analysis. *Faseb Journal,* 33(12)**,** 14542-14555.

Ruiz-Villalba, A., Van Pelt-Verkuil, E., Gunst, Q. D., Ruijter, J. M. & Van Den Hoff, M. J. (2017) Amplification of nonspecific products in quantitative polymerase chain reactions (qPCR). *Biomolecular detection and quantification,* 14**,** 7-18.

Rydberg, B. & Lindahl, T. (1982) NON-ENZYMATIC METHYLATION OF DNA BY THE INTRACELLULAR METHYL-GROUP DONOR S-ADENOSYL-L-METHIONINE IS A POTENTIALLY MUTAGENIC REACTION. *Embo Journal,* 1(2)**,** 211-216.

Samstag, C. L., Hoekstra, J. G., Huang, C.-H., Chaisson, M. J., Youle, R. J., Kennedy, S. R. & Pallanck, L. J. (2018) Deleterious mitochondrial DNA point mutations are overrepresented in Drosophila expressing a proofreading-defective DNA polymerase gamma. *Plos Genetics,* 14(11).

Samuels, D. C., Schon, E. A. & Chinnery, P. F. (2004) Two direct repeats cause most human mtDNA deletions. *Trends in Genetics,* 20(9)**,** 393-398.

Santalucia, J., Jr. (2007) Physical principles and visual-OMP software for optimal PCR design. *Methods in molecular biology (Clifton, N.J.),* 402**,** 3-34.

Santoro, A., Spinelli, C. C., Martucciello, S., Nori, S. L., Capunzo, M., Puca, A. A. & Ciaglia, E. (2018) Innate immunity and cellular senescence: The good and the bad in the developmental and aged brain. *Journal of Leukocyte Biology,* 103(3)**,** 509-524.

Sarup, P., Sorensen, P. & Loeschcke, V. (2014) The long-term effects of a life-prolonging heat treatment on the Drosophila melanogaster transcriptome suggest that heat shock proteins extend lifespan. *Experimental Gerontology,* 50**,** 34-39.

Schaible, R., Sussman, M. & Kramer, B. H. (2014) Aging and Potential for Self-Renewal: Hydra Living in the Age of Aging - A Mini-Review. *Gerontology,* 60(6)**,** 548-556.

Schapira, A. H. V. (2012) Mitochondrial diseases. *Lancet,* 379(9828)**,** 1825-1834.

Scheckhuber, C. Q., Erjavec, N., Tinazli, A., Hamann, A., Nystrom, T. & Osiewacz, H. D. (2007) Reducing mitochondrial fission results in increased life span and fitness of two fungal ageing models. *Nature Cell Biology,* 9(1)**,** 99-U129.

Sen, A. & Cox, R. T. (2017) Fly Models of Human Diseases: Drosophila as a Model for Understanding Human Mitochondrial Mutations and Disease. *Fly Models of Human Diseases,* 121**,** 1-27.

Sfeir, A. & Symington, L. S. (2015) Microhomology-Mediated End Joining: A Back-up Survival Mechanism or Dedicated Pathway? *Trends in Biochemical Sciences,* 40(11)**,** 701-714.

Shen, J., Wan, J., Huff, C., Fang, S. Y., Lee, J. E. & Zhao, H. (2016) Mitochondrial DNA 4977-base pair common deletion in blood leukocytes and melanoma risk. *Pigment Cell & Melanoma Research,* 29(3)**,** 372-378.

Shoffner, J. M., Lott, M. T., Voljavec, A. S., Soueidan, S. A., Costigan, D. A. & Wallace, D. C. (1989) SPONTANEOUS KEARNS-SAYRE CHRONIC EXTERNAL OPHTHALMOPLEGIA PLUS SYNDROME ASSOCIATED WITH A MITOCHONDRIAL-DNA DELETION - A SLIP REPLICATION MODEL AND METABOLIC THERAPY. *Proceedings of the National Academy of Sciences of the United States of America,* 86(20)**,** 7952-7956.

Short, K. R., Bigelow, M. L., Kahl, J., Singh, R., Coenen-Schimke, J., Raghavakaimal, S. & Nair, K. S. (2005) Decline in skeletal muscle mitochondrial function with

aging in humans. *Proceedings of the National Academy of Sciences of the United States of America,* 102(15)**,** 5618-5623.

Shutt, T. E. & Gray, M. W. (2006) Bacteriophage origins of mitochondrial replication and transcription proteins. *Trends in Genetics,* 22(2)**,** 90-95.

Sinha, R. P. & Hader, D. P. (2002) UV-induced DNA damage and repair: a review. *Photochemical & Photobiological Sciences,* 1(4)**,** 225-236.

Stangegaard, M., Hjort, B. B., Hansen, T. N., Hoflund, A., Mogensen, H. S., Hansen, A. J. & Morling, N. (2013) Automated extraction of DNA from biological stains on fabric from crime cases. A comparison of a manual and three automated methods. *Forensic Science International-Genetics,* 7(3)**,** 384-388.

Stewart, J. B. & Chinnery, P. F. (2015) The dynamics of mitochondrial DNA heteroplasmy: implications for human health and disease. *Nature Reviews Genetics,* 16(9)**,** 530-542.

Stocco, D. M., Cascarano, J. & Wilson, M. A. (1977) QUANTITATION OF MITOCHONDRIAL-DNA, RNA, AND PROTEIN IN STARVED AND STARVED-REFED RAT-LIVER. *Journal of Cellular Physiology,* 90(2)**,** 295-306.

Suen, D. F., Narendra, D. P., Tanaka, A., Manfredi, G. & Youle, R. J. (2010) Parkin overexpression selects against a deleterious mtDNA mutation in heteroplasmic cybrid cells. *Proceedings of the National Academy of Sciences of the United States of America,* 107(26)**,** 11835-11840.

Suffys, P., Vanderborght, P. R., Dos Santos, P. B., Correa, L. A. P., Bravin, Y. & Kritski, A. L. (2001) Inhibition of the polymerase chain reaction by sputum samples from tuberculosis patients after processing using a silica-guanidiniumthiocyanate DNA isolation procedure. *Memorias Do Instituto Oswaldo Cruz,* 96(8)**,** 1137-1139.

Sun, N., Youle, R. J. & Finkel, T. (2016) The Mitochondrial Basis of Aging. *Molecular Cell,* 61(5)**,** 654-666.

Sun, Y., Yolitz, J., Wang, C., Spangler, E., Zhan, M. & Zou, S. (2013) Aging studies in Drosophila melanogaster. *Methods in molecular biology (Clifton, N.J.),* 1048**,** 77-93.

Suomalainen, A. & Kaukonen, J. (2001) Diseases caused by nuclear genes affecting mtDNA stability. *American Journal of Medical Genetics,* 106(1)**,** 53-61.

Sutovsky, P., Moreno, R. D., Ramalho-Santos, J., Dominko, T., Simerly, C. & Schatten, G. (1999) Development - Ubiquitin tag for sperm mitochondria. *Nature,* 402(6760)**,** 371-372.

Svec, D., Tichopad, A., Novosadova, V., Pfaffl, M. & Kubista, M. (2015) How good is a PCR efficiency estimate: Recommendations for precise and robust qPCR efficiency assessments.

Sykora, P., Wilson, D. M. & Bohr, V. A. (2012) Repair of persistent strand breaks in the mitochondrial genome. *Mechanisms of Ageing and Development,* 133(4)**,** 169-175.

Szczepanowska, K. & Trifunovic, A. (2015) Different faces of mitochondrial DNA mutators. *Biochimica Et Biophysica Acta-Bioenergetics,* 1847(11)**,** 1362-1372.

Szklarczyk, R. & Huynen, M. A. (2010) Mosaic origin of the mitochondrial proteome. *Proteomics,* 10(22)**,** 4012-4024.

Tadi, S. K., Sebastian, R., Dahal, S., Babu, R. K., Choudhary, B. & Raghavan, S. C. (2016) Microhomology-mediated end joining is the principal mediator of

double-strand break repair during mitochondrial DNA lesions. *Molecular Biology of the Cell,* 27(2)**,** 223-235.

Tanhauser, S. M. & Laipis, P. J. (1995) MULTIPLE DELETIONS ARE DETECTABLE IN MITOCHONDRIAL-DNA OF AGING MICE. *Journal of Biological Chemistry,* 270(42)**,** 24769-24775.

Tatar, M. (2010) Reproductive aging in invertebrate genetic models. *Reproductive Aging,* 1204**,** 149-155.

Tennessen, J. M., Barry, W. E., Cox, J. & Thummel, C. S. (2014) Methods for studying metabolism in Drosophila. *Methods,* 68(1)**,** 105-115.

Thannickal, V. J. & Fanburg, B. L. (2000) Reactive oxygen species in cell signaling. *American Journal of Physiology-Lung Cellular and Molecular Physiology,* 279(6)**,** L1005-L1028.

Toni, L. S., Garcia, A. M., Jeffrey, D. A., Jiang, X., Stauffer, B. L., Miyamoto, S. D. & Sucharov, C. C. (2018) Optimization of phenol-chloroform RNA extraction. *Methodsx,* 5**,** 599-608.

Trifunovic, A., Hansson, A., Wredenberg, A., Rovio, A. T., Dufour, E., Khvorostov, I., Spelbrink, J. N., Wibom, R., Jacobs, H. T. & Larsson, N. G. (2005) Somatic mtDNA mutations cause aging phenotypes without affecting reactive oxygen species production. *Proceedings of the National Academy of Sciences of the United States of America,* 102(50)**,** 17993-17998.

Trifunovic, A., Wredenberg, A., Falkenberg, M., Spelbrink, J. N., Rovio, A. T., Bruder, C. E., Bohlooly-Y, M., Gidlof, S., Oldfors, A., Wibom, R., Tornell, J., Jacobs, H. T. & Larsson, N. G. (2004) Premature ageing in mice expressing defective mitochondrial DNA polymerase. *Nature,* 429(6990)**,** 417-423.

Tsuji, J., Frith, M. C., Tomii, K. & Horton, P. (2012) Mammalian NUMT insertion is non-random. *Nucleic Acids Research,* 40(18)**,** 9073-9088.

Tudek, B., Boiteux, S. & Laval, J. (1992) BIOLOGICAL PROPERTIES OF IMIDAZOLE RING-OPENED N7-METHYLGUANINE IN M13MP18-PHAGE DNA. *Nucleic Acids Research,* 20(12)**,** 3079-3084.

Tyynismaa, H., Mjosund, K. P., Wanrooij, S., Lappalainen, I., Ylikallio, E., Jalanko, A., Spelbrink, J. N., Paetau, A. & Suomalainen, A. (2005) Mutant mitochondrial helicase Twinkle causes multiple mtDNA deletions and a late-onset mitochondrial disease in mice. *Proceedings of the National Academy of Sciences of the United States of America,* 102(49)**,** 17687-17692.

Udvardi, M. K., Czechowski, T. & Scheible, W. R. (2008) Eleven golden rules of quantitative RT-PCR. *Plant Cell,* 20(7)**,** 1736-1737.

Valko, M., Leibfritz, D., Moncol, J., Cronin, M. T. D., Mazur, M. & Telser, J. (2007) Free radicals and antioxidants in normal physiological functions and human disease. *International Journal of Biochemistry & Cell Biology,* 39(1)**,** 44-84.

Van Bon, B. W. M., Oortveld, M. A. W., Nijtmans, L. G., Fenckova, M., Nijhof, B., Besseling, J., Vos, M., Kramer, J. M., De Leeuw, N., Castells-Nobau, A., Asztalos, L., Viragh, E., Ruiter, M., Hofmann, F., Eshuis, L., Collavin, L., Huynen, M. A., Asztalos, Z., Verstreken, P., Rodenburg, R. J., Smeitink, J. A., De Vries, B. B. A. & Schenck, A. (2013) CEP89 is required for mitochondrial metabolism and neuronal function in man and fly. *Human Molecular Genetics,* 22(15)**,** 3138-3151.

Van Deursen, J. M. (2014) The role of senescent cells in ageing. *Nature,* 509(7501)**,** 439-446.

Van Houten, B., Hunter, S. E. & Meyer, J. N. (2016) Mitochondrial DNA damage induced autophagy, cell death, and disease. *Frontiers in Bioscience-Landmark,* 21**,** 42-54.

Vantuyle, G. C., Gudikote, J. P., Hurt, V. R., Miller, B. B. & Moore, C. A. (1996) Multiple, large deletions in rat mitochondrial DNA: Evidence for a major hot spot. *Mutation Research-Fundamental and Molecular Mechanisms of Mutagenesis,* 349(1)**,** 95-107.

Vellai, T., Takacs-Vellai, K., Zhang, Y., Kovacs, A. L., Orosz, L. & Muller, F. (2003) Genetics - Influence of TOR kinase on lifespan in C-elegans. *Nature,* 426(6967)**,** 620-620.

Vermulst, M., Wanagat, J., Kujoth, G. C., Bielas, J. H., Rabinovitch, P. S., Prolla, T. A. & Loeb, L. A. (2008) DNA deletions and clonal mutations drive premature aging in mitochondrial mutator mice. *Nature Genetics,* 40(4)**,** 392-394.

Viguera, E., Canceill, D. & Ehrlich, S. D. (2001) Replication slippage involves DNA polymerase pausing and dissociation. *Embo Journal,* 20(10)**,** 2587-2595.

Villa-Cuesta, E. & Rand, D. M. (2015) Preparation of Mitochondrial Enriched Fractions for Metabolic Analysis in Drosophila. *Jove-Journal of Visualized Experiments*(103).

Von Wurmb-Schwark, N., Ringleb, A., Schwark, T., Broese, T., Weirich, S., Schlaefke, D., Wegener, R. & Oehmichen, M. (2008) The effect of chronic alcohol consumption on mitochondrial DNA mutagenesis in human blood. *Mutation Research-Fundamental and Molecular Mechanisms of Mutagenesis,* 637(1-2)**,** 73-79.

Von Wurmb-Schwark, N., Schwark, T., Caliebe, A., Drenske, C., Nikolaus, S., Schreiber, S. & Nebel, A. (2010) Low level of the mtDNA(4977) deletion in blood of exceptionally old individuals. *Mechanisms of Ageing and Development,* 131(3)**,** 179-184.

Wallace, D. C., Shoffner, J. M., Trounce, I., Brown, M. D., Ballinger, S. W., Corraldebrinski, M., Horton, T., Jun, A. S. & Lott, M. T. (1995) MITOCHONDRIAL-DNA MUTATIONS IN HUMAN DEGENERATIVE DISEASES AND AGING. *Biochimica Et Biophysica Acta-Molecular Basis of Disease,* 1271(1)**,** 141-151.

Wang, X. F. & Son, A. (2013) Effects of pretreatment on the denaturation and fragmentation of genomic DNA for DNA hybridization. *Environmental Science-Processes & Impacts,* 15(12)**,** 2204-2212.

Wang, Y., Cooper, R., Kiladjian, A., Bergelson, S. & Feschenko, M. (2019) A Digestion-free Method for Quantification of Residual Host Cell DNA in rAAV Gene Therapy Products. *Molecular Therapy-Methods & Clinical Development,* 13**,** 526-531.

Wei, Y. H. (1992) MITOCHONDRIAL-DNA ALTERATIONS AS AGING-ASSOCIATED MOLECULAR EVENTS. *Mutation Research,* 275(3-6)**,** 145-155.

Wei, Y. H., Lee, C. F., Lee, H. C., Ma, Y. S., Wang, C. W., Lu, C. Y. & Pang, C. Y. (2001) Increases of mitochondrial mass and mitochondrial genome in association with enhanced oxidative stress in human cells harboring 4,977 BP-deleted

mitochondrial DNA. *Healthy Aging for Functional Longevity: Molecular and Cellular Interactions in Senescence,* 928**,** 97-112.

Wilhelm, J., Hahn, M. & Pingoud, A. (2000) Influence of DNA target melting behavior on real-time PCR quantification. *Clinical Chemistry,* 46(11)**,** 1738-1743.

Williams, C. S., Mann, M. & Dubois, R. N. (1999) The role of cyclooxygenases in inflammation, cancer, and development. *Oncogene,* 18(55)**,** 7908-7916.

Williams, G. C. (1957) PLEIOTROPY, NATURAL-SELECTION, AND THE EVOLUTION OF SENESCENCE. *Evolution,* 11(4)**,** 398-411.

Wong, M. L. & Medrano, J. F. (2005) Real-time PCR for mRNA quantitation. *Biotechniques,* 39(1)**,** 75-85.

Yamashita, S., Nishino, I., Nonaka, I. & Goto, Y. I. (2008) Genotype and phenotype analyses in 136 patients with single large-scale mitochondrial DNA deletions. *Journal of Human Genetics,* 53(7)**,** 598-606.

Yang, W. & Hekimi, S. (2010) A Mitochondrial Superoxide Signal Triggers Increased Longevity in Caenorhabditis elegans. *Plos Biology,* 8(12).

Yasukawa, T. & Kang, D. (2018) An overview of mammalian mitochondrial DNA replication mechanisms. *Journal of Biochemistry,* 164(3)**,** 183-193.

Ye, K. X., Lu, J., Ma, F., Keinan, A. & Gu, Z. L. (2014) Extensive pathogenicity of mitochondrial heteroplasmy in healthy human individuals. *Proceedings of the National Academy of Sciences of the United States of America,* 111(29)**,** 10654-10659.

Yen, T. C., Chen, Y. S., King, K. L., Yeh, S. H. & Wei, Y. H. (1989) LIVER MITOCHONDRIAL RESPIRATORY FUNCTIONS DECLINE WITH AGE. *Biochemical and Biophysical Research Communications,* 165(3)**,** 994-1003.

Yen, T. C., Su, J. H., King, K. L. & Wei, Y. H. (1991) AGING-ASSOCIATED 5 KB DELETION IN HUMAN LIVER MITOCHONDRIAL-DNA. *Biochemical and Biophysical Research Communications,* 178(1)**,** 124-131.

Yin, P. H., Lee, H. C., Chau, G. Y., Wu, Y. T., Li, S. H., Lui, W. Y., Wei, Y. H., Liu, T. Y. & Chi, C. W. (2004) Alteration of the copy number and deletion of mitochondrial DNA in human hepatocellular carcinoma. *British Journal of Cancer,* 90(12)**,** 2390-2396.

Young, M. J. & Copeland, W. C. (2016) Human mitochondrial DNA replication machinery and disease. *Current Opinion in Genetics & Development,* 38**,** 52-62.

Yu-Wai-Man, P., Lai-Cheong, J., Borthwick, G. M., He, L. P., Taylor, G. A., Greaves, L. C., Taylor, R. W., Griffiths, P. G. & Turnbull, D. M. (2010) Somatic Mitochondrial DNA Deletions Accumulate to High Levels in Aging Human Extraocular Muscles. *Investigative Ophthalmology & Visual Science,* 51(7)**,** 3347-3353.

Yuan, S. Q., Cohen, D. B., Ravel, J., Abdo, Z. & Forney, L. J. (2012) Evaluation of Methods for the Extraction and Purification of DNA from the Human Microbiome. *Plos One,* 7(3).

Yui, R. & Matsuura, E. T. (2006) Detection of deletions flanked by short direct repeats in mitochondrial DNA of aging Drosophila. *Mutation Research-Fundamental and Molecular Mechanisms of Mutagenesis,* 594(1-2)**,** 155-161.

Yui, R., Ohno, Y. & Matsuura, E. T. (2003) Accumulation of deleted mitochondrial DNA in aging Drosophila melanogaster. *Genes & Genetic Systems,* 78(3)**,** 245-251.

Yusoff, A. A. M., Abdullah, W. S. W., Khair, S. & Abd Radzak, S. M. (2019) A comprehensive overview of mitochondrial DNA 4977-bp deletion in cancer studies. *Oncology Reviews,* 13(1)**,** 54-64.

Zhang, H. X., Burr, S. P. & Chinnery, P. F. (2018) The mitochondrial DNA genetic bottleneck: inheritance and beyond. *Mitochondrial Diseases,* 62(3)**,** 225-234.

Zhang, Y. Q., Ikeno, Y., Qi, W. B., Chaudhuri, A., Li, Y., Bokov, A., Thorpe, S. R., Baynes, J. W., Epstein, C., Richardson, A. & Van Remmen, H. (2009) Mice Deficient in Both Mn Superoxide Dismutase and Glutathione Peroxidase-1 Have Increased Oxidative Damage and a Greater Incidence of Pathology but No Reduction in Longevity. *Journals of Gerontology Series a-Biological Sciences and Medical Sciences,* 64(12)**,** 1212-1220.

Zinovkina, L. A. (2018) Mechanisms of Mitochondrial DNA Repair in Mammals. *Biochemistry-Moscow,* 83(3)**,** 233-249.

Zipper, H., Brunner, H., Bernhagen, J. & Vitzthum, F. (2004) Investigations on DNA intercalation and surface binding by SYBR Green I, its structure determination and methodological implications. *Nucleic Acids Research,* 32(12).